



Høgskulen
på Vestlandet

BACHELOR'S THESIS

Optimization of green extraction conditions and determination of Fucoxanthin from *Laminaria hyperborea*

Benjamin Alexander Johannesen

Bachelor's programme in Engineering, Chemical Engineering

Faculty of Engineering and Science/Department of Safety, Chemistry and Biomedical laboratory sciences/Chemical Engineering/Specialization Environmental Technology

Submission Date

30th of May 2022

I confirm that the work is self-prepared and that references/source references to all sources used in the work are provided, cf. Regulation relating to academic studies and examinations at the Western Norway University of Applied Sciences (HVL), § 12-1.

Foreword

This thesis was written during the spring semester of 2022 as a final part of bachelor's program in Chemical Engineering with a specialization in Environmental Technology at Western University of Applied Sciences.

The experiments were done at the laboratories at Western University of Applied Sciences in Bergen, Norway.

Firstly, I want to thank my employer and external supervisor, Georg Kopplin. Both for his guidance as an expert in macroalgae chemistry and for asking me to work on this project that was demanding and interesting. I've become a better chemist for it, that's for sure.

I also want to thank my internal supervisor, Jarle Sidney Diesen. His extensive knowledge in organic and green chemistry was a great fit for this project, and his door was always open for guidance and laughter. Torun Synnøve Skøld was a great help in the practical lab work involved in the project.

Finally, I want to thank Bjørn Grung for his answers with regards to factorial design and Kevin Brahm for his answers on the carotenoid column.

Bergen 30th of May 2022

Benjamin A. Johannesen

Benjamin Alexander Johannesen

Abstract

Alginor was in the process of establishing a biorefinery focused on products from *Laminaria hyperborea* and wanted to develop methods to extract carotenoids, polyphenols, and chlorophylls from it. *Laminaria hyperborea* is a brown macroalgae, and the main pigment that gives the macroalgae its color is Fucoxanthin. Fucoxanthin is a high value product because of its antioxidant behavior, and therefore it was the focus of this thesis. The goals of this thesis were to develop a reverse-phase HPLC determination method for Fucoxanthin, and to optimize extraction conditions for Fucoxanthin using a Soxhlet system. Since Fucoxanthin is a product for the food-, cosmetics-, and pharmaceutical industry it would have to be done with green solvents. Traditionally organic solvents like n-hexane, dichloromethane, or diethyl ether have been used, and to compete using green solvents an optimization study was needed. The significant factors for the extraction conditions were found to be solvent type, sample to solvent ratio, and extraction time. Previous work done at the behest of Alginor had found the optimal extraction time to be five cycles. The solvent types that were suitable with regards to greenness were ethanol, methanol, and 2-propanol. The sample to solvent ratios that were tested were 1:20 and 1:30. A factorial design with 18 experiments was set up to find the optimal extraction conditions, but first, the determination method had to be developed. The column used was YMC Carotenoid (250 mm x 4.6 mm I.D., 5 μ m particle size) with a temperature set at 36 °C, and the injection volume for the samples was 20 μ L. The mobile phases used were water (A), Methanol (B), and Ethyl acetate (C), and the gradient program (A%:B%:C%) was made up by the following linear gradients: 3:94:3 from start to 10 minutes, 3:62:35 at 15 minutes, 3:47:50 at 22 minutes, 3:7:90 at 30 minutes, 3:7:90 at 40 minutes, 3:94:3 at 50 minutes, and 3:94:3 at 60 minutes. The resolutions for the extracts varied from 1.455 ± 0.056 for the 2-propanol extracts to 2.012 ± 0.236 for the methanol extracts, suitable for quantification. The linearity coefficients varied from 0.96675 to 0.98577, which was acceptable for this comparison. The limits of detection varied from 0.0981 mg/l to 0.2290 mg/l, and the limits of quantification varied from 0.3270 mg/l to 0.7632 mg/l. The precision of the peak area was 8.8 %RSD, 2.8 %RSD for the retention time, and 0.2 RSD% for the peak width. A factorial analysis showed that methanol with a sample to solvent ratio of 1:20 was the optimal extraction conditions. A plot of the main effects revealed that there were interaction effects between the solvent type and sample to solvent ratio factors, and that methanol had a decrease in extracted Fucoxanthin, whilst 2-propanol had a slight increase. The results for the optimal extraction conditions were confirmed by a significant variance by a one-way ANOVA-test, and a least significant difference test between the methanol and 2-propanol extracts. The concentration of Fucoxanthin divided by dry weight for the ethanol extracts with a 1:20 sample to solvent ratio was 0.2835 ± 0.1398 (mg/l)/g dry weight, and with a 1:30 sample to solvent ratio -0.0039 ± 0.0232 (mg/l)/g dry weight. The concentration of Fucoxanthin divided by dry weight for the methanol extracts with a 1:20 sample to solvent ratio was 0.9802 ± 0.0461 (mg/l)/g dry weight, and with a 1:30 sample to solvent ratio 0.6077 ± 0.0948 (mg/l)/g dry weight. The concentration of Fucoxanthin divided by dry weight for the 2-propanol extracts with a 1:20 sample to solvent ratio was 0.6567 ± 0.0352 (mg/l)/g dry weight, and with a 1:30 sample to solvent ratio 0.4819 ± 0.0802 (mg/l)/g dry weight.

Sammendrag

Alginor var i ferd med å etablere et bioraffineri med fokus på produkter fra *Laminaria hyperborea* og ønsket å utvikle metoder for å trekke ut karotenoider, polyfenoler og klorofyller fra det. *Laminaria hyperborea* er en brun makroalge, og hovedpigmentet som gir makroalgen farge er Fucoxanthin. Fucoxanthin er et høyverdig produkt på grunn av dets antioksidierende oppførsel, og ble derfor fokus for denne oppgaven. Målene med denne oppgaven var å utvikle en reversfase HPLC-bestemmelsesmetode for Fucoxanthin og å optimalisere ekstraksjonsforholdene for Fucoxanthin ved bruk av et Soxhlet-system. Siden Fucoxanthin er et produkt til mat-, kosmetikk- og farmasi-industrien, må ekstraksjonen gjøres med grønne løsemidler. Tradisjonelt har organiske løsningsmidler som n-heksan, diklormetan eller dietyleter blitt brukt, og for å være konkurransedyktig med grønne løsningsmidler var det nødvendig med en optimaliseringsstudie. De signifikante faktorene for ekstraksjonsbetingelsene ble funnet å være løsemiddeltipe, forhold mellom prøve og løsemiddel, og ekstraksjonstid. Tidligere arbeid utført på vegne av Alginor hadde funnet ut at den optimale utvinningstiden var fem sykluser. Løsemidlene som var egnet med hensyn til grønnhet var etanol, metanol og 2-propanol. Forholdene mellom prøve og løsemiddel som ble testet var 1:20 og 1:30. Et faktorielt design med 18 eksperimenter ble satt opp for å finne de optimale ekstraksjonsforholdene, men først måtte bestemmelsesmetoden utvikles. Kolonnen som ble brukt var YMC Carotenoid (250 mm x 4,6 mm I.D., 5 µm partikkelstørrelse) med en temperatur satt til 36 °C, og injeksjonsvolumet for prøvene var 20 µL. De mobile fasene som ble brukt var vann (A), metanol (B) og etylacetat (C), og gradientprogrammet (A%:B%:C%) ble bygd opp av følgende lineære gradienter: 3:94:3 fra start til 10 minutter, 3:62:35 etter 15 minutter, 3:47:50 etter 22 minutter, 3:7:90 etter 30 minutter, 3:7:90 etter 40 minutter, 3:94:3 etter 50 minutter, og 3:94:3 etter 60 minutter. Oppløsningene for ekstraktene varierte fra $1,455 \pm 0,056$ for 2-propanol-ekstraktene til $2,012 \pm 0,236$ for metanol-ekstraktene, egnet for kvantifisering. Linearitetskoeffisientene varierte fra 0,96675 til 0,98577, noe som var akseptabelt for denne sammenligningen. Deteksjonsgrensene varierte fra 0,0981 mg/l til 0,2290 mg/l, og kvantifiseringsgrensene varierte fra 0,3270 mg/l til 0,7632 mg/l. Presisjonen av arealet til toppene var 8,8 %RSD, 2,8 %RSD for retensjonstiden og 0,2 %RSD for bredden av toppene. En faktoriell analyse viste at metanol med et forhold mellom prøve og løsemiddel på 1:20 var de optimale ekstraksjonsbetingelsene. Et plott av hovedeffektene viste at det var interaksjonseffekter mellom løsemiddeltypen og forholdet mellom prøve og løsemiddel, og at metanol hadde en reduksjon i ekstrahert Fucoxanthin, mens 2-propanol hadde en svak økning. De optimale ekstraksjonsforholdene ble funnet til å være signifikant av en enveis ANOVA-test, og en "minst-signifikant-differansemetode" mellom metanol- og 2-propanol-ekstraktene. Konsentrasjonen av Fucoxanthin delt på tørrvekt for etanolekstraktene med et 1:20 prøve/løsemiddelforhold var $0,2835 \pm 0,1398$ (mg/l)/g tørrvekt, og med et 1:30 prøve/løsemiddelforhold $-0,0039 \pm 0,0232$ (mg/l)/g tørrvekt. Konsentrasjonen av Fucoxanthin delt på tørrvekt for metanolekstraktene med et 1:20 prøve til løsemiddelforhold var $0,9802 \pm 0,0461$ (mg/l)/g tørrvekt, og med et 1:30 prøve til løsemiddelforhold $0,6077 \pm 0,0948$ (mg/l)/g tørrvekt. Konsentrasjonen av Fucoxanthin delt på tørrvekt for 2-propanolekstraktene med 1:20 prøve til løsemiddelforhold var $0,6567 \pm 0,0352$ (mg/l)/g tørrvekt, og med 1:30 prøve til løsemiddelforhold $0,4819 \pm 0,0802$ (mg/l)/g tørrvekt.

List of abbreviations

EIC - European Innovation Council

AORTA - Alginor's Ocean Refining Total utilizing Application

Fx - Fucoxanthin

RP-HPLC-DAD – Reverse-phased High Performance Liquid Chromatography

ANOVA – Analysis of Variance

β -car - β -carotene

RSD

LOD-

LOQ-

Table of contents

Introduction	11
Background	11
A description of the thesis problem and the reasons for the study	12
Theory	14
Bioactive compounds	14
Liquid-solid extraction	17
Chromatography	17
Liquid chromatography	17
High performance liquid chromatography	21
Method validation	22
Experimental design	24
Materials and Methods	27
Results and discussion	33
Strategy	33
Literary analysis for method development	33
Screening test	34
Developing a determination method	38
Method validation	51
Optimization of a Soxhlet extraction	56
Analysis of optimization study	63
Factorial analysis	63
Relationship between temperature and Fx concentration	65
ANOVA analysis	66
Analytes other than Fucoxanthin	69
Conclusion	72
Future work	72
References	73
Attachments	76
Attachment 1 – Calculations of uncertainty	76
Attachment 2 – Calculations for modified mobile phases	83
Attachment 3 – Screening test runs	88
Attachment 4 – YMC modified runs	90
Attachment 5 – Method validation	97
Attachment 6 – HPLC data from the optimization study	100

Figure list for the main report

Figure 1 - A kelp forest of <i>Laminaria hyperborea</i> off the coast of Haugesund, Norway. The picture was reproduced with permission from Alginor.....	11
Figure 2 - An illustration and description of a the different parts of a kelp plant. The picture was reproduced with permission from Alginor. (https://alginor.no/about-us/our-raw-material/)	12
Figure 3 - A comparison of the molecular length of β -carotene with the film thickness of C18 and C30 column material, determined with small angle neutron scattering. The picture was reproduced with permission from YMC (https://www.ymc.co.jp/en/columns/ymc_carote	18
Figure 4 - A chromatogram of the separation of carotenes and xanthophylls with a legend on the right, and the y-axis for detector signal cut out for design purposes. The picture was reproduced with permission from YMC (https://www.ymc.co.jp/en/columns/ymc_carote	18
Figure 5 - A picture of the HPLC system that was used in the thesis, a Dionex Ultimate 3000 system located in Bergen, Norway.....	21
Figure 6 - The process of lyophilization of seaweed leaves	28
Figure 7 - The process of drying the raw sample material.....	28
Figure 8 - Set up of the Soxhlet extraction system	29
Figure 9 - Color of the solution at the end of the fifth cycle, and the extraction solution in relation to the remaining seaweed material.....	29
Figure 10 - A chromatogram of an unmodified YMC program with 20 μ l of an ethanol extract at 450 nm. The concentration of the extract was about 15 000 mg/l.	39
Figure 11 – A chromatogram of unmodified YMC program with 20 μ l of a 100 mg/l Fucoxanthin standard in ethanol at 450 nm.	39
Figure 12 - A chromatogram for the modified gradient program #1 with 20 μ l of an ethanol extract at 450 nm. The concentration of the extract was about 15 000 mg/l.....	40
Figure 13 - A chromatogram for the modified gradient program #2 with 20 μ l of an ethanol extract at 450 nm. The concentration of the extract was about 15 000 mg/l.....	42
Figure 14 - A chromatogram for the modified gradient program #1 with 20 μ l of a methanol extract at 450 nm. The concentration of the extract was about 45 000 mg/l.....	43
Figure 15 – A contour plot of a run with gradient program #1 with 20 μ l of a methanol extract recorded from 200 nm to 800 nm. The concentration of the extract was about 45 000 mg/l. .	43
Figure 16 - A chromatogram for the modified gradient program #3 with 20 μ l of a methanol extract at 450 nm. The concentration of the extract was about 45 000 mg/l.....	44
Figure 17 - Zoom of a chromatogram of modified YMC gradient program #4 with 20 μ l of a methanol extract at 450 nm. The concentration of the extract was about 45 000 mg/l.....	46
Figure 18 - A contour plot of modified YMC gradient program #4 with 20 μ l of a methanol extract at 450 nm. The concentration of the extract was about 45 000 mg/l.....	46
Figure 19 - Zoom of a chromatogram of modified YMC gradient program #4 with 20 μ l of a methanol extract at 450 nm. The concentration of the extract was about 45 000 mg/l, and the flow rate was 0.9 ml/min.....	47

Figure 20 - Zoom of a chromatogram of modified YMC gradient program #4 with 20 μ l of a methanol extract at 450 nm. The concentration of the extract was about 45 000 mg/l, and the flow rate was 0.7 ml/min.....	47
Figure 21 - Zoom of a chromatogram of modified YMC gradient program #4 with 20 μ l of a methanol extract at 450 nm. The concentration of the extract was about 45 000 mg/l, the flow rate was 0.9 ml/min, and the column temperature was set to 50 °C.	48
Figure 22 - Zoom of a chromatogram of modified YMC gradient program #5 with 20 μ l of a methanol extract at 450 nm. The concentration of the extract was about 45 000 mg/l, the flow rate was 1.0 ml/min, and the column temperature was set to 40 °C.	49
Figure 23 - Zoom of a chromatogram of modified YMC gradient program #5 with 20 μ l of a methanol extract at 450 nm. The concentration of the extract was about 45 000 mg/l, the flow rate was 1.0 ml/min, and the column temperature was set to 36 °C.	50
Figure 24 - Calibration curves used for the extracts in the optimization study. The calibration curve used for the ethanol extracts is on top, for the methanol extracts in the middle, and for the 2-propanol extracts on the bottom.....	55
Figure 25 - Plot of standardized concentration of extracted Fx for the different factors in the optimization study, with mean values (marked as x in the plot) and error bars (standard deviation).....	63
Figure 26 - A plot for main effects on standardized concentration of Fx in the extracts. Points 1, 3 and 5 had STSRs of 1:20, and points 2, 4 and 6 had STSRs of 1:30	64
Figure 27 - A plot of standardized concentration of Fx against the boiling temperature of the solvent type with a STSR of 1:20. Orange points are for methanol extracts, yellow points are for ethanol extracts, and blue points are for 2-propanol extracts	65
Figure 28 - A plot of standardized concentration of Fx against the boiling temperature of the solvent type with a STSR of 1:30. Orange points are for methanol extracts, yellow points are for ethanol extracts, and blue points are for 2-propanol extracts	66
Figure 29 - Sample preparation of the extracts from Op-1 to Op-6.....	69
Figure 30 - A chromatogram of a standard-extract-mixture at 231 nm on the left compared to extract number 12 (Op-13) on the right at 231 nm, the maximum absorption point of phloroglucinol	70
Figure 31 - A chromatogram of a standard-extract-mixture at 431 nm on the left compared to extract number 12 (Op-13) on the right at 431 nm, the maximum absorption point of chlorophyll a.....	71
Figure 32 - A chromatogram of a standard-extract-mixture at 448 nm on the left compared to extract number 12 (Op-13) on the right at 448 nm, the maximum absorption point of fucoxanthin.....	71
Figure 33 - A chromatogram of a standard-extract-mixture at 451 nm on the left compared to extract number 12 (Op-13) on the right at 451 nm, the maximum absorption point of β -carotene	71

Table list for the main report

Table 1 - The most abundant carotenoids in seaweeds and their molecular structure.	14
Table 2 - The molecular structure of the most used standard for polyphenols, phloroglucinol.	15
Table 3 - The most abundant chlorophylls in seaweeds and their molecular structure.....	16
Table 4 - A general example of a 23 full factorial design with coded values for the factor levels.....	25
Table 5 – CAS-number, purity and supplier of chemicals, additives, and standards used in the project.....	27
Table 6 - Measurements and means for a generalized one-way ANOVA (2: p. 54)	31
Table 7 - ANOVA-table with sums of squares and a resulting f-value	32
Table 8 - Gradient program of alternative #1 for the screening test.	35
Table 9 - Column type and settings for alternative #1 in the screening test.	35
Table 10 - Gradient program of alternative #2 for the screening test.	35
Table 11 - Column type and settings for alternative #2 for the screening test.....	36
Table 12 - Gradient program of alternative #3 for the screening test.	36
Table 13 - Column type and settings for alternative #3 for the screening test.....	37
Table 14 - Design of experiments for a screening test to evaluate HPLC determination methods	37
Table 15 - Column type and settings for alternative #4 from YMC	38
Table 16 - Modified YMC gradient program #1	40
Table 17 - Modified YMC gradient program #2.....	41
Table 18 - Modified YMC gradient program #3.....	44
Table 19 - Modified YMC gradient program #4.....	45
Table 20 - Modified YMC gradient program #5:.....	49
Table 21 - Gradient program for the determination method of Fx.....	50
Table 22 - Settings for the gradient program of the determination method for Fx determination	51
Table 23 - Concentration levels #1 for the calibration curves for Fx	52
Table 24 - Altered concentration levels #2 for the calibration curves for Fx	52
Table 25 - Data from the calibration curves for all the extracts.....	54
Table 26 - limit of detection and lower limit of quantification for all calibration curves used for the extracts.....	56
Table 27 - Precision data for peak area, RT, and peak width	56
Table 28 - Possible combinations in factorial design.....	57
Table 29 - DoE for a Soxhlet extraction optimization study.....	57
Table 30 - Weight and concentration of extracts in the optimization study.....	57
Table 31 - RT, peak area, peak width, and resolution for the runs in the optimization study .	59
Table 32 - Peak area, weight (DW), concentration of Fx extracted, and standardized concentration of Fx extracted in optimization study	61
Table 33 - Main effects of the solvent types sorted by STSR.....	64
Table 34 - The measurements from different extraction conditions in the optimization study, the means of these measurements, and an overall mean	67
Table 35 - ANOVA-table with sums of squares and a resulting F-value.....	68

Introduction

Background

Alginor is a marine biotechnology company in Haugesund that is developing methods for harvesting and biorefining products from *Laminaria hyperborea*, a brown macroalgae (kelp or seaweed) that grows in the North Atlantic Ocean (1). The company was founded in 2014 and has over 30 employees with production facilities in Skudeneshavn and Avaldnes. Alginor has a goal of establishing the first biorefinery for marine resources in Europe, and as a starting point it is focusing on achieving a total utilization of *Laminaria hyperborea* downstream that is sustainable. There are an estimated 60 million tonnes of standing biomass of the kelp along the coastline in Norway, and the harvesting of the kelp is regulated to ensure the sustainability of the process (1). By harvesting in different zones at periodic intervals the kelp is allowed to grow back, providing a sustainable raw material stream.



Figure 1 - A kelp forest of *Laminaria hyperborea* off the coast of Haugesund, Norway. The picture was reproduced with permission from Alginor (2).

Major companies in the biorefinery sector like Borregaard and the European Innovation Council Fund (EIC Fund) have invested approximately 300 million NOK in Alginor as a part in the upscaling efforts of the company. The investment of the EIC Fund was made as a part of the “Green Deal” initiative of the European Union (3).

In the pursuit of a total utilization of kelp materials a portfolio of twelve products have been developed for pharmaceutical and food applications (4). Traditionally the kelp industry has used preservatives like formaldehyde, which has been linked to certain types of cancer (5). The use of formaldehyde creates approximately 85% waste because of the need to wash out the formaldehyde with great amounts of water, rendering the extraction of all products except for alginates unviable. Alginor’s Ocean Refining Total utilizing Application (abbreviated as AORTA) is a technological solution developed by Alginor that creates no waste by avoiding formaldehyde in methods for harvesting, separating and biorefining. Two of these product

groups are carotenoids (6) and polyphenols (7). Additionally, chlorophylls were of interest in this thesis as a potential product group. These compounds can be extracted from the leaves of *Laminaria hyperborea*, and an illustration of the seaweed can be found in figure 2 below.

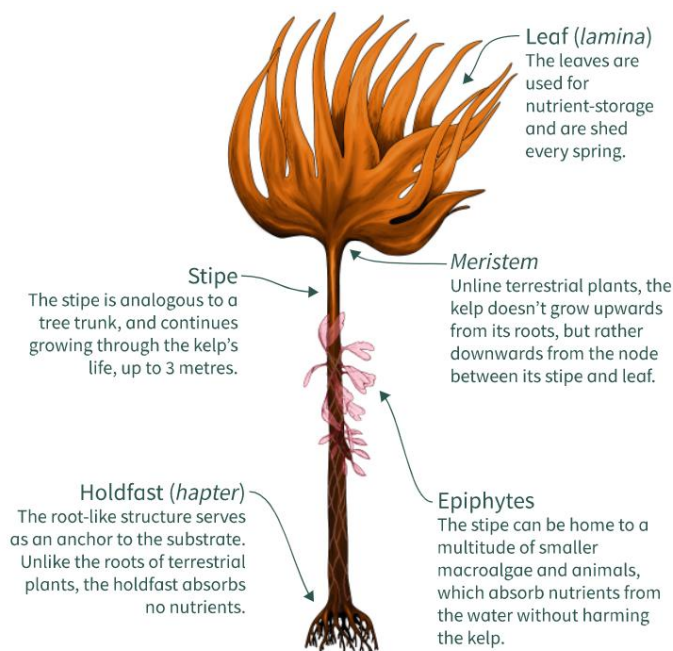


Figure 2 - An illustration and description of the different parts of a kelp plant. The picture was reproduced with permission from Alginor (8).

A description of the thesis problem and the reasons for the study

The green shift has brought forth a need for green extractions of lipophilic compounds commonly extracted with organic solvents like n-hexane, acetone, diethyl ether or chloroform (9) (p.3) (10) (p.2-3) (11) (p. 171) . An extraction of lipophilic compounds from *Laminaria hyperborea* with green solvents would open market segments in the food and pharmaceutical industry for products from this kelp (12). The most abundant bioactive compound in brown macroalgae is Fucoxanthin (abbreviated as Fx) (13) (p.495) (14) (p.326) , so this was the main analyte of the study. Solvents such as n-hexane, diethyl ether and chloroform are unsuitable for extracting products for the food and pharma industry because even trace amounts of the solvent can be hazardous to health (15) (p.5). Green solvents such as methanol, ethanol and 2-propanol were to be considered in this study because of their sustainability and because of their lower toxicity (15) (p.5-6). An optimization study of a green extraction conditions to increase the extraction yield of analytes such as Fx using a Soxhlet extraction system. Fx is a commodity as a food supplement because of its high antioxidant behavior (16) (p. 2-3) (13) (p. 495). Studies report that Fx and other carotenoids have beneficial effects against obesity, macular degeneration, and cancerous activity (17) (p. 109) (18) (p.98) (19) (p. 95) (20) (p.2560) (21) (p. 1). A secondary analyte in the study was polyphenols separated as a crude mix given its potential value as a food supplement, and its relatively high occurrence in brown macroalgae (13) (p. 495) (22) (p. 1119). Chlorophylls were also of interest in this study, although with a lower priority because of a low occurrence in brown macroalgae compared to

compounds like Fx (23) (p.15). The development of a determination method for Fucoxanthin was the first and foremost goal of the thesis, since the optimization study would depend entirely on a reliable determination method. The determination method of choice was a reverse phase high performance liquid chromatographic (abbreviated as RP-HPLC) method coupled to a diode array detector (abbreviated as DAD) so that it could be used as a separation method with preparative column chromatography as well. The determination of polyphenols and chlorophylls were a secondary goal, either isolated or as a crude mix.

Purpose of the project

The purpose of the study was to develop a determination method for Fx and other bioactive molecules from *Laminaria hyperborea* using RP-HPLC-DAD. The determination method would then be used to optimize extraction conditions for Fx using a Soxhlet-system. The extraction method of Fx with a Soxhlet system and the determination method used as a separation method would then be used by Algisor in two process steps to produce Fx commercially

Research questions

1. Which gradient system of mobile phases and columns provides the best resolution of a reverse phase HPLC determination of Fx using green solvents suitable for food and pharma products?
2. Is there a baseline separation of polyphenols and chlorophylls as well?
3. Does ethanol, methanol or 2-propanol extract the highest yield of Fx from *Laminaria hyperborea* using a Soxhlet system?
4. Does a sample to solvent ratio of 1:20 or 1:30 of solvents extract the highest yield of Fx from *Laminaria hyperborea* using a Soxhlet system?

Objectives of the project

1. Developing a determination method for the quantification of Fx using RP- HPLC-DAD with baseline separation. The columns used should be of a preparative column type to enable the use of the method as a separation method as well.
2. Finding out if ethanol, methanol, and 2-propanol gives the highest yields of Fx in a Soxhlet extraction system, with a proven significance using a one-way analysis of variance (abbreviated ANOVA)
3. Achieving a baseline separation for polyphenols and chlorophylls, the former of which is prioritized over the latter
4. Getting chromatographic data on other analytes from *Laminaria hyperborea* for future reference

Research method and strategy

The objectives of the thesis were to be solved by comparing extracts using the chromatograms from RP-HPLC-DAD determination method to determine the concentration of Fx in extracts from a Soxhlet extraction system with ethanol, methanol, and 2-propanol. The extracts would either have sample to solvent ratios (abbreviated as STSR) of 1:20 and 1:30 to determine the best ratios for an extraction of Fx.

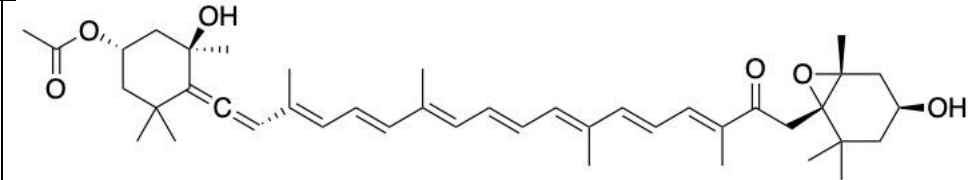
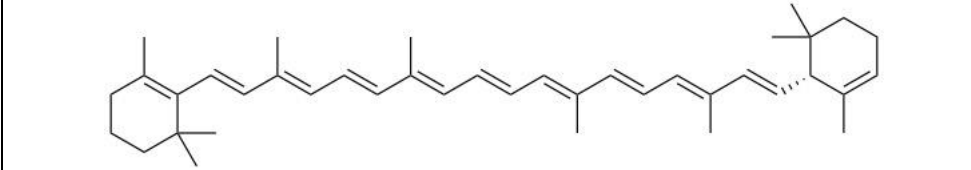
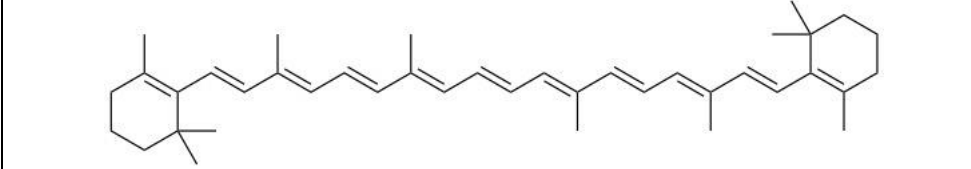
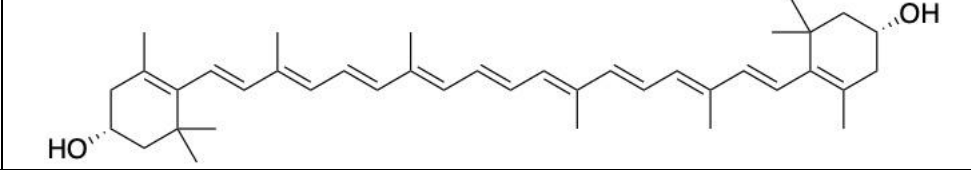
Theory

Bioactive compounds

Carotenoids

Carotenoids are pigments that are found naturally in plants, both terrestrial and aquatic, and most are yellow, brown, orange, or red in color (6). Over 600 carotenoids have been isolated from natural sources (18) (p.97). Structurally carotenoids are classified as tetraterpenes and derive from isoprenoid lycopene, a type of long acyclic chain (24) (p. 298-299). Tetraterpenes consists of eight isoprene units, a unit that consists of five carbon atoms, so the name tetraterpene means that it is a chain with forty carbon atoms. The molecular structure of the most abundant carotenoids found in seaweeds is shown in table 1 below (13) (p. 495-496) (14) (p. 325-326) (24) (p. 301).

Table 1 - The most abundant carotenoids in seaweeds and their molecular structure.

Name of the compound	Molecular structure
Fucoxanthin (abbreviated as Fx)	
α -carotene	
β -carotene (abbreviated as β -car)	
Zeaxanthin	

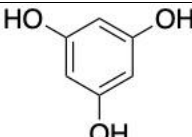
Carotenoids are divided into carotenes and xanthophylls, the latter of which is a collective term for carotenoids that have an oxygenated fraction. Carotene chains only contain carbon and hydrogen making them unsaturated and non-polar, which gives these carotenoids more lipophilic character than xanthophylls (14) (p. 325-326). All these pigments occur naturally in a trans configuration but can be induced into a cis configuration through thermal isomerization. The most abundant pigment in brown seaweed is Fx, which masks the green color from chlorophyll pigments with an orange color resulting in a brown color overall (13) (p. 495). Carotenoid pigments protect plant material from photooxidation by scavenging singlet oxygen and peroxy radicals (14) (p. 325-326) (6). Zeaxanthin is a derivative from β -car through a photoprotective hydroxylation and epoxidation reaction.

Research has shown beneficial effects as fat-soluble antioxidants for the protection against a whole range of diseases, including cancer, cardiovascular diseases, and macular degeneration. α -carotene and β -car are turned into vitamin A in the body (14) (p. 325-326) (13) (p. 495).

Polyphenols

Polyphenols are one of the largest plant groups with over 8000 polyphenol compounds, with a 150 of them isolated from seaweeds alone (7). The major phenolic compound group found in macroalgae is phlorotannin, a group of polymers and oligomers of phloroglucinol (1,3,5-trihydroxybenzene) (13) (p.495) (25) (p. 104). The structure of phloroglucinol (abbreviated Phl), the most used standard for polyphenols (26) (p. 325) (27) (p. 326), can be seen in table 2 below.

Table 2 - The molecular structure of the most used standard for polyphenols, phloroglucinol.

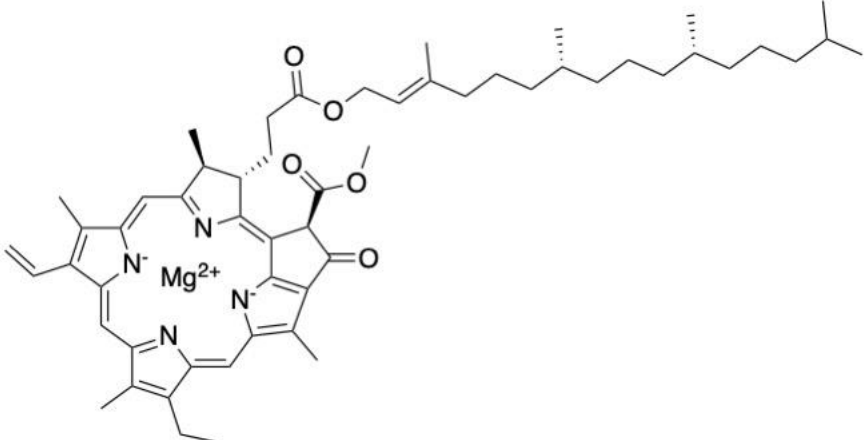
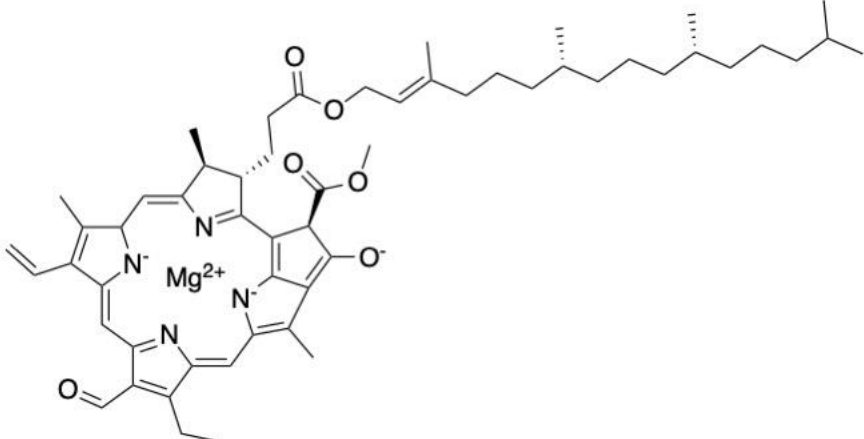
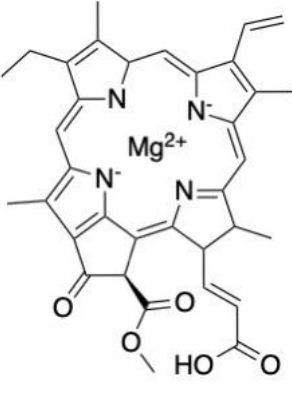
Name of the compound	Molecular structure
Phloroglucinol, 1,3,5-trihydroxybenzene	

Phlorotannins is a large subgroup of polyphenols because of the high number of possible chemical linkages between aromatic groups (p. 2, review phlorotannin compounds in brown seaweeds). The main linkages are through aryl-aryl (C-C) bonds and aryl-ether (C-O) bonds. These compounds are very hydrophilic and polar because of the many groups of hydroxy (O-H) in the molecular structure (28) (p. 327).

Chlorophylls

Most macroalgae is green in color because of a pigment called chlorophyll a (abbreviated chl a), but the color in brown macroalgae is masked by carotenoids (14) (p.325). Chlorophylls are cyclic tetrapyrroles that are crucial for the photosynthesis in plants and the main pigments in higher plants in general are chl a and chl b. Brown macroalgae can have substantial amounts of chl c as well, and some amounts of pheophytin a (14) (p.325). The molecular structure of the most abundant chlorophylls found in brown macroalgae can be found in table 3 below (13) (p.495).

Table 3 - The most abundant chlorophylls in seaweeds and their molecular structure.

Name of the compound	Molecular structure
Chlorophyll a	 <p>The structure of Chlorophyll a features a central magnesium atom (Mg²⁺) coordinated by four nitrogen atoms in a porphyrin-like ring. The ring is substituted with a vinyl group, a methyl group, and an ethyl group. A long phytyl side chain is attached to the ring via an ester linkage. The side chain contains two double bonds and is terminated with a methyl group. A methyl ester group is also present on the ring.</p>
Chlorophyll b	 <p>The structure of Chlorophyll b is similar to Chlorophyll a, with a central magnesium atom coordinated by four nitrogen atoms. It has a vinyl group, a methyl group, and an ethyl group on the ring. The side chain is a long phytyl chain with two double bonds and a methyl group at the end. A methyl ester group and a formyl group (-CHO) are also present on the ring.</p>
Chlorophyll c	 <p>The structure of Chlorophyll c has a central magnesium atom coordinated by four nitrogen atoms. The ring is substituted with a vinyl group, a methyl group, and an ethyl group. The side chain is a long phytyl chain with two double bonds and a methyl group at the end. A methyl ester group and a hydroxyl group (-OH) are also present on the ring.</p>

Liquid-solid extraction

An extraction is a separation method that separates an analyte from other compounds in a sample (29) (p. 387), and a liquid-solid extraction (abbreviated LSE) utilizes different phases involved to separate the compounds (29) (p. 402). The compounds in the solid phase are separated because of a differential in solubility in the solvent. An extraction method using a Soxhlet system is a classic LSE technique that is classified as an exhaustive extraction technique with batch equilibrium and preequilibrium (29) (p. 390). The contact between the solid and liquid phase is broken between equilibrium stages in stages. Advantages with a Soxhlet system is that it is possible to maintain a fresh solvent contact throughout the extraction, and it is not necessary with filtration of the extract afterwards (30) (p. 1408).

A solid sample contained in a paper thimble is washed continually by boiling solvent in an apparatus called a Soxhlet extractor (29) (p. 402). The solvent is heated in a sample flask causing it to boil, and a condenser placed above the Soxhlet extractor condenses the solvent gas (29) (p. 399). The condensed solvent washes over the solid sample extracting the analyte from the solid material and the analytes is transferred to the sample flask in stages (29) (p. 399 – 400). LSE that utilizes a high pressure below the supercritical point of the solvent is called a pressurized fluid extraction (PFE), which is a common way to assist a Soxhlet extraction (29) (p. 402).

Chromatography

Chromatography is a separation method, and a separation is defined as the process of isolating analytes from a mixture of compounds (29) (p. 39). When a mobile phase flows over a stationary phase a differential in the affinity to absorb or adsorb to the stationary phase separates the compounds from each other (29) (p. 39-40). Adsorption is the process of attraction to a surface and absorption, also called partition, is the process of diffusion into a surface (29) (p. 44-45).

Liquid chromatography

In liquid chromatography (abbreviated as LC) the mobile phase that flows over the stationary phase is a liquid, and the sample is added to the mobile phase in elution chromatography (29) (p.41-43). The stationary phase is contained in a column, and elution is defined as the process of passing a mobile phase with a sample through a stationary phase continually. The stationary phase in a column can be liquid or solid (29) (p. 41), although the liquid stationary phases have mostly been replaced by bonded phases that are chemically bonded to a solid support (29) (p. 185). Columns are either packed with particles of stationary phase or open with a coat of liquid stationary phase on the walls inside of the column (31) (p. 610). As an example, the difference of affinity between β -carotene and two different stationary phases, C18 and C30, can be seen in figure 3 below.

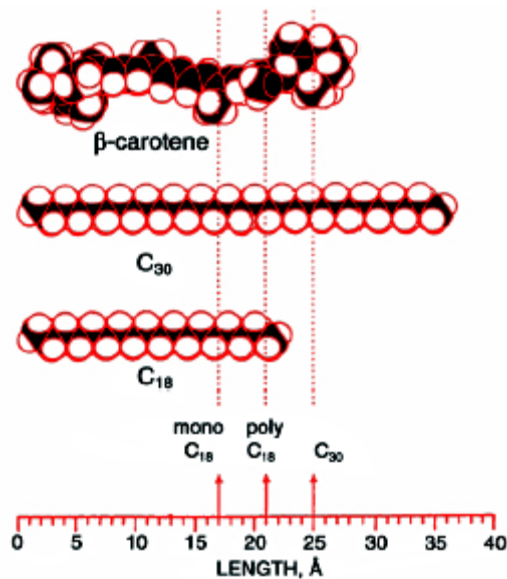


Figure 3 - A comparison of the molecular length of β -carotene with the film thickness of C18 and C30 column material, determined with small angle neutron scattering. The picture was reproduced with permission from YMC (32)

The time when an analyte elutes out of the column is called the retention time of that analyte (29) (p. 43). A common way to record data from the chromatographic process is by recording the eluting compounds as peaks in a plot of detector signal versus time, and such a plot is called a chromatogram (29) (p. 45-46). The retention time for an analyte can be measured as distance along the x-axis on a chromatogram from the start to the maximum of the peak (29) (p. 47). As an example of a chromatogram the separation of carotenes and xanthophylls can be seen in figure 4 below.

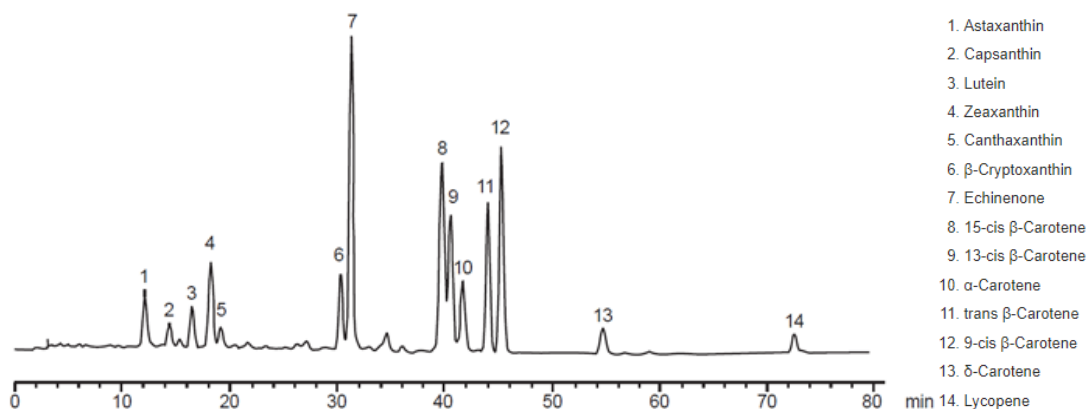


Figure 4 - A chromatogram of the separation of carotenes and xanthophylls with a legend on the right, and the y-axis for detector signal cut out for design purposes. The picture was reproduced with permission from YMC (32)

The retention time depends on how long the analyte was retained by its affinity to the stationary phase, which makes it a characteristic feature. This means that the retention time can be used for identification of an analyte (31) (p. 625). A retention time adjusted for the retention time of the mobile phase is defined by formula 1 below (31) (p. 612).

$$t_r^l = t_r - t_m \quad (1)$$

The subscript of r denotes the analyte and m denotes the mobile phase, and the apostrophe denotes that the retention time is adjusted. Other important parameters for retention time are

the retention factor and relative retention (31) (p. 612), defined in formula 2 and 3, respectively.

$$k = \frac{t_r - t_m}{t_m} \quad (2)$$

The retention factor (k) is always a positive number (31) (p. 613). The numerator in the expression is equal to the time that the compound spends in the column and the denominator is equal to the time the mobile phase spends in the column. If the compound is not retained by the stationary phase at all the retention time of the compound is equal to the retention time of the mobile phase, making the expression equal to zero (31) (p. 613). Referring to figure # a baseline can be thought of as the horizontal line in a chromatogram where there are no peaks, and the retention time of the mobile phase can usually be found by a shift in the baseline before all other peaks in the chromatogram (p. 48).

$$\alpha = \frac{t'_{r2}}{t'_{r1}} = \frac{k_2}{k_1} \quad (3)$$

Relative retention is used to compare two compounds in a chromatogram and is independent on the flow rate. This enables identification if the flow rate is not comparable for the two compounds (31) (p. 612).

An assumption that the compounds do not interact with each other is made in these formulas. This is justified by the relatively low concentration of compounds in the separation system, and the fact that the separation of the compounds increases throughout the column (29) (p. 49).

The efficiency of a separation of two compounds relies on two factors: The difference in retention time between the peaks and the peak widths of the compounds (31) (p. 615) If the peaks are close in retention time and have wide peaks the resolution is poor. An expression for resolution can be found below as formula 4 below (31) (p. 615).

$$Resolution = \frac{\Delta t_r}{w_{av}} = \frac{\Delta V_r}{w_{av}} = \frac{0.589 \Delta t_r}{w_{1/2av}} \quad (4)$$

The numerator in formula 4 is the separation between two peaks in time (t_r) or volume units (V_r), and the denominator is the average width of the two peaks (w_{av}) (31) (p. 615). The width is measured at the base of the peak, or as the half-height of a *Gaussian* peak ($w_{1/2av}$) if the last expression is used. A *Gaussian* peak is an idealized peak without asymmetries and is a theoretical shape that can be approximately realized if there are no unfavorable interactions with the compound (31) (p. 615-616) (29) (p. 51).

Unfavorable interactions and asymmetry in peaks

An ideal peak shape is sharp and narrow like a gaussian peak, but the longer compounds are retained in the column the longer the peak width get (31) (p. 616). A main reason for this peak broadening is diffusion, which is the random rate of molecules moving from a region with high concentration to a region with low concentration (31) (p. 616 – 617). This movement follows a *Gaussian* distribution called *brownian motion* (31) (p. 616), and the flux of diffusion is proportional to a concentration gradient and diffusion constant (31) (p. 617). The diffusion will approximately broaden a peak two-fold if the retention time of a compound is increased with a factor of four-fold (31) (p. 618). A parameter measuring the efficiency of the

column is plate height (31) (p. 618). Plate height is defined as the proportionality constant between the distance travelled across the length of a column and the variance of *Gaussian* peak width, expressed in formula 5 below.

$$\text{Plate height, } H = \frac{\sigma^2}{x} \quad (5)$$

Plate height (H) is also known as *height equivalent to a theoretical plate* and can be approximated as the column length required for an equilibration for the compound between the mobile and stationary phases (31) (p. 618 – 619). A low number of plate heights are associated with efficient columns. Another parameter of column efficiency is the number of plates, expressed with units of length in formula 6 below.

$$\text{Number of plates, } N = \frac{L}{H} = \frac{16L^2}{w^2} \quad (6)$$

Considering that L is the entire column length, and the number of plates (N) should be maximized for a better separation, it follows that the column length should be maximized to increase separation (31) (p. 619). However, increasing the column length increases the separation time, which increases the peak width (31) (p. 620). The number of plates (N) is expressed in units of time in formula 7 below.

$$\text{Number of plates, } N = \frac{16t_r^2}{w^2} = \frac{5.55t_r^2}{w_{1/2}^2} \quad (7)$$

There are competing factors in maximizing the number of plates (N) while keeping the separation time as low as possible, and the relationship between the factors are expressed in the *van Deemter equation* given in formula 8 below.

$$\text{Plate height, } H \approx A + \frac{B}{u_x} + Cu_x \quad (8)$$

The constants A , B and C are specified by the column used, and u_x is the linear velocity along the length of the column. A accounts for the fact that components can take multiple paths through the column, B accounts for diffusion along the path and C accounts for the time required for the equilibration between the mobile and stationary phase (31) (p. 622). The term with the constant C is also called the *mass transfer* term (31) (p. 623). A plot derived from this equation can be used to find an optimal flow rate while keeping the number of plates as high as possible.

The retention time of a *Gaussian* peak is independent of the concentration of the analyte and can be used for identification with minimal uncertainty (31) (p. 625). In practice real peaks are skewed depending on the variation of analyte concentration in the column. An *overloading* of the column with analyte causes either *fronting* or *tailing* peaks. In *fronting* peaks there is a slow and gradual increase in peak height coupled with an abrupt fall, leading to an increase in the actual retention time of the compound. In *tailing* peaks there is an abrupt increase in peak height coupled with a slow and gradual decrease, leading to a decrease in the actual retention time of the compound. Another possible cause of tailing is sites on the column walls that react strongly with the analyte, but this effect is reduced by column manufacturers by *end capping*, which blocks the silanol groups from reacting with the analyte (31) (p. 625).

High performance liquid chromatography

To achieve a satisfactory separation of complex samples fine particles packed in closed columns are often necessary, which promotes the need for high pressure in the system to achieve the separation whilst keeping an optimal flow rate through the column (31) (p. 668). Typical particle sizes for column used in HPLC are 1.7 – 5 μm . The plate number increases with a decrease in particle size, resulting in an increase of the peak sharpness. This effect is explained by an increase in the uniform flow and a decrease in the diffusion distance, with reference to *van Deemter* curves (31) (p. 622 – 624 + p. 669). Such a system is called a high-performance liquid chromatography system (abbreviated as an HPLC system). The HPLC system used for this thesis can be found in figure 5 below as an example.



Figure 5 - A picture of the HPLC system that was used in the thesis, a Dionex Ultimate 3000 system located in Bergen, Norway.

With reference to figure 5 the components in a HPLC system are solvent reservoirs for the mobile phase on top, with a gradient pump below, an autosampler with a sample injection valve, a column housed in an oven with temperature control, and a detector at the bottom. The components are connected to a computer with HPLC software. HPLC systems operate with pressures in the range of 7-40 MPa (31) (p. 668), and a common detector system uses ultraviolet light with a photodiode array (abbreviated as PDA) that can record the spectrum of the analyte (31) (p. 686-687). The spectrum of the analyte can then be compared to spectra for identification.

Columns are susceptible to impurities because of the tight packing of the stationary phase so it is crucial to not introduce these through samples or solvents (31) (p. 671, instr). Samples should be filtered through a $\geq 0.5 \mu\text{m}$ filter before injection, and solvent should be of HPLC grade. A higher column temperature leads to a shorter separation time and a higher peak sharpness, but temperatures above 60 $^{\circ}\text{C}$ are not recommended for most columns to avoid degradation of column lifetime (31) (p. 671). The most used stationary material in liquid-liquid absorption chromatography is bonded covalently to a silica surface, and the most common bonded stationary phase is *octadecyl* (abbreviated as ODS) with 18 carbon atoms bonded to the silica support (31) (p. 672). A limitation of this kind of setup is that the pH can

not exceed the range of pH 2-8 to avoid a hydrolyzing reaction with the column material (31) (p. 673).

Reversed-phase chromatography and gradient elution

The most used mode of HPLC is the reversed-phased (abbreviated as RP) chromatography, where the mobile phase is more polar than the stationary phase (31) (p. 675). A less polar solvent in the mobile phase elutes the analytes faster, and the polarity of a solvent is dependent on its dipole moment and its ability to accept or donate a hydrogen. A normal-phase chromatography is the reverse with a more polar stationary phase than the mobile phase. The term mobile phase strength is used to describe the polarity of a mobile phase, which determines the ability of the mobile phase to elute compounds from a column (31) (p. 676). In RP HPLC a non-polar mobile phase elutes compounds quicker.

An isocratic elution is a linear elution performed with one solvent in the mobile phase, whilst a gradient elution is performed with multiple solvents and can regulate the mobile phase strength continuously (31) (p. 666-667).

Determination method development

To find a suitable HPLC mode for a determination method a good starting point is to look at the molecular mass of the analyte and the solubility of the analyte in water (31) (p. 684). From there the next step would be to find a suitable solvent based on differentiating characteristics of the analyte molecule, namely the polarity of the analyte. Different chromatographic modes are for example reversed phase mode or normal phase mode.

A gradient separation is likely needed to separate analytes in complex molecules, but an isocratic elution should be checked first. An isocratic elution has a constant mobile phase composition, whilst a gradient elution is continuously changing the composition. A good starting point is to run a broad scouting gradient (31) (p. 699). An example of this is a 10-90% linear gradient of acetonitrile and buffer over 40 minutes (31) (p. 699-700). If all the peaks are eluted over a narrow solvent range isocratic elution is an option, if not, gradient elution is preferable. The point of a gradient elution is to avoid a long and inefficient elution with chromatograms free of any compounds in some regions.

The next step is to improve the separation by reducing the flow rate or introducing a segmented gradient in stead of a linear gradient (31) (p. 700). By using a segmented gradient, the regulation of mobile phase strength can close inefficient segments of the chromatogram while keeping the peaks separated. Other possibilities to increase the separation with a higher difficulty is to change the stationary phase, particle size, mobile phase or to increase the length of the column. In HPLC small changes in mobile phase composition leads to relatively large changes in the retention factor for two analytes being separated (29) (p. 114). An equilibration of the column and mobile phase is required between runs, and for reversed-phase separations 10-20 column volumes should be passed through before an injection of the next run (31) (p. 701).

Method validation

Method validation is a process of proving that a method is suitable for its intended use (31) (p. 100). Parameters that measure aspects of this can be found with formulas throughout this chapter.

Selectivity

The ability of the method to differentiate analyte from interferences for quantification purposes (31) (p.100-101). Interferences might include impurities, derivatives from analytes and the matrix in general. A matrix refers to everything that is not the analyte in a sample (31) (p. 98). A baseline separation between analytes is required for a sufficient selectivity, meaning that the detector signal reaches the baseline before the next analyte reaches the detector (31) (p. 101). This can be verified by a resolution above 1.5 (31) (p. 616), and the resolution can be calculated with formula 4.

Linearity

The ability of the method to produce peak area and height proportional to the concentration of the analyte in a specified range (31) (p. 101, instr.). If the target concentration is known, a common range for an assay is between 50% and 150% of that target concentration (31) (p. 101, instr.). A measure of linearity is the square of the linearity coefficient, R^2 , of a calibration curve, which should be above 0.995. A calibration curve is created as a regression line by the least squares method and the linearity coefficient is a measure between zero and one that describes the global fit of the data points to the regression line (31) (p. 101). The calibration plot has concentration as the x-axis and the response in signal as the y-axis. Another measure of linearity is how close the y-intercept of the calibration curve is to zero if the signal is corrected by subtracting the blank response, which should then be below 2% of zero (31) (p. 101). The sensitivity of the method can be measured by looking at the slope of the calibration curve, which is a measure of change in the response signal corresponding to a change in the concentration (31) (p. 97).

Accuracy

Accuracy is a measure of trueness to the actual value (31) (p. 101). This can be evaluated by measuring a known quantity from certified reference material, comparing the methods measurement with the measurement from a different method, or by measuring the response from spiked blank samples (31) (p. 101-102). A blank sample contains the matrix of the sample without the analyte (31) (p. 97) and is required to measure spike recovery, which should be $100\pm 2\%$ (31) (p. 102). Spike recovery is measured from three levels spanning 50-150% of the target concentration with three replicates. If the blanks cannot be replicated the accuracy is measured by measuring the response from additions of a standard with a known concentration to the unknown sample (31) (p. 101).

Precision

Precision is a measure of the agreement between repeated measurements, usually expressed as standard deviation or uncertainty (31) (p. 102). One aspect of precision is repeatability, which evaluates the precision of the method over a small amount of time measured by the same person at the same concentration. Repeatability should not be above 2% RSD and can be measured with six repeated measurements of a target concentration of 100%. Another aspect is intermediate precision, which measures precision of the measurements when they're done by different people, on different days and with different instruments. Last, there is reproducibility, which compares precision between different laboratories (31) (p. 102).

Limit of detection and quantification

A limit of detection (abbreviated LOD) is the lowest concentration of analyte that can be detected with a stated level of confidence, usually set to 95% confidence (29) (p. 135). An assumption is made that each point of the regression line has a normal distributed variance

(29) (p. 136). A reasonable estimation of the LOD can be made from formula (9) below with the stated assumption (31) (p. 103) (29) (p. 135-136).

$$\text{Minimal detectable concentration, } c_{dl} = \frac{3s_y}{m} \quad (9)$$

Where s_y is the standard deviation of the regression line and m is the slope of the regression line. A limit of quantification (abbreviated LOQ) can be estimated by formula (10) below (31) (p. 105) (29) (p.135-136).

$$\text{Minimal detectable concentration, } c_{ql} = \frac{10s_y}{m} \quad (10)$$

Where s_y is the standard deviation of the regression line and m is the slope of the regression line.

Robustness

The ability of a method to give constant measurements regardless of small, deliberate changes in operating parameters such as solvent composition, temperature, pH et cetera (31) (p. 105). Requirements for products are variations under 2%.

Experimental design

Source 1: “Statistics and Chemometrics for Analytical Chemistry”

Source 2: https://bibsys-almaprimo.hosted.exlibrisgroup.com/primo-explore/fulldisplay?docid=BIBSYS_ILS71540186410002201&context=L&vid=HIB&lang=en_NO&search_scope=default_scope&adaptor=Local%20Search%20Engine&isFrbr=true&tab=default_tab&query=any,contains,chemometrics:%20statistics%20and%20computer%20application%20in%20analytical%20chemistry&offset=0

Planning a design of experiments (DoE) ahead of running experiments can avoid systematic errors and minimize random errors (29) (p. 11). Systematic error, often called bias, refers to errors that cause all the measurements to differ from the true value in the same direction (29) (p. 3). Random error cause error in parallel measurements and will always be a factor (29) (p. 11). A factor can be defined as an identifiable aspect of the conditions in an experiment that causes significant change in the results of the experiments. Often the features of a method will depend on multiple experimental factors so there should be an initial screening design to find to the most important factors. Then the possible combinations of the significant factors can be run to find the optimal setting for feature being optimized.

The factors that can be varied during the experiment are called controlled variables, and the different values of the factor in the experiment are called levels (29) (p. 199). Factorial experiments are done by varying the factors at a fixed number of levels and can detect factor interactions (33) (p. 105). Most factors are not independent of each other and are affected by interaction with other factors (29) (p. 206).

A common method to study experimental factors is the “one factor at a time” approach (abbreviated OFAT), where only one factor is changed for each experiment and the rest are kept the same to identify the effect of the factor being changed (29) (p. 12). The general principle of studying the effect of a selected set of factors whilst keeping all other factors as

constant as possible is known as the *ceteris paribus principle*, which is a fundamental principle in experimental design (33) (p. 102-103). The drawback of using the OFAT-principle instead of a factorial design is that any interaction effect would not be discovered (Source). This could then lead to a misconception that the altered factor was the reason for an effect in the response variable when it was an interaction effect.

Experimental design can be summed up to the following stages (29) (p. 199):

- 1. Identifying significant factors in an experiment
- 2. Minimizing the effects of uncontrolled factors in the experiment by design
- 3. Using statistical analysis to interpret the effects of the different factors

By controlling the significant factors that affect the results of the experiments the error should only be random, but uncontrolled factors like temperature may affect the results in a systematic way. To avoid misconstruing any trends in the results as an effect of any of the controlled factors the DoE should be randomized (29) (p. 200-201). The technique of randomization involves picking the order of the experiments at random, but if the random order happens to produce a systematic order in any natural subdivisions it should be modified. This is especially relevant if the measurements must be divided across several days, and a consideration should be made to ensure that at least one of the combinations of the significant factors are run on each of the days, with randomization within the day (29) (p. 201). This is called a randomized block design. Another consideration is that factorial experiment designs should be symmetric to avoid confounding factor effects (33) (p. 105-106).

An example of a 2^3 full factorial design can be seen in table 4 below (33) (p. 106). 2^3 describes a full factorial design with two levels and three factors.

Table 4 - A general example of a 2^3 full factorial design with coded values for the factor levels.

Experiment	Factors			Response
	X ₁	X ₂	X ₃	
1	-1	-1	-1	Y ₁
2	+1	-1	-1	Y ₂
3	+1	+1	-1	Y ₃
4	-1	+1	-1	Y ₄
5	-1	-1	+1	Y ₅
6	+1	-1	+1	Y ₆
7	+1	+1	+1	Y ₇
8	-1	+1	+1	Y ₈

Using coded values for the factor levels means scaling the factors so that the factors can be compared quantitatively (33) (p. 106). The coding scheme for continuous variables with two levels are +1 for the higher level and -1 for the lower level. If the variable is categorical this coding scheme cannot be used since there is no natural higher or lower level, and coding scheme such as dummy coding will need to be used for regression and other quantitative analysis (34).

The main effect of a factor is calculated as the absolute difference, $|D|$, in the response variable between the higher and lower levels. As an example, formula 11 shows the calculation of the main effect of variable X₁ (33) (p. 111) from table 4.

$$|D_{X_1}| = \frac{Y_2 + Y_4 + Y_6 + Y_8}{4} - \frac{Y_1 + Y_3 + Y_5 + Y_7}{4} \quad (11)$$

A plot for main factor effects and the response variable can be used to find interaction effects between the factors (33) (p. 113-114). If there are no factor interactions the main effects will produce parallel lines in the plot, whilst any deviation indicates interaction effects between the factors.

Materials and Methods

Chemicals, standards, and additives

Table 5 – CAS-number, purity and supplier of chemicals, additives, and standards used in the project

Name	Grade	CAS	Purity [%]	Supplier
Methanol	HPLC	67-56-1	> 99.9	VWR
Ethanol	Analysis	64-17-5	99.9	Antibac
2-propanol	Analysis	67-63-0	> 99.7	VWR
Ethyl acetate	HPLC	141-78-6	> 99.8	Supelco
Tert-Butyl methyl ether	HPLC	1634-04-4	> 99.9	VWR
Acetic acid	HPLC-additive	64-19-7	99.9	Merck
Triethylamine (TEA)	HPLC-additive	121-44-8	99.9	Merck
Phloroglucinol	HPLC-standard	108-73-6	> 99.0	Sigma-Aldrich
B-carotene	HPLC-standard	7235-40-7	> 95.0	Sigma-Aldrich
Chlorophyll a	HPLC-standard	479-61-8	> 95.0	Supelco
Fucoxanthin	HPLC-standard	3351-86-8	> 95.0	Supelco

Instrumentation and equipment

- RP-HPLC-UV-Vis
 - Instrument: Ultimate 3000 / Dionex
 - Quaternary gradient pump
 - Autosampler loop of 50 μ l
 - Columns:
 - YMC-Pack ODS-AQ (250 mm x 4.6 mm I.D., 5 μ m particle size)
 - Referred to as C18
 - YMC Carotenoid (250 mm x 4.6 mm I.D., 5 μ m particle size)
 - Referred to as C30
 - Detector: Diode Array Detector (DAD)
 - 5 ml Braun Omnifix syringes (with Luer lock solo technology) coupled to Chromafil PET-45/25 (PET – polyethylene terephthalate) 0.45 μ m syringe filters
 - HPLC vials: VWR 5 ml short thread vials with 9 mm PP (PP – polypropylene) short thread caps (Ultraclean closure technology, silicone (white), PTFE (red) (PTFE – polytetrafluoroethylene), 55 degrees shore A, 1.0 mm, screw cap ND9)
- Analytical balance weight
 - Instrument: XS204 / Mettler Toledo
- Software
 - Chromeleon 7
 - Excel version 2204, Microsoft 365

Raw material preparation and storage



Figure 6 - The process of lyophilization of seaweed leaves

Seaweed leaves from *Laminaria hyperborea* were collected from the Rogaland Field ID: 54D off the western coast of Norway on the 4th of November 2021. The leaves were sliced up, lyophilized, and stored in ethanol in the dark at -20 °C to avoid oxidation and isomerization. By storing the seaweed leaves in an organic solvent, a positive pressure from within the container will stop any oxygen from reacting with the raw material. Preparation of the raw material was done by Alginor, and the batch used throughout the project was OEWA-00578 (HY210041/SW21002).

Sample preparation for extraction

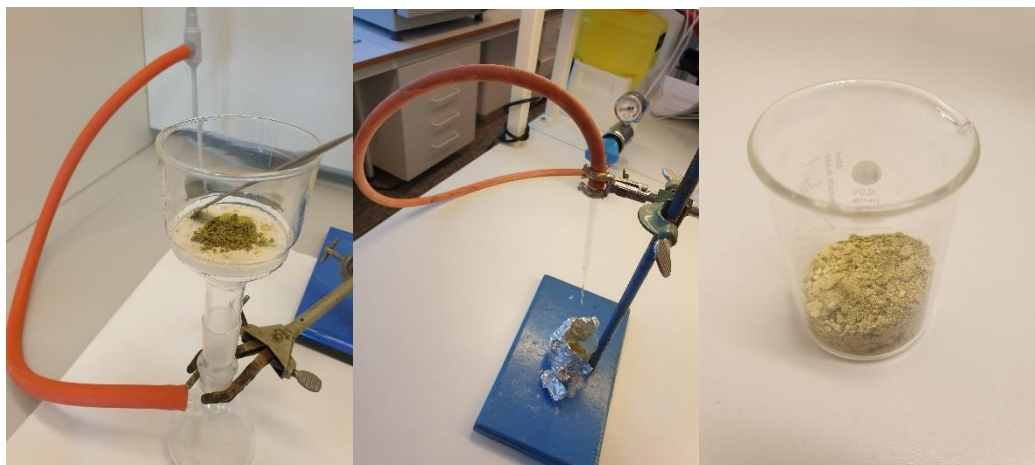


Figure 7 - The process of drying the raw sample material

The stored seaweed leaves were dried using a sinter nutch and with a continuous flow of nitrogen gas until the ethanol was evaporated. The flow of nitrogen gas created an inert atmosphere and increased the rate of evaporation by convection with the nitrogen gas. When the weight of the sample was constant either 6,67 grams or 10 grams of the dried leaves were transferred to a thimble for an extraction.

Extraction with a Soxhlet system

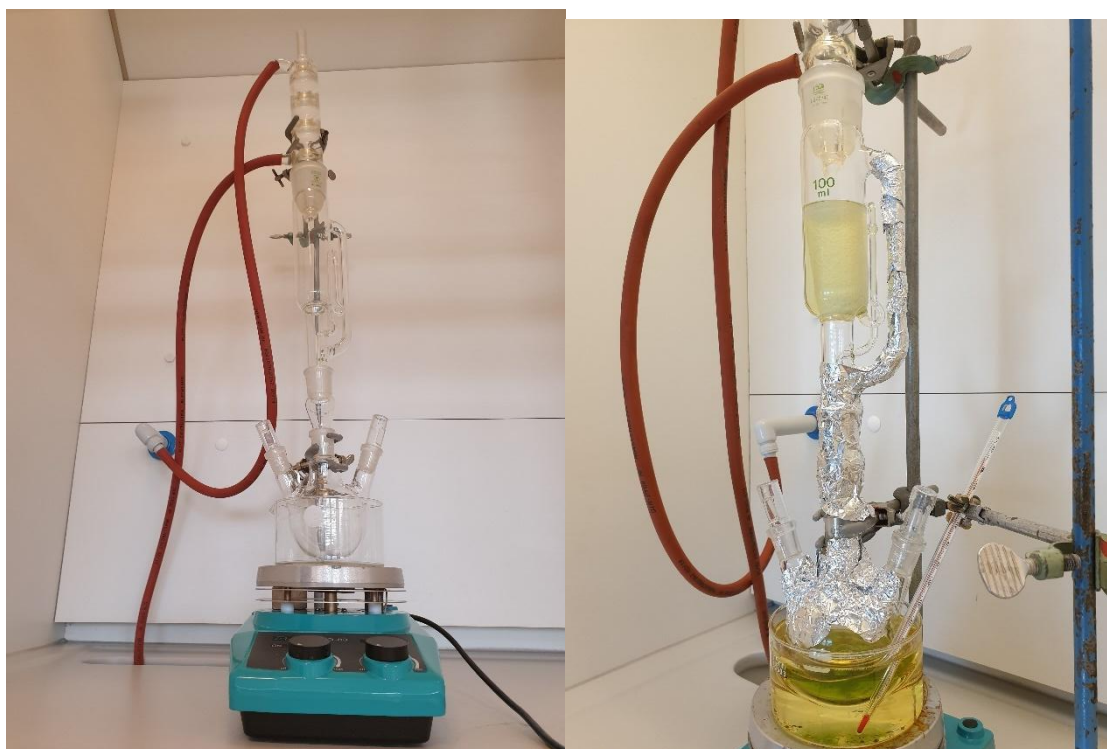


Figure 8 - Set up of the Soxhlet extraction system

The setup consisted of an oil bath of rapeseed oil placed on top of a heating plate with a magnetic stirrer at the bottom, and a 250 ml round bottom flask containing a magnet was fastened with vices above the oil vat. 200 ml of either methanol, ethanol or 2-propanol was added to the round bottom flask, and it was lowered into the oil vat until half of the solvent level was reached by the oil level. A 100 ml Soxhlet apparatus containing a cellulose thimble (25 mm diameter x 60 mm height, Grade 603) with the dried sample was fastened above the round bottom flask. Above the Soxhlet apparatus a Liebig cooler was fastened with a countercurrent of water to condense the solvent gas.

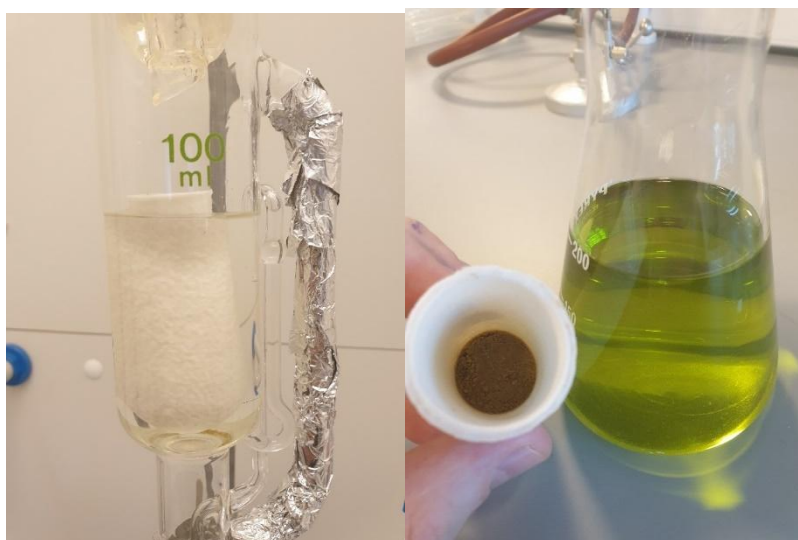


Figure 9 - Color of the solution at the end of the fifth cycle, and the extraction solution in relation to the remaining seaweed material

The temperature in the oil vat was set to about 15 °C above the boiling point of the solvent to provide a steady flow of solvent through the Soxhlet apparatus. After five cycles the extraction was considered done, and extracted solution was brought to room temperature. The volume of the solution was measured and refilled up to 200 ml. The solution was filtered through a polyethylene terephthalate (PET) 0.45 µm microfilter and injected into the HPLC system without dilution.

Optimization of an extraction with a Soxhlet system

A design of experiments was set up with variables of solvent type and sample to solvent ratio, and the yield of Fucoxanthin was considered as the main effect investigated. The solvent types tested were methanol, ethanol, and isopropanol (2-propanol), and the sample to solvent ratios tested had levels of 1:20 (grams of dried sample to ml of solvent) and 1:30. Every run was injected into the HPLC in a triplicate, resulting in 18 experiments in total. The order of the experiments was randomized to enable detection of systematic error.

Statistical analysis

Three calibration curves were constructed with 5 concentration levels for a Fucoxanthin standard in solutions of ethanol, methanol, and 2-propanol. Each concentration level was measured twice. An analysis was performed with factorial design to find the main effects, and the possible combinations of factors were measured thrice. The variance between the solvent types were compared used a one-way ANOVA test to check significance.

Multipoint calibration curves by the external standard method

A calibration curve is a regression line that shows the spectroscopic response of known concentrations of analyte (31) (p. 84, instr.), which is then presented in a plot of detector response and concentration. Solutions with a known concentration of analyte are called standard solutions and solutions containing nothing but the reagents and solvents used in the standard solutions are called blank solutions.

The construction of a calibration curve is done by preparing standard solutions covering a range of the expected concentration of the analyte in unknown samples (31) (p. 85, instr.). The response of the standard solutions is then measured, and the curve is constructed by linear regression (p. 301, chrom.). To correct for the absorbance of blank samples subtract the average blank response from the absorbance of the standard solutions. The equation of a linear calibration curve is given in formula 12 below.

$$\text{absorbance, } Y = m \times x + b \quad (12)$$

Where m refers to the slope of the calibration curve, x refers to the concentration and b is the offset to the curve. The calibration curve can not be used for quantification outside of the linear range of the curve, which is the analyte concentration range where the response is proportional to the concentration (31) (p. 86, instr.).

External standards are known solutions of the analyte without other components from the unknown solution (31) (p. 95). The fixed-volume loops used in HPLC systems make the external standard method suitable for HPLC because of the high regularity of the volumes produced (29) (p. 302, chrom.).

One-way ANOVA

ANOVA stands for analysis of variance and is used for comparing the variance of more than two means by separating and estimating the causes of variation (31) (p. 52-59). The means analyzed are of factor effects at different levels called groups, and a one-way ANOVA analyzes a single factor at different levels. A significance test such as ANOVA is necessary to know if the variation is large enough to discount random error being the cause of the variation (31) (p. 54). A one-way ANOVA has one controlled factor in addition to the random error present in the measurements. An assumption that the variance of the measurements of the controlled variable is independent and that the uncontrolled variation is truly random must be made to use an ANOVA test (31) (p. 59). If the measurements are made with the same procedure that assumption is usually valid.

A generalized one-way ANOVA test with h samples and n parallels with measurements and means can be found in table 6 below.

Table 6 - Measurements and means for a generalized one-way ANOVA (2: p. 54)

							Mean
Sample 1	X_{11}	X_{12}	..	X_{1j}	..	X_{1n}	\bar{X}_1
Sample 2	X_{21}	X_{22}	..	X_{2j}	..	X_{2n}	\bar{X}_2
	:	:		:		:	
Sample i	X_{i1}	X_{i2}	..	X_{ij}	..	X_{in}	\bar{X}_i
	:	:		:		:	
Sample h	X_{h1}	X_{h2}	..	X_{hj}	..	X_{hn}	\bar{X}_h
Overall mean = \bar{X}							

X_{ij} in table 6 stands for the j th measurement of the i th sample, and \bar{X} is the mean of all measurements.

The null hypothesis, H_0 , is that the variance within the samples is not significantly different from the variance between the samples. The test hypothesis, H_1 , is that there is a significant difference between the sources of variation (31) (p. 54-55).

Null hypothesis: The within-sample variation = The between-sample variation

Test hypothesis: The within-sample variation < The between-sample variation

Variation within the samples (31) (p. 54-55)

Calculation of the variance for each sample is done with formula 13:

$$\sum \frac{(x_i - \bar{x})^2}{(n-1)} \quad (13)$$

An estimate of the variation within the samples, σ_0^2 , is calculated with formula 14:

$$\sigma_0^2 = \sum_i \sum_j \frac{(x_{ij} - \bar{x}_i)^2}{h(n-1)} \quad (14)$$

Variation between the samples (31) (p. 55-56)

An estimate of the variation between the samples, σ_0^2 , is calculated with formula 15:

$$\sigma_0^2 = n \times \sum_i \frac{(\bar{x}_i - \bar{x})^2}{(h-1)} \quad (15)$$

A one-sided F-test is used to test if the null hypothesis is true, or that the null hypothesis must be discarded because the variation between the samples is significantly greater than the variation within the samples. The F-value for the F-test is calculated by formula 16 below and compared to the critical F-values found for a one-tailed test (31) (p. 280).

$$F - value = \frac{\sigma_0^2 \text{ between samples}}{\sigma_0^2 \text{ within samples}} \quad (16)$$

The F-test can find a significant difference because of one of many means, and that mean might confound an insignificant difference between the other means in the test (31) (p. 56). The least significant difference method can find the reason for the difference by checking the differences between the means. The test value can be calculated from formula 17:

$$\text{least significant difference} = s \times \sqrt{\left(\frac{2}{n}\right)} \times t_{h(n-1)} \quad (17)$$

The critical t-value is two-tailed and can be found for P = 0.05. If the difference between the means is less than resulting value of least significant difference the difference is considering insignificant (31) (p. 56). A t-test is a comparison of two means (31) (p. 39).

A summary of the sums of squares and the resulting f-value can be found below in table 7 (31) (p. 57).

Table 7 - ANOVA-table with sums of squares and a resulting f-value

Source of variation	Sum of variation	F-value
Within-sample		
Between-sample		

Results and discussion

An overview of standard deviations and the calculation of combined standard deviations can be found in attachment 1.

Strategy

Developing a determination method from scratch can be time consuming without any prior information about the significant factors and the factor levels. Hence, the strategy was to begin with a comprehensive literary analysis of articles concerning the determination of carotenoids from algae, and to a lesser degree polyphenols and chlorophylls. Finding an appropriate chromatogram mode as a starting point could save a lot of time and increase the chances of achieving a baseline separation for Fx. This would involve finding the gradient program, column, column temperature and flow rate used to separate and determine Fx from complex natural samples. After finding a starting point for the determination method the strategy was to use the OFAT-principle to tune the separation of the analytes with changes in mobile phase composition, column temperature and flow rate. The resolution of the Fx-peak was the criterion for the efficiency of the separation, and the Fx-peak were to be identified comparing the sample peaks with a check standard of Fx. A secondary confirmation for the identification of Fx would be done with reference to spectral data for Fx for similar gradient programs.

Developing a determination method for HPLC would likely be time consuming even with a good starting point considering the complexity of the natural sample. An optimization study with response surface methods to find the optimal levels for the significant factors would be a good strategy (33) (p. 119-122), but to limit the scope of the project the study was limited to two levels for significant variables. The optimization study with two factor levels should be considering a start of an optimization, and not a full optimization study. To determine the the optimal factors and levels a full factorial analysis and a ANOVA-test would for significance in the measured variance.

Literary analysis for method development

A wide search was made on databases like PubMed, ScienceDirect, SpringerLink, Taylor & Francis Online, Web of Science and on the resources of the school library directly through a search engine called Oria.

Only peer-reviewed articles were considered in the analysis, and this was checked by running the articles through Oria and confirming that the articles had a check mark for peer review. Articles involving the determination of carotenoids like Fucoxanthin from macroalgae using HPLC-DAD was prioritized, especially if it involved brown macroalgae. Simultaneous determination methods for more than one analyte in complex matrixes were given special attention. Other considerations were citations per year since publication, and age of the article considering the rapid development in column technology.

The extraction of lipophilic compounds using a Soxhlet system was researched first to prepare for the development of the HPLC determination method. Significant factors for an extraction with a Soxhlet system was investigated through interviews with the internal and external supervisors to the thesis, and through a literary analysis of nine selected articles. The

significant factors affecting the extraction were found to be solvent type, extraction time and STSR. Extraction temperature was not a factor since the Soxhlet extraction would require a fixed temperature at the solvents boiling point. A constraint for Alginor was that the solvent had to be green with regards to sustainability and toxicity in even trace amounts in dried product. This was important considering market possibilities in the food-, cosmetic- and pharma-industry (15). Most of the articles got greater yields of the analytes using ethanol (35) (p. 3) (36) (p. 53) and methanol as solvent (22) (p. 1121) (37) (p. 998) . Alginor had gotten good yields of lipophilic compounds using 2-propanol in a study done by Pilodist at the behest of Alginor. The Pilodist study also found the optimal number of cycles in a Soxhlet apparatus to be five cycles, which enabled the elimination of one factor in a factorial analysis. Most STSR's for lipophilic extractions varied from 1:20 (37) (p. 998) (38) (p. 12) to 1:25 (35) (p. 3) (36) (p. 53) and the levels for STSR were set to 1:20 and 1:30. The highest level for STSR was set to 1:30 to see if a greater yield could be obtained by increasing the ratio beyond the norm.

About 24 articles with a high degree of relevance were reviewed thoroughly in the analysis for the determination method, and some general trends were observed for most of the methods by compiling the parameters in a datasheet. The significant factors were found to be different columns and gradient programs. Factors like flow rate and column temperature were also significant but considered a part of the gradient programs.

The most popular columns for separating complex samples like macroalgae or other complex natural samples were 250 mm in length with an inner diameter of 4.6 mm. (23) (p. 6) (39) (p. 5) (11) (p. 172) (26) (p. 328) 250 mm columns are not ideal with regards to increased runtimes and solvent use, but it was necessary with a long column to achieve the separations. The most popular stationary phases were C30 and C18 columns (40) (p. 7) (25) (p. 105) with particle sizes of 5 μm and the most popular column manufacturer was YMC. With a basis of these findings a C18 and C30 column with these specifications were acquired by Alginor for the project.

From the literary analysis three alternatives for a gradient program were possible starting points for a screening test. These alternatives all determined antioxidants in macroalgae with good resolution for the analytes. All gradient programs were extended to 45 minutes of runtime to ease comparison of the alternatives, and an increase of runtime would not negatively affect a separation.

Screening test

The alternatives used in the screening test can be found onwards, along with details of necessary modifications of the mobile phases.

#1 Phenolic Content and Antioxidant Capacity in Algal Food Products (22)

This article determined phenolic content from edible macroalgae, some of which were brown macroalgae, making this article relevant for the thesis. The analytes were not Fucoxanthin, but polyphenols, but nonetheless determining several analytes during a short runtime.

The gradient program is shown in table 8, and the mobile phases were:

- A: water-acetic acid (99:1, v/v)
- B: water-acetonitrile-acetic acid (67:32:1, v/v/v)

Table 8 - Gradient program of alternative #1 for the screening test.

Time (min)	% A	% B	Flow (ml/min)
0 – 10	90	10	1.0
10 – 16	90 – 80	10 – 20	1.0
16 – 20	80 - 60	20 – 40	1.0
20 – 25	60 – 50	40 – 50	1.0
25 – 27	50 – 60	50 – 40	1.0
27 – 35	60 – 90	40 – 10	1.0

Acetonitrile is not a green solvent and had to be substituted. The modification of the mobile phase B was done considering the relative polarity (41) and viscosity of the mobile phases, and the calculations can be found in attachment 2.

Modified mobile phases:

- A: water – acetic acid (99:1, v/v)
- B: methanol - acetic acid (99:1, v/v)

Table 9 - Column type and settings for alternative #1 in the screening test.

Column type	C18 Kinetex column (Phenomenex, 150 mm × 4.6 mm, 2.6 µm particle size)
Column temperature [°C]	23
Injection volume [µL]	10
Wavelength setpoint [nm]	275

#2 HPLC Detection and Antioxidant Capacity Determination of Brown, Red and Green Algal Pigments in Seaweed Extracts (14)

This article was highly relevant since the raw material was different kinds of macroalgae, including brown algae, and the analytes included all the analytes in this thesis, including Fucoxanthin.

The gradient program is shown in table 10, and the mobile phases were:

- A: methanol-acetonitrile (50:50, v/v) with 0.1% triethylamine (TEA)
- B: Acetone

Table 10 - Gradient program of alternative #2 for the screening test.

Time (min)	% A	% B	Flow (ml/min)
0 – 15	100	0	1.5
15 – 25	100 – 30	0 – 70	1.5
25 – 40	30 – 0	70 – 100	1.5

Neither of the mobile phases are green considering acetonitrile and acetone, so both had to be modified using green solvents. Triethylamine is a common flavoring additive and was not a problem as an additive in the modified mobile phase according to the database in PubChem. The calculations for the modification can be found in attachment 2.

Modified mobile phases:

- A: methanol – ethyl acetate – triethylamine (72:28, v/v, additive: v: 0,1)
- B: ethyl acetate

A PDA was utilized to record wavelengths from 200 nm to 800 nm continuously.

Table 11 - Column type and settings for alternative #2 for the screening test.

Column type	Waters YMC C30 (250 mm × 4.6 mm, 5- μ m particle size)
Column temperature [°C]	35
Injection volume [μ L]	20
Wavelength setpoint [nm]	450, 650, 665

#3 Antioxidant compounds in edible brown seaweeds (13)

This article was highly relevant due to the raw materials being several brown seaweeds, and all the analytes in the article study was of interest in this thesis, including Fucoxanthin. However, only the pigments were analyzed using the HPLC determination method, reducing the complexity of the matrix.

The gradient program is shown in table 12, and the mobile phases were:

- A: methanol
- B: water
- C: dichloromethane-hexane (50:50, v/v)

Table 12 - Gradient program of alternative #3 for the screening test.

Time (min)	% A	% B	% C	Flow (ml/min)
0 – 4,5	85	15	0	1.0
4,5 – 5	85 – 100	15 – 0	0	1.0
5 – 10	100 – 70	0	30	1.0
10 – 14	70	0	30	1.0
14 – 15	70 – 100	0	30 – 0	1.0
15 – 20	100 – 85	0 – 15	0	1.0

Mobile phase C had to be modified considering both dichloromethane (DCM) and hexane. Calculations for the modification can be found in attachment 2.

Modified mobile phases:

- A: methanol
- B: water

- C: ethyl acetate

A PDA was utilized to record wavelengths from 200 nm to 800 nm continuously.

Table 13 - Column type and settings for alternative #3 for the screening test.

Column type	Tracer Extrasil C18 ODS 2 column (250 x 4 mm, 5 µm particle size)
Column temperature [°C]	35
Injection volume [µL]	20
Wavelength setpoint [nm]	450, 650, 665

Before the screening test could be started a procedure for sample preparation and Soxhlet extraction had to be developed. This involved making procedures to dry the raw material and to extract lipophilic compounds from the dried material.

A screening test with the factors column type and gradient program was run in a randomized order to minimize the risk of introducing systematic error. A factorial design was not necessary for the screening test considering that the variables were categorical and nominal. Also, the response variable was considered qualitatively by comparing the separation of the analytes in general. The design of experiments can be found in table 14 below.

Table 14 - Design of experiments for a screening test to evaluate HPLC determination methods

Experiment	Randomized order	Column type	Gradient program
1	13	C18	1
2	4	C18	1
3	9	C18	1
4	3	C18	2
5	7	C18	2
6	6	C18	2
7	10	C18	3
8	17	C18	3
9	18	C18	3
10	16	C30	1
11	14	C30	1
12	8	C30	1
13	2	C30	2
14	1	C30	2
15	11	C30	2
16	5	C30	3
17	15	C30	3
18	12	C30	3

All the experiments were recorded at 275 nm, 450 nm, 650 nm, and 665 nm, but the chromatogram used for comparison was recorded at 450 nm in compliance to the absorption maxima of Fx found in the literary analysis. An ethanol extract with a concentration of about 15 000 mg/l was used in the screening test, corresponding to a STSR of about 1:66,7. To begin with a diluted extract was used because of issues with a high back pressure in the system and uncertainty around the need to dilute the samples from the Soxhlet extraction. There were also issues with leakage from the gradient pump, but the issues were resolved after the screening test. The chromatograms at 450 nm are given in attachment #.

Evaluation of the experiments

None of the alternatives from the literary analysis were suitable as a starting point for a method, and the screening test was stopped after the fifth experiment. None of the gradient programs separated the peaks in the ethanol extract sufficiently, with the latest peaks eluting at around 15-17 minutes and most of the peaks eluting in a bundle at the start of the chromatograms. A considerable baseline shift was observed with the influx of ethyl acetate, showing that ethyl acetate had a considerable absorbance in the bandwidth range that was recorded. Also, an addition of a mobile phase that absorbs in the area being recorded should be linear to ensure a baseline suitable for quantification.

A fourth alternative was found for the C30 column on the website of the manufacturer, YMC. (32)

Developing a determination method

The gradient program found for the C30 column was advertised to separate carotenes and xanthophylls, analytes found in abundance in natural products like brown seaweed. A binary gradient elution was used without modified mobile phases and with the settings given in table 15 to check the reproducibility of the advertised separation. The chromatogram of the unmodified run can be found in figure 10.

Mobile phases:

- A: methanol-MTBE-water (81/15/4)
 - MTBE – Methyl tert-butyl ether
- B: methanol-MTBE-water (7/90/3)

Gradient program:

- 0-100% B during a 90-minute runtime with a flow rate of 1 ml/min

Table: Settings for YMC program

Table 15 - Column type and settings for alternative #4 from YMC

Column temperature [°C]	Ambient (set to 26 °C)
Injection volume [µL]	20
Wavelength setpoint [nm]	450 (200-800 nm PDA)

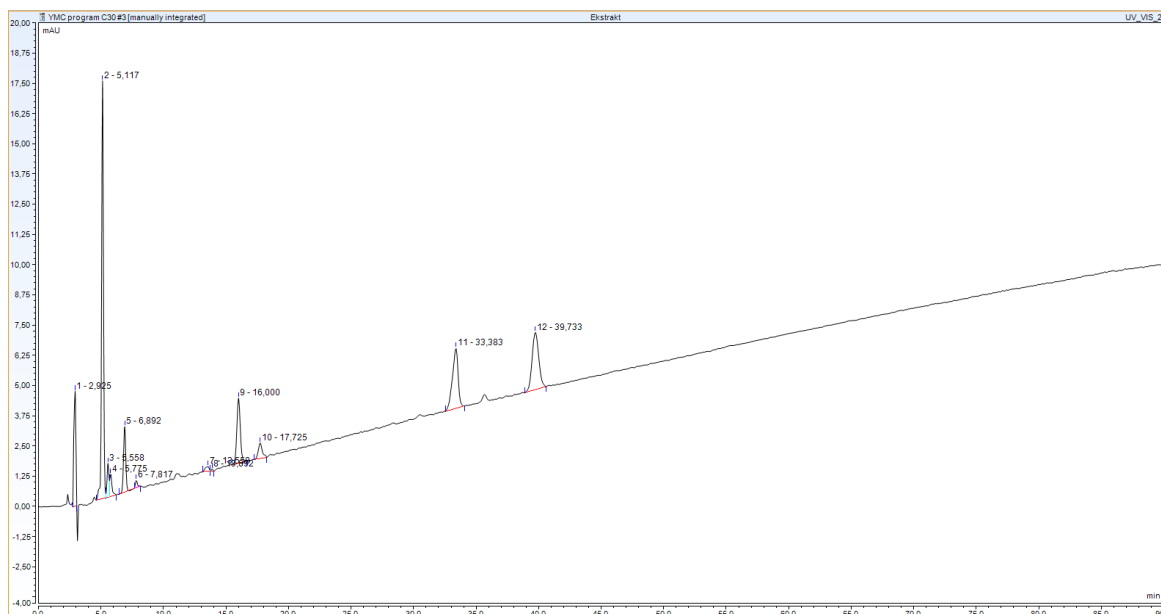


Figure 10 - A chromatogram of an unmodified YMC program with 20 μ l of an ethanol extract at 450 nm. The concentration of the extract was about 15 000 mg/l.

As seen by figure 10 the separation with the YMC gradient program was promising with the latest peaks eluting at around 41 minutes, whilst the latest peaks in any of the alternatives in the screening test eluted at around 15 – 17 minutes. Now that there was a promising starting point, 20 μ l of a 100 mg/L Fx standard in a solution with ethanol was injected. The concentration of the standard would have been made with a lower concentration if it would not have detrimental effects on the uncertainty of the weight and volume measurements. The total weight of the standard was 5 mg, and the analytical weights available had four decimal points measuring in grams. This meant that a minimum of 1 mg had to be diluted keeping the uncertainty in the fourth decimal, which was diluted in a 10 ml measuring flask.



Figure 11 – A chromatogram of unmodified YMC program with 20 μ l of a 100 mg/l Fucoxanthin standard in ethanol at 450 nm.

Figure 11 showed that 100 mg/L of the Fucoxanthin standard had an absorption of about 2400 mAU and a RT of about 4,9 minutes. The only similar peak in that range in figure 10 was peak number 2 with an absorption of about 18 mAU and a RT of about 5,1 minutes. The separation of the suspected Fx-peak seemed plausible, so the next step was to modify the mobile phases using green solvents. The settings for the gradient programs onward were the same as the settings for the unmodified YMC-program given in table 15, unless stated otherwise.

The first modified gradient program had the following mobile phases:

- A: Methanol
- B: Ethyl acetate

The first modified YMC gradient program (#1) can be found in table 16, and the chromatogram can be found in figure 12.

Table 16 - Modified YMC gradient program #1

Stages in gradient program [min]	Mobile phase composition [A%:B%]
0	90:10
90	10:90



Figure 12 - A chromatogram for the modified gradient program #1 with 20 μ l of an ethanol extract at 450 nm. The concentration of the extract was about 15 000 mg/l.

As seen by figure 12 the modified variant of the YMC program yielded an even better separation for the compounds in ethanol extract with the latest peaks eluting at about 44 minutes. The linear gradient in the program resulted in a good baseline like the one in the unmodified program (figure 10) considering the baseline shift caused by the increase of absorbance in the mobile phase caused by ethyl acetate.

With a suitable starting point for the determination method the strategy onwards was to get a baseline separation for Fucoxanthin with the OFAT-principle. Fx has been the most abundant compound in previous work with lipophilic extracts from brown seaweeds ([Sources](#)), so peak number 3 at 4,9 minutes in figure 12 was tentatively identified as a Fx-peak. There was a need to increase the retention of the analytes since several of them bundled up together between 5 and 10 minutes. This could be achieved by increasing the polarity in the mobile phase at the start of the gradient program, which would differentiate the analytes better and therefore increase the separation. The relative polarity of water is 1, 0.762 for methanol, and 0.228 for ethyl acetate.

To increase the lifetime of the column it is recommended that gradient programs don't have stages with a 100% of organic solvents like methanol or a 100% of water to avoid harmful interactions with the stationary phase. Harmful interactions could involve a phase collapse of the column, where the stationary phase would react chemically with the polar mobile phase (42) (p. 8). Modified gradient programs had an upper limit of 90% of methanol and water for this reason.

A new program was made with the mobile phases of:

- A: Water
- B: Methanol
- C: Ethyl acetate

The first modified YMC gradient program (#2) can be found in table 17, and the chromatogram can be found in figure 13.

Table 17 - Modified YMC gradient program #2

Stages in gradient program [min]	Mobile phase composition [A%:B%:C%]
0	85:15:0
15	85:15:0
20	0:85:15
90	0:10:90

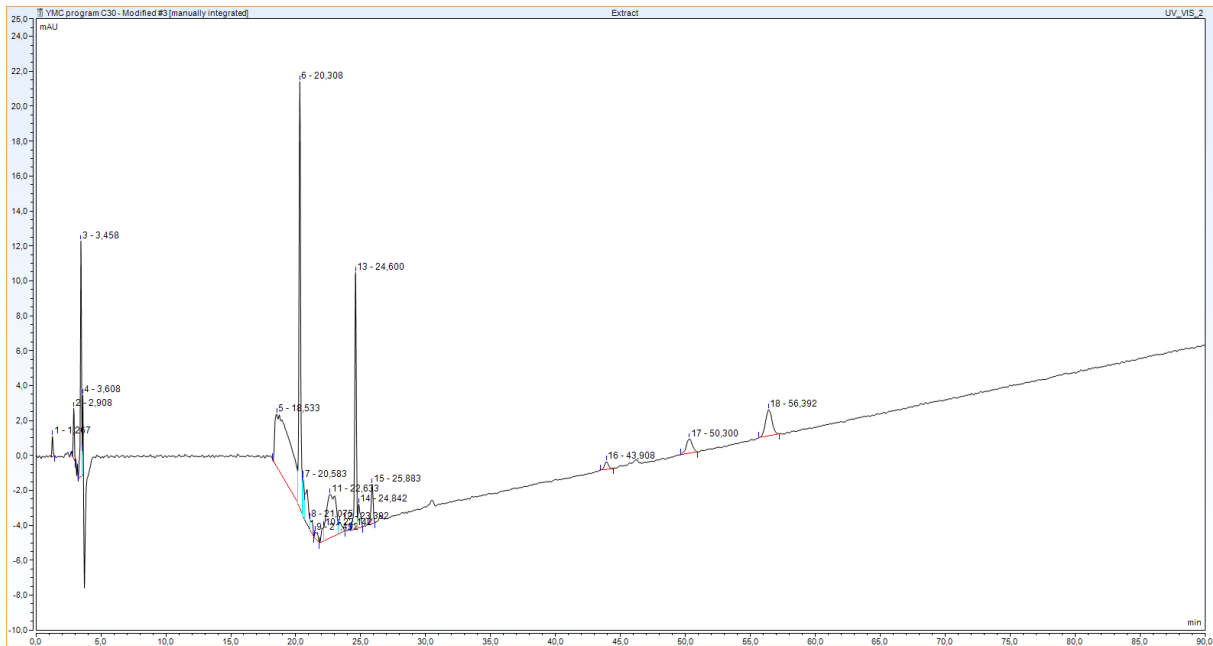


Figure 13 - A chromatogram for the modified gradient program #2 with 20 μ l of an ethanol extract at 450 nm. The concentration of the extract was about 15 000 mg/l.

As seen by figure 13 the peaks bundled up between 5 and 10 minutes (RT) in figure # now eluted between 20 and 27 minutes (RT), with Fucoxanthin (an assumption, not a confirmed identification) coming out as peak number 6 with a RT of 20,308 minutes. A dramatic shift in the baseline made quantification impossible in this area, and it was suspected that there was an issue with a non-uniform mobile phase front, which was backed up by a discovery that ethyl acetate is immiscible in water. The latest peak eluted at about 56 minutes, which was a better separation, but analytes could not be determined given the irregular baseline.

Next, gradient program #1 from table 16 was reproduced to start over, and the chromatogram of that run can be found in figure 14 below. Given the low absorbance values some noise was to be expected in general because of the scaling of the chromatogram, and another extraction with a lower STSR was planned. A new extraction was done with about 9,15 grams of dried seaweed leaves and 200 ml of methanol (approximately a 1:22 STSR, and a concentration of 45 000 mg/l). Methanol was chosen as the solvent to align the matrix of the sample with the mobile phase to minimize interference from solvent peaks.

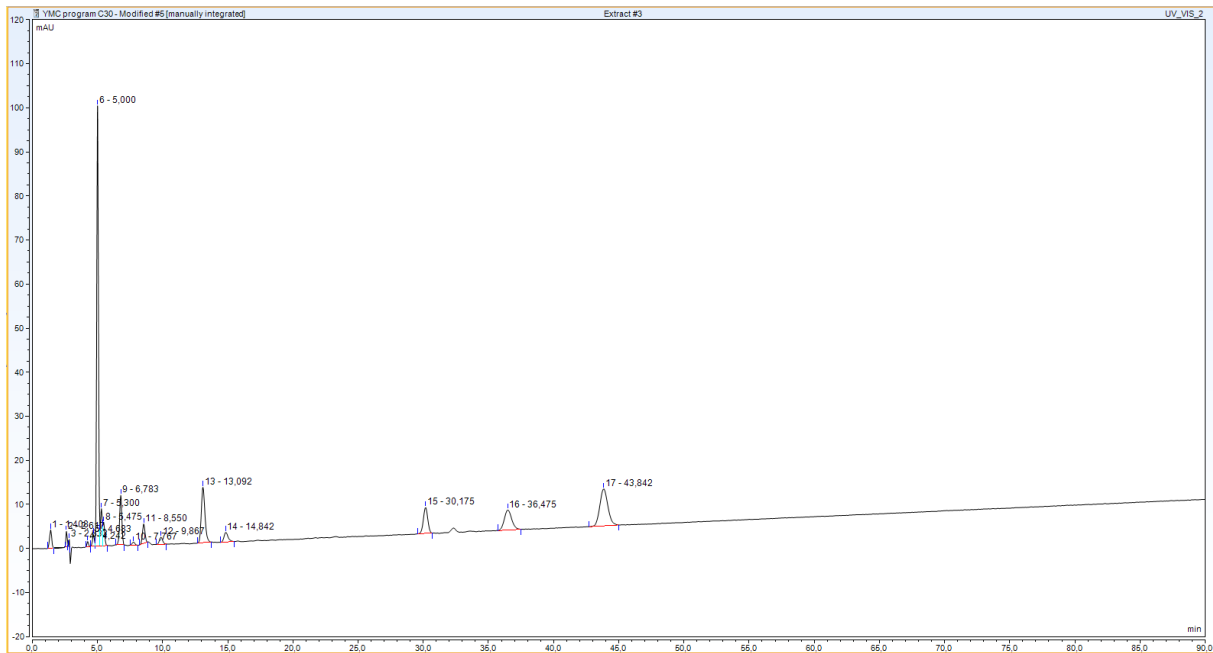


Figure 14 - A chromatogram for the modified gradient program #1 with 20 μ l of a methanol extract at 450 nm. The concentration of the extract was about 45 000 mg/l.

As seen by figure 14 the peak absorbance of the assumed Fx-peak increased to over a 100 mAU, which amounts to about a fivefold increase in response signal from the ethanol extract used earlier. The retention time of the assumed Fx-peak was now about 5 minutes. The increased scale of the analytes in the chromatogram eased the interpretation since the baseline noise now was less of a factor.

Up until now the absorption maxima of Fucoxanthin was assumed to be at 450 nm with reference to the literary analysis, but a range of 200 to 800 nm was recorded for each run so the absorption maxima could be found by considering the contour plot produced by the PDA. However, as seen by figure 15 below, there was an issue with an enormous absorption at 244,31 nm.

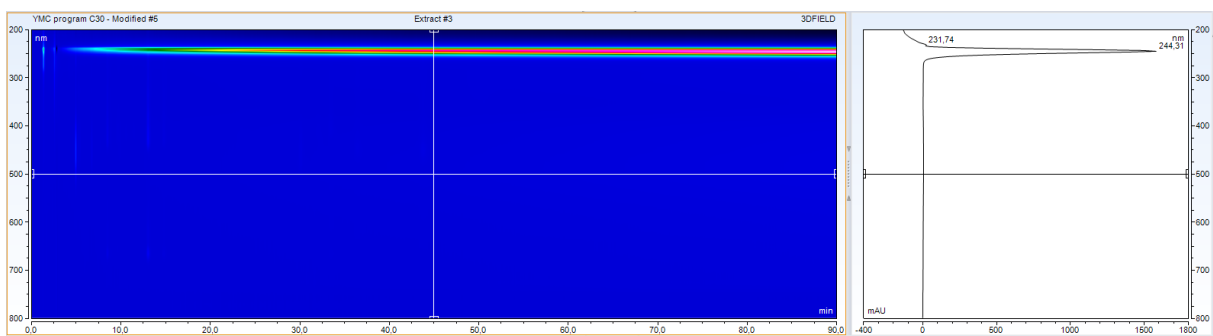


Figure 15 – A contour plot of a run with gradient program #1 with 20 μ l of a methanol extract recorded from 200 nm to 800 nm. The concentration of the extract was about 45 000 mg/l.

As seen by figure 15 a substantial absorption at 244,3 nm made identification of an absorption maxima for Fx difficult. Such an absorption could only come from the mobile phase itself. Onwards the bandwidth range for the PDA was set from 250 nm to 800 nm. From the literary analysis it was found that polyphenols have absorption maxima around 275 nm, so the lower limit of the PDA was kept as low as possible.

As seen in figure 13 there was a need for an alteration in polarity to increase separation, especially in the start of the chromatogram. A third gradient program given in table 18 was made with the following mobile phases:

- A: Methanol
- B: Ethyl acetate

Table 18 - Modified YMC gradient program #3

Stages in gradient program [min]	Mobile phase composition [A%:B%]
0	90:10
20	90:10
90	10:90

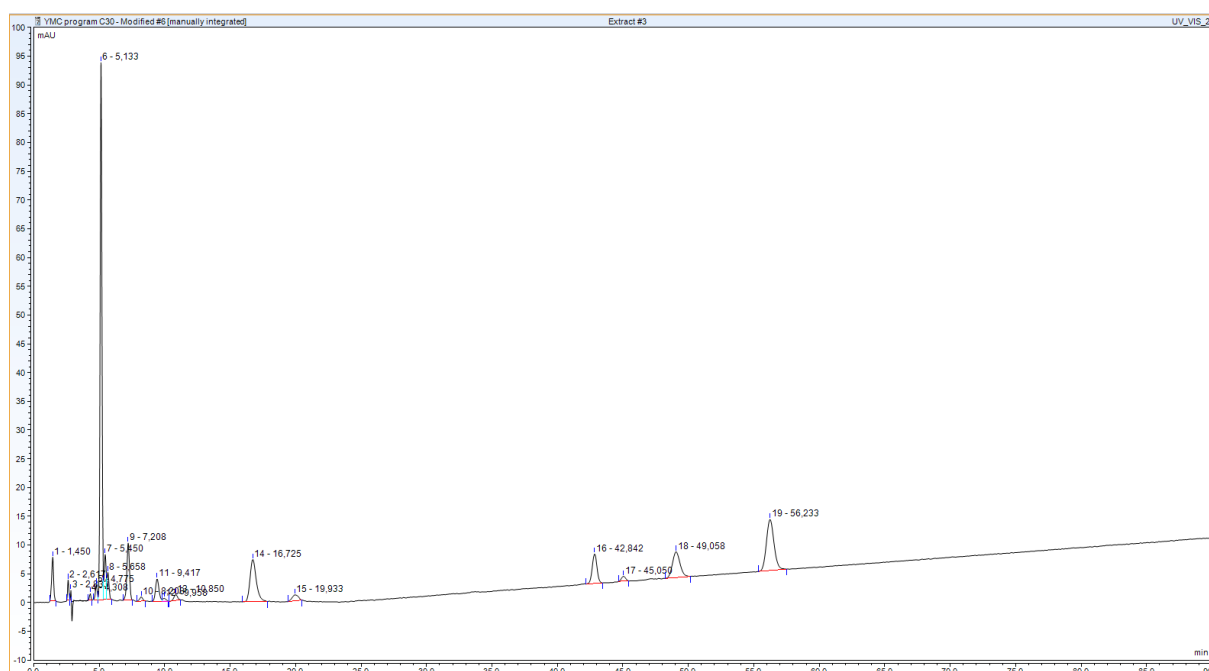


Figure 16 - A chromatogram for the modified gradient program #3 with 20 μ l of a methanol extract at 450 nm. The concentration of the extract was about 45 000 mg/l.

As seen by figure 16 above an increase from about 5 minutes to 5,1 minutes in retention time was observed for the assumed Fx-peak compared to gradient program #1 in figure 14. This was a miniscule difference, but the separation of the other analytes was greatly improved with the last peak eluting at about 56,2 minutes compared to 43,8 minutes for figure 14. There were two regions where no peaks eluted in the chromatogram for gradient program #3. These regions spanned the area from 22 minutes to 42 minutes, and from 59 minutes until the runtime stop. To create a more efficient gradient program a quicker increase in mobile phase strength to elute faster in these areas was needed.

Also, the contour plot given in attachment 4 showed that the absorption of ethyl acetate still eclipsed all other absorptions. The range for the PDA was changed to span from 270 nm to 800 nm, keeping a small area around 275 nm for polyphenols. To identify more peaks in the beginning of the chromatograms a run with 20 μ l of a methanol extract and gradient program #3 at 450 nm was done and can be found in attachment 4. The mobile phase front with a

sample of a methanol extract hit the detector at a retention time of about 2,8 with a positive absorption of about 2, followed by a negative absorption of about 4.

After consulting with a representative from YMC a new upper limit for methanol in the gradient program was established at 97%. This allowed for more retention of polar compounds at the start of the run, thereby separating the earlier peaks better from the assumed Fx-peak. Ideally some water could be included considering the higher relative polarity compared to methanol. A source claimed that 3% of water was miscible in water which was evaluated by mixing 300 µl of water, 700 µl of methanol and 9000 µl of ethyl acetate in a solubility test. The solubility test confirmed solubility with 3% water and a new gradient program was made. This fourth gradient program can be found in table 19 below.

The following mobile phases were in the gradient program:

- A: Water
- B: Methanol
- C: Ethyl acetate

Table 19 - Modified YMC gradient program #4

Stages in gradient program [min]:	Mobile phase composition [A%:B%:C%]:
0	3:94:3
17	3:94:3
25	3:62:35
35	3:47:50
40	3:7:90
50	3:7:90
55	3:94:3
70	3:94:3

Plateaus were added to the new gradient programs to hold the polarity higher in the regions with bundled peaks, and a quicker decrease in polarity was incorporated in regions without peaks, which allowed for a decrease of twenty minutes runtime. Fifteen minutes of column conditioning was added at the end of the program to facilitate for multiple runs in a row. The first run with gradient program #4 can be found in figure below with a zoom of the chromatogram. Onwards all the chromatograms were zoomed in to help the evaluation of the separation for the Fx-peak, but first the assumed identity of the Fx-peak needed to be confirmed.

In a precursor of gradient program #4 a chromatogram of the Fx standard was run in comparison to a methanol extract to positively identify the peak, the results of which can be found in attachment 4. In the chromatogram for the methanol extract peak number six had an absorption of about 75 mAU and a retention time of about 6,37 minutes, and peak number two in the chromatogram for the Fx standard had an absorption of about 1700 mAU and a retention time of about 6,25 minutes. The absorption maximum of the Fucoxanthin standard in a contour plot in attachment 4 was also used in the identification, which was measured to be at around 448,6 nm. These results positively identified the assumed Fx peak as Fx with a comparison of both the retention time and the absorption maxima.

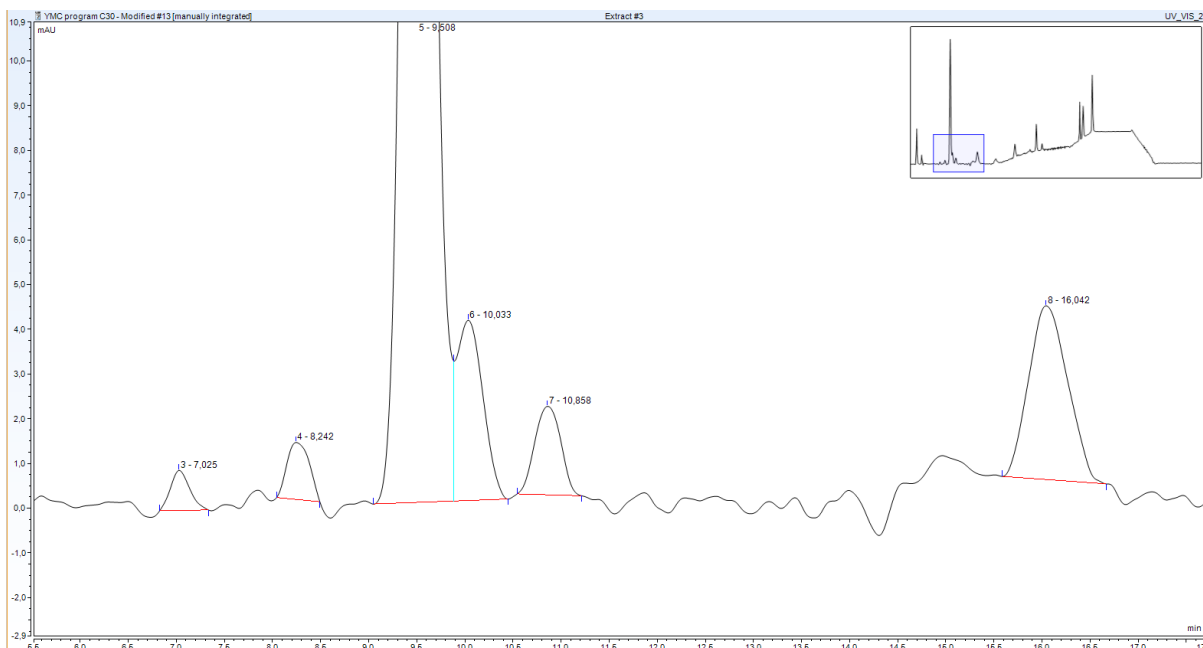


Figure 17 - Zoom of a chromatogram of modified YMC gradient program #4 with 20 μ l of a methanol extract at 450 nm. The concentration of the extract was about 45 000 mg/l.

Peak 5 in figure 17 above with a RT of 9,508 minutes and an absorption of about 46 mAU was identified as Fx, and with an absorption maximum at about 447,6 nm found in figure 18 below. A shoulder peak of another compound co-eluted but compared to earlier runs baseline separation seemed possible. The full chromatogram can be found in attachment 4.

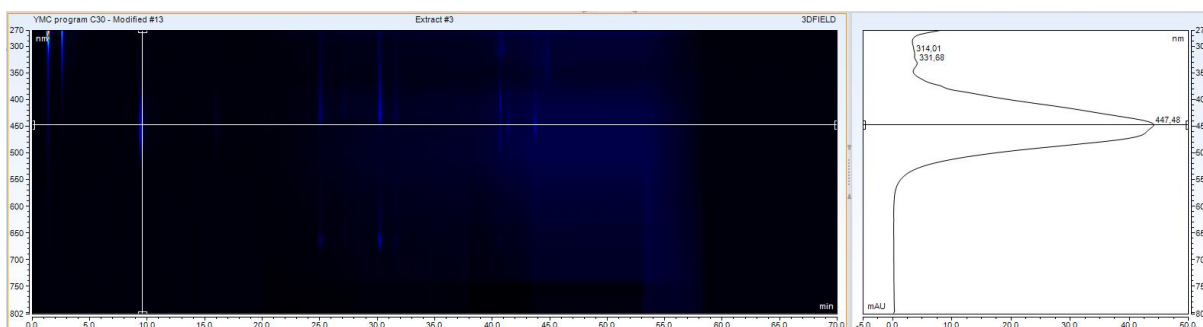


Figure 18 - A contour plot of modified YMC gradient program #4 with 20 μ l of a methanol extract at 450 nm. The concentration of the extract was about 45 000 mg/l.

Gradient program #4 was run with a flow rate of 0.9 ml/min, and the chromatogram of that run can be found below in figure.

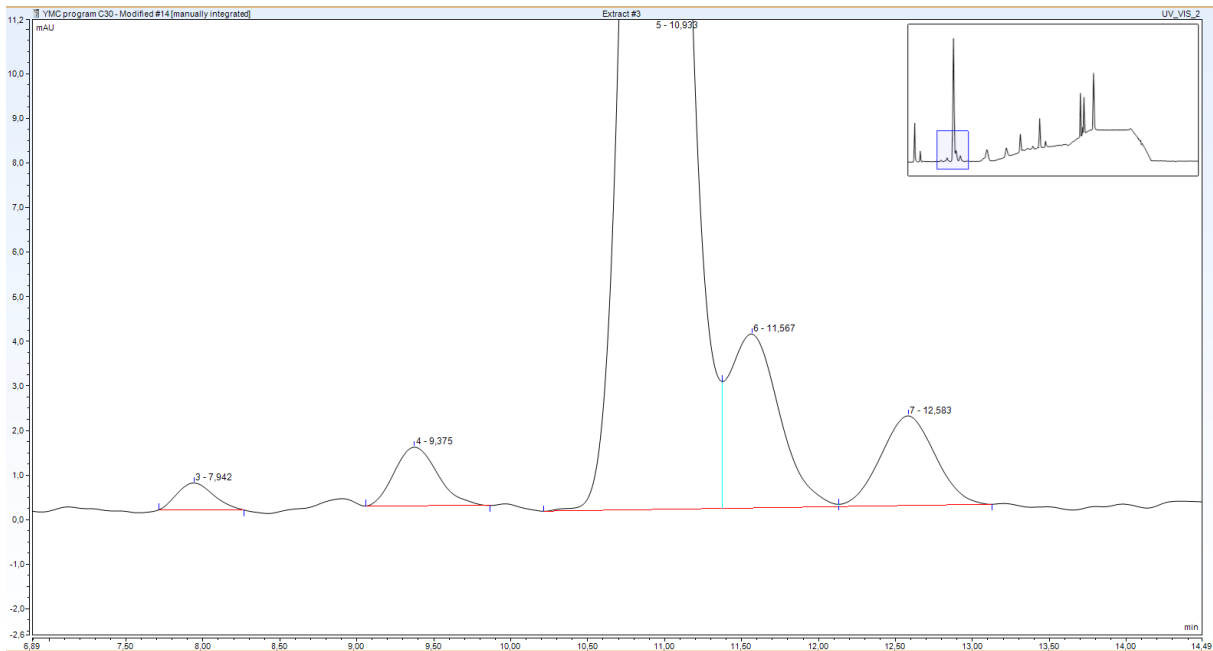


Figure 19 - Zoom of a chromatogram of modified YMC gradient program #4 with 20 μ l of a methanol extract at 450 nm. The concentration of the extract was about 45 000 mg/l, and the flow rate was 0.9 ml/min.

As seen by figure 19 the shoulder peak had gotten slightly smaller, but the peak width increased because of the lower flow rate, resulting in diminishing returns of resolution. Another run was done with the same program, but with a flow rate of 0.7 ml/min and an increase in runtime to 75 minutes in case of very late peaks. The chromatogram of that run can be seen in figure 20 below.

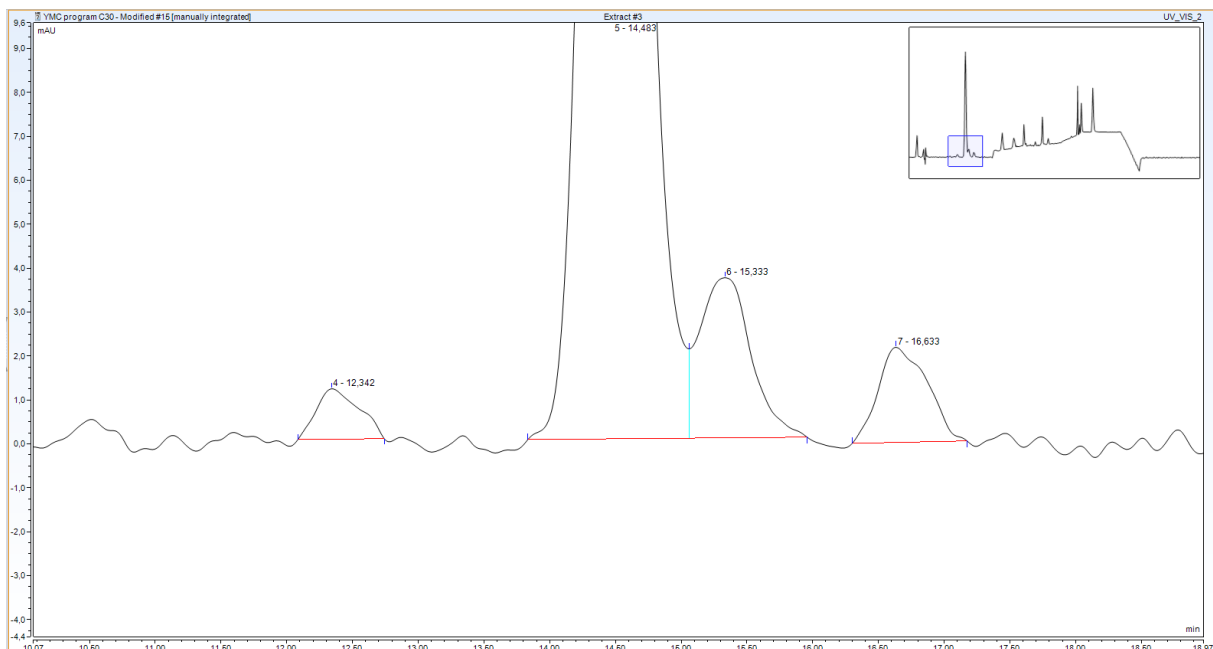


Figure 20 - Zoom of a chromatogram of modified YMC gradient program #4 with 20 μ l of a methanol extract at 450 nm. The concentration of the extract was about 45 000 mg/l, and the flow rate was 0.7 ml/min.

A slight improvement on the resolution because of a reduction in the shoulder peak can be seen in figure 20, but the effect was miniscule. Another run was done with 0.9 ml/min flow

rate, 50 °C on the column and a runtime set back to 70 minutes. The chromatogram of that run can be seen in figure 21 below.

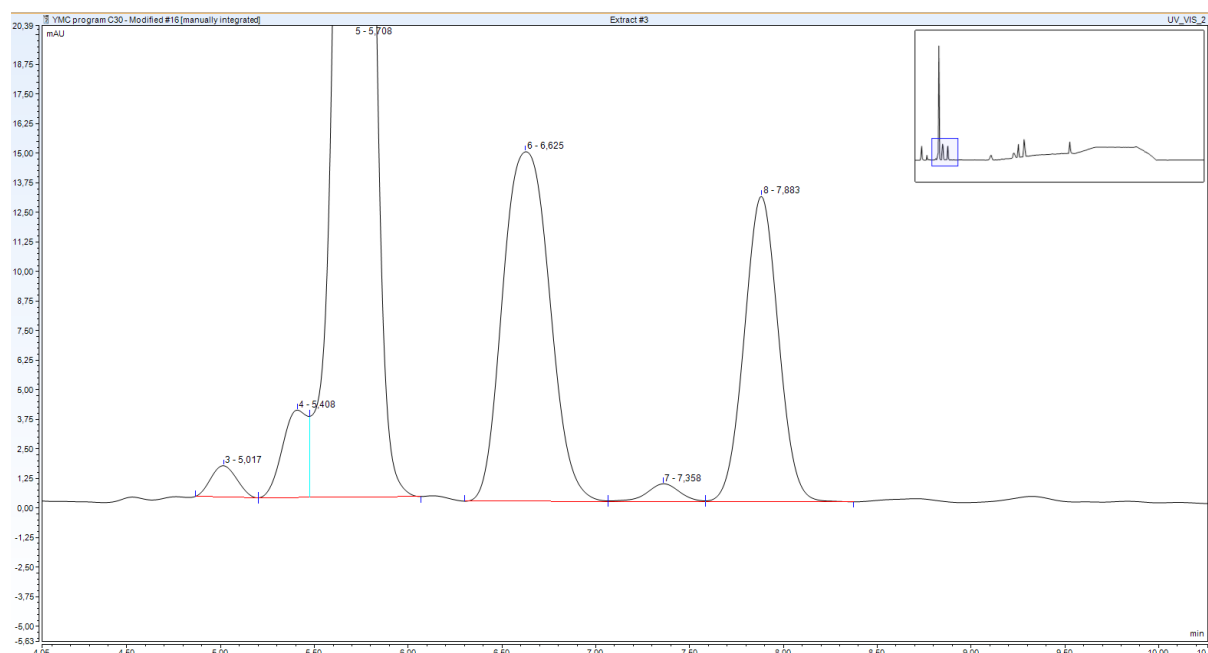


Figure 21 - Zoom of a chromatogram of modified YMC gradient program #4 with 20 µl of a methanol extract at 450 nm. The concentration of the extract was about 45 000 mg/l, the flow rate was 0.9 ml/min, and the column temperature was set to 50 °C.

As seen by figure 21 the shoulder peak co-eluting with Fx earlier had now switched positions with Fx to elute slower than the Fx-peak, and the resolution improved in general because of lower peak widths from the heightened column temperature. The RT of Fx had changed from about 10,9 minutes in figure 19 with a column temperature of 26 °C to about 5,7 minutes with 50 °C. The absorption of 20 µl of Fx standard in ethanol was measured to be about 2200 mAU, given in a chromatogram in attachment 4. Previously the absorption was about 1700 mAU (Attachment 4), but that was from a HPLC vial that had gotten left out for two days in room temperature and light. This was an indication of how quickly Fucoxanthin degrades into derivatives, and this vial was only used for identification purposes. It was possible to increase the temperature further than 50 °C, but according to the manual of the column it is not recommended to exceed 50 °C to preserve a normal lifetime for the column.

A chromatogram of the same program with an increased flow rate of 1.0 ml/min was run, and the chromatogram of that run can be found in attachment 4. The RT of Fx was now about 5,4 minutes, and the shoulder peak in front of the Fx peak had almost completely merged with the Fx-peak.

Several modifications of the plateaus were done to decrease the runtime to 60 minutes, and the gradient program can be found in table 20 below.

The following mobile phases were in the gradient program:

- A: Water
- B: Methanol
- C: Ethyl acetate

Table 20 - Modified YMC gradient program #5:

Stages in gradient program [min]:	Mobile phase composition [A%:B%:C%]:
0	3:94:3
10	3:94:3
15	3:62:35
22	3:47:50
30	3:7:90
40	3:7:90
50	3:94:3
60	3:94:3

Gradient program #5 was run with 40 °C on the column and a flow rate of 1.0 ml/min, and the chromatogram of that run can be found in figure 22 below.

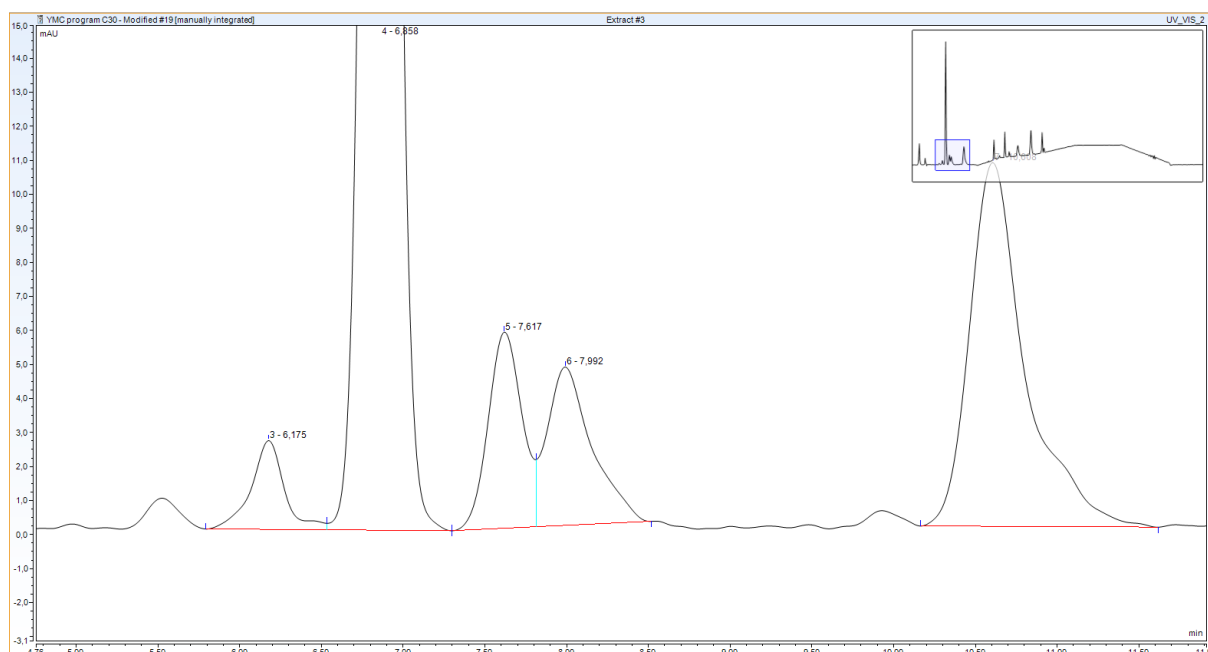


Figure 22 - Zoom of a chromatogram of modified YMC gradient program #5 with 20 µl of a methanol extract at 450 nm. The concentration of the extract was about 45 000 mg/l, the flow rate was 1.0 ml/min, and the column temperature was set to 40 °C.

As seen by figure 22 the shoulder peak and the Fx peak had been separated enough for an approximate baseline separation. A run with the same program and settings other than a column temperature of 35 °C can be found in attachment 4. The resolution of the Fx peak was worsened as the Fx peak was now separated from the foremost peak, but was slightly joined with the backmost peak. Chromatograms of runs with 30 °C, 37 °C and 39 °C on the column and the same settings otherwise can be seen in attachment 4. Finally, a run was done with 36 °C on the column and the same settings otherwise, the chromatogram of which can be found in figure below.

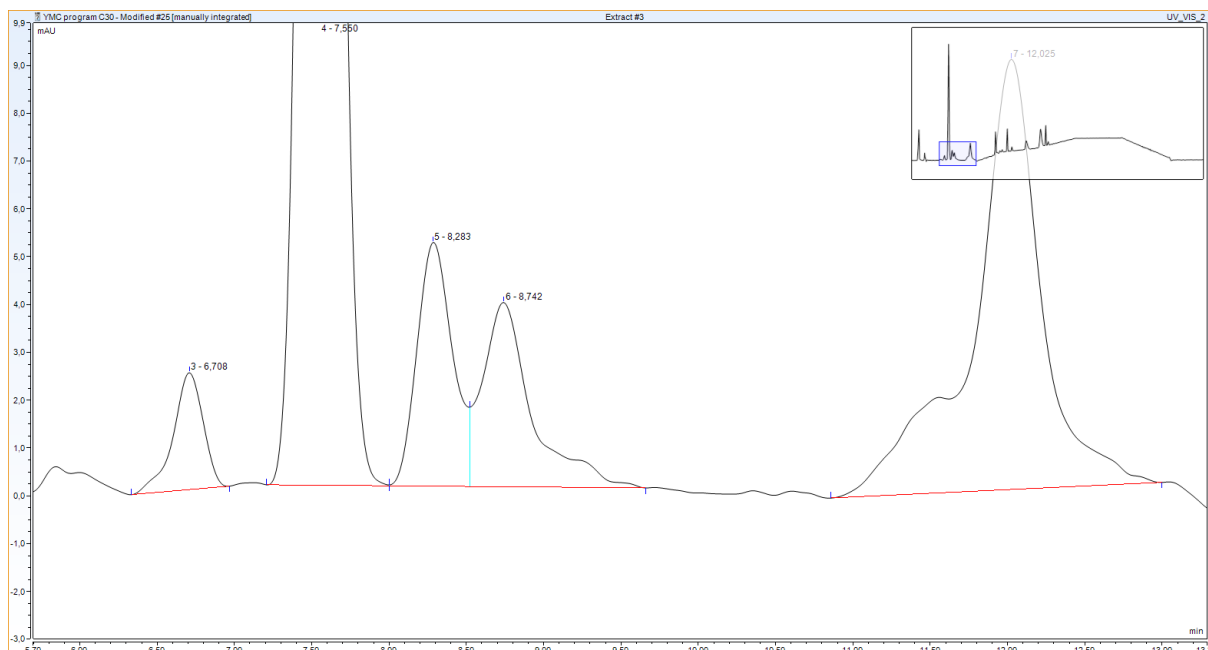


Figure 23 - Zoom of a chromatogram of modified YMC gradient program #5 with 20 μ l of a methanol extract at 450 nm. The concentration of the extract was about 45 000 mg/l, the flow rate was 1.0 ml/min, and the column temperature was set to 36 $^{\circ}$ C.

As seen in figure 23 a baseline separation was achieved for the Fx peak, and the gradient program was now considered suitable for quantification. A full chromatogram of this run at 450 nm can be found in attachment 4. There might have been room for a reduction in runtime given that the latest eluting peak came out at a RT of about 28,1 minutes. However, there should be some area without eluting peaks at the end of a gradient program to ensure that there is no carry over of analytes to a following run. The resolution for the Fx peak was considered acceptable at above 1.5, but ideally the resolution for main analytes should be above 2. The focus now shifted to the optimization of extraction conditions for the Soxhlet system, and an overview of the determination method can be found below, with the gradient program in table 21 and settings in table 22.

The following mobile phases were in the gradient program:

- A: Water
- B: Methanol
- C: Ethyl acetate

Table 21 - Gradient program for the determination method of Fx

Stages in gradient program [min]	Mobile phase composition [A%:B%:C%]
0	3:94:3
10	3:94:3
15	3:62:35
22	3:47:50
30	3:7:90
40	3:7:90
50	3:94:3
60	3:94:3

Table 22 - Settings for the gradient program of the determination method for Fx determination

Column temperature [°C]	36 °C
Injection volume [μL]	20
Wavelength setpoint [nm]	448

As seen by table 22 the wavelength for the absorption maximum for Fucoxanthin was set to 448 nm for the measurements done in the Soxhlet extraction optimization study, with reference to the contour plot in figure 18. The Soxhlet optimization study was performed after a method validation.

Method validation

Selectivity

The selectivity was calculated with the formula (4) for resolution for each of the extracts in the optimization study, and the results can be found in table # in the chapter for the optimization study following this chapter.

Linearity

Five concentration levels were measured for the Fucoxanthin standard from 50% to 150% of target concentration to construct a calibration curve used in an external standard method for determination. Considering the variation observed with different solvents in the extracts, calibration curves were constructed for each solvent used.

The target concentration (set as a concentration of 100%) was estimated from the known quantity of the Fucoxanthin standard used for identification purposes in the method development and an approximation of a ratio from the peak area ratio between the standard and the largest area recorded of the extracts at the time. At the time six of the runs in the optimization study had been done, and an estimating of the target concentration was possible.

The peak area of the Fx standard in ethanol divided by concentration was 4 533 130 mAU*min / mgL⁻¹ (Attachment #), and the largest peak area divided by concentration at the time was recorded for Op-5 at about 412,9 mAU*min / mgL⁻¹ (table # in attachment 6). The peak height of the Fx standard divided by concentration was about 11000 times greater than that of the highest peak of the extracts divided by concentration. With a standard concentration of 100 ±10 mg/L that gave an estimate of about 9 mg/L as a target concentration. With respect to minimizing the standard uncertainty in the dilution using the same autopipette, target concentration was set to 8 mg/L (attachment 1). To get a range of approximately 50-150% of the estimated target concentration the concentration levels in table 23 were made. The dilution factors were used to create standard solutions from a the between standard with a concentration of 100 ±10 mg/L.

Table 23 - Concentration levels #1 for the calibration curves for Fx

Levels:	Dilution factor:	Concentration [mg/L]
Level 1	7,5	13.3333 ± 1.3542
Level 2	10	10.0000 ± 1.0131
Level 3	12.5	8,0000 ± 0.8080
Level 4	15	6,6667 ± 0.6732
Level 5	17,5	5,7143 ± 0.5769

After ten measurements of five standard solutions for methanol, and five measurements of five standard solutions for ethanol it became clear that the lowest concentration level (level 5) was not low enough for the ethanol and 2-propanol extracts (with reference to peak areas in table #). The lowest peak area measured should have been considered, but luckily the two first datasets were done for methanol which had higher peak areas. The second dataset for the ethanol extracts and the remaining two datasets for 2-propanol were altered to accommodate this. The altered concentration levels (#2) can be found in table 24 below.

Table 24 - Altered concentration levels #2 for the calibration curves for Fx

Levels:	Dilution factor:	Concentration [mg/L]
Level 1	7,5	13,3333± 1.3542
Level 2	22	4,5455 ± 0.4584
Level 3	38,8	2,6455 ± 0.4579
Level 4	54	1,8519 ± 0.1863
Level 5	70	1,4286 ± 0.1437

Calibration curve for ethanol extracts

Ten measurements for nine different concentration levels from table 23 and 24, with a resulting calibration curve given in figure # in attachment 5. There were nine concentration levels since all levels were altered except the highest one at level 1, which means that only level 1 had two measurements. This calibration curve had to be altered because of the lower peak areas recorded for the ethanol extracts in general.

Calibration curve for ethanol extracts:

$$Y_{signal} = 1.7495 \times X_{concentration} + 8.1379$$

$$X_{concentration} = \frac{Y_{signal} - 8.1379}{1.7495}$$

This calibration curve had a coefficient of determination of 0.94184, and the concentration of the ethanol extracts were as low as about -0.54 mg Fx/L. The four levels that were altered to correct for the lower peaks areas were removed, resulting in six measurements on five concentration levels. The calibration curve can be found with the calibration curves for the

methanol and 2-propanol extracts in figure 24 at the end of the chapter about the linearity of the method.

This calibration curve had a coefficient of determination of 0.97366, an improvement on the linearity that made it acceptable for quantification. The constraint from having very low amounts of the Fucoxanthin standard resulted in a high standard deviation for the concentration of the between standard (ref. attachment 5), making the construction of calibration curves with standard solutions difficult. Additionally, the lowest concentration of the ethanol extracts was about -0.08 mg Fx/L compared to -0.54 mg Fx/L for the former calibration curve. The altered calibration curve was used for the optimization study, given in equation # below.

$$Y_{signal} = 1.6951 \times X_{concentration} + 7.3266$$

$$X_{concentration} = \frac{Y_{signal} - 7.3266}{1.6951}$$

Calibration curve for methanol extracts

Two measurements for each of the concentration levels from table 24, with a resulting calibration curve given in figure # with the other calibration curves.

The lowest peak area was slightly below the peak area for the lowest concentration level, but it was considered close enough to be acceptable without an alteration in the concentration levels. There was a considerable time constraint in this project because of the periodic unavailability of the HPLC system and the long runtimes in general. The HPLC system could only be used in tandem with faculty. This calibration curve had a coefficient of determination of 0.96675, which was considered acceptable.

Calibration curve for methanol extracts:

$$Y_{signal} = 0.9127 \times X_{concentration} + 9.1984$$

$$X_{concentration} = \frac{Y_{signal} - 9.1984}{0.9127}$$

Calibration curve for 2-propanol extracts

Two measurements for each of the concentration levels from table 24, with a resulting calibration curve that can be found in attachment 5.

This calibration curve had a coefficient of determination of 0.95606, which was a bit under an acceptable linearity. Figure # shows that concentration level 2 (second highest) was an outlier in reference to the calibration curve, and it was removed to alter the calibration curve. The calibration curve used in the optimization study had eight measurements on four concentration levels, which can be found with the other calibration curves in figure 24.

This calibration curve had a coefficient of determination of 0.98577, an acceptable linearity.

Calibration curve for 2-propanol extracts:

$$Y_{signal} = 1.2915 \times X_{concentration} + 2.7586$$

$$X_{concentration} = \frac{Y_{signal} - 2.7586}{1.2915}$$

Calibration curves for all the extracts

In figure # below the calibration curve used for the ethanol extracts can be found on top, in the middle for the methanol extracts, and on the bottom for the 2-propanol extracts. The coefficient of determination of the calibration curve was the worst for the methanol extracts at 0.96675, and second worst for the ethanol extracts with 0.97366, and the least bad for the 2-propanol extracts with 0.98577. None of these coefficients were considered good since they were not above 0.995, which was not surprising considering the large concentration range. To get a good linearity for a method the concentration range should go from 80% to 120%, which was not possible in this project considering the changing solvent types. With reference to table 25 below, the sensitivity of the method was the highest for the ethanol extracts, middling for the 2-propanol extracts, and lowest for the methanol extracts. Looking back the injection volume for the extracts with the highest level of STSR should have been increased to reduce the span of the concentration range. There were considerable constraints on time and availability of the HPLC system, which is why there were only two measurements for each concentration at the most. Ideally the number of measurements at each concentration level should have been five. Also, if time allowed the extracts would have been injected with altered injection volume to correct for the STSR of the extract, which would allow for a narrower concentration range.

Table 25 - Data from the calibration curves for all the extracts

Solvent type	Standard deviation, s_y [%RSD]	Slope, m	Offset, b
Ethanol	9.8586	1.6951	7.3266
Methanol	2.9843	0.9127	9.1984
2-propanol	9.8565	1.2915	2.7586

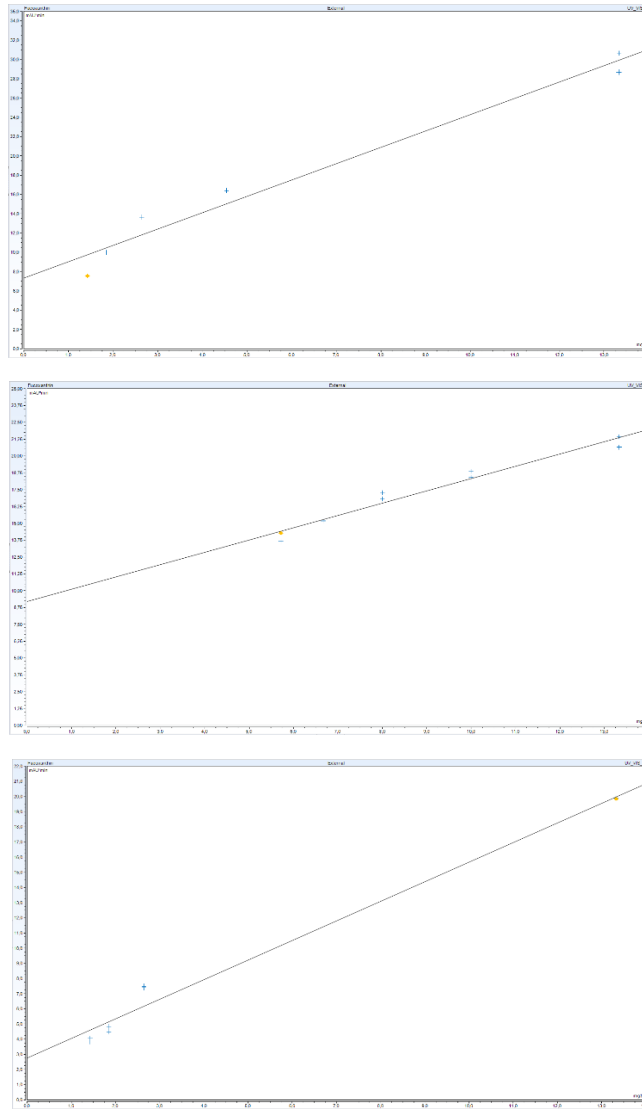


Figure 24 - Calibration curves used for the extracts in the optimization study. The calibration curve used for the ethanol extracts is on top, for the methanol extracts in the middle, and for the 2-propanol extracts on the bottom.

Limits of detection and quantification

Data from the calibration curves used for ethanol, methanol, and 2-propanol extracts can be found in table 25 above figure 24.

As an example, a calculation of the LOD for the ethanol extracts can be found below, calculated with formula (9).

$$\text{Minimal detectable concentration, } c_{dl,ethanol} = \left(\frac{3 \times 0.098586}{1.6951} \right) \frac{\text{mg Fx}}{\text{L}} = 0.174478 \frac{\text{mg Fx}}{\text{L}} \sim \mathbf{0.1745} \frac{\text{mg Fx}}{\text{L}}$$

As an example, a calculation of the LOQ for the ethanol extracts can be found below, calculated with formula (10).

$$\text{Minimal detectable concentration, } c_{dl,ethanol} = \left(\frac{10 \times 0.098586}{1.6951} \right) \frac{\text{mg Fx}}{\text{L}} = 0.581594 \frac{\text{mg Fx}}{\text{L}} \sim \mathbf{0.5816} \frac{\text{mg Fx}}{\text{L}}$$

The LOD and LOQ for all extracts can be found in table 26 below.

Table 26 - limit of detection and lower limit of quantification for all calibration curves used for the extracts

Solvent type	LOD [(mg Fx)/L]	LOQ [(mg Fx)/L]
Ethanol	0.1745	0.5816
Methanol	0.0981	0.3270
2-propanol	0.2290	0.7632

As seen by table 26 the LOD and LOQ for the calibration curve used for the methanol extracts were the lowest, middling for the ethanol extracts and highest for the 2-propanol extracts. This could be an effect of the fact that the determination method was made with a methanol extract.

Precision

Precision was measured by six repeated injections of the Op-13 extract, which was deemed a good candidate because of its middling resolution for the Fx-peak. The chromatograms were measured at 448 nm and can be found in attachment 5. The data extracted from the runs can be found in table 27 below.

Table 27 - Precision data for peak area, RT, and peak width

	Mean	Standard deviation	Relative standard deviation, [%RSD]
Peak area [mAU*min]	13.4781	0.5278	8.8
RT [min]	7.95	0.17	2.8
Peak width [min]	0.388	0.010	0.2

As seen by table 27 the precision on peak area was not good with a %RSD of 8.8, but since it was not above a %RSD of 10 it was considered acceptable. The precision for RT was nearly good at 2.8 %RSD, and the precision for peak width was good at 0.2 %RSD.

Unfinished method validation

Time would not allow for more validation runs of the determination method. Time and resources were an issue with this project with runtimes of 60 – 90 minutes and a limited window for use of the HPLC system.

Optimization of a Soxhlet extraction

The significant variables were solvent type and STSR. Solvent type is a nominal categorical variable with three levels for each solvent, and STSR is a continuous variable with two levels, 1:20 and 1:30. This amounted to six possible combinations of the factors in the design, illustrated in table 28 below. The combinations were run in triplicate experiments, resulting in a total of 18 experiments for the optimization study. The design of experiments can be found in table 29.

Table 28 - Possible combinations in factorial design

Ethanol, 1:20 sample to solvent ratio	Methanol, 1:20 sample to solvent ratio	2-propanol, 1:20 sample to solvent ratio
Ethanol, 1:30 sample to solvent ratio	Methanol, 1:30 sample to solvent ratio	2-propanol, 1:30 1:20 sample to solvent ratio

The experiments were randomized, and the order of experiments were referred to as Op-#, with reference to table 29 below.

Table 29 - DoE for a Soxhlet extraction optimization study

Experiment	Randomized order (Op-#)	Solvent type	STSR
1	12	Ethanol	1:20
2	18	Ethanol	1:20
3	3	Ethanol	1:20
4	7	Ethanol	1:30
5	8	Ethanol	1:30
6	15	Ethanol	1:30
7	16	Methanol	1:20
8	4	Methanol	1:20
9	9	Methanol	1:20
10	5	Methanol	1:30
11	17	Methanol	1:30
12	13	Methanol	1:30
13	14	2-propanol	1:20
14	2	2-propanol	1:20
15	11	2-propanol	1:20
16	6	2-propanol	1:30
17	10	2-propanol	1:30
18	1	2-propanol	1:30

The raw material data for the extractions can be found in table 25 below.

Table 30 - Weight and concentration of extracts in the optimization study

Extraction number	Weight DW [g]	Concentration [g DW/l]
1 (Op-12)	9,9986 ±0.0001	49.9930 ±0.4999
2 (Op-18)	9,9983 ±0.0001	49.9915 ±0.4999
3 (Op-3)	10,0012 ±0.0001	50.0060 ±0.5001
Mean value	9.9994 ±0.0001	49.9968 ±0.5000

4 (Op-7)	6.6759 ±0.0001	33.3795 ±0.3338
5 (Op-8)	6,6809 ±0.0001	33.4045 ±0.3340
6 (Op-15)	6,6736 ±0.0001	33.3680 ±0.3337
Mean value	6.6768 ±0.0001	33.3840 ±0.3338
7 (Op-16)	10,0031 ±0.0001	50.0155 ±0.5002
8 (Op-4)	9,9992 ±0.0001	49.9960 ±0.5000
9 (Op-9)	10,0040 ±0.0001	50.0200 ±0.5002
Mean value	10.0021 ±0.0001	50.0105 ±0.5001
10 (Op-5)	6,6642 ±0.0001	33.3210 ±0.3332
11 (Op-17)	6,6729 ±0.0001	33.3645 ±0.3336
12 (Op-13)	6,6750 ±0.0001	33.3750 ±0.3338
Mean value	6.6707 ±0.0001	33.3535 ±0.3335
13 (Op-14)	9,9949 ±0.0001	49.9745 ±0.4997
14 (Op-2)	10.0213 ±0.0001	50.1065 ±0.5011
15 (Op-11)	10,0070 ±0.0001	50.0350 ±0.5004
Mean value	10.0077 ±0.0001	50.0387 ±0.5004
16 (Op-6)	6.6638 ±0.0001	33.3190 ±0.3332
17 (Op-10)	6,6657 ±0.0001	33.3285 ±0.3333
18 (Op-1)	6.6828 ±0.0001	33.4140 ±0.3341
Mean value	6.6708 ±0.0001	33.3538 ±0.3335

RT, peak area, peak width, and resolution for the extracts in the optimization study can be found in table 31, and the chromatograms for each extract measured at 448 nm can be found in attachment 6.

The resolution was calculated as an average of the resolution between the foremost and backmost peak from the Fx peak, divided by an average of the peak widths of the peaks. The calculation for extraction number 1 (Op-12) was done with formula (4) and can be found below.

$$\text{Resolution of the foremost peak} = \frac{|6.100 - 6.625|}{\left(\frac{0.424 + 0.375}{2}\right)} = 1.3141$$

$$\text{Resolution of the backmost peak} = \frac{|7.442 - 6.625|}{\left(\frac{0.388 + 0.375}{2}\right)} = 2.1415$$

$$\text{Average resolution of Fx peak for extract 1} = \frac{(1.3141 + 2.1415)}{2} = 1.7278 \sim 1.728$$

Table 31 - RT, peak area, peak width, and resolution for the runs in the optimization study

Extraction number	Solvent type	RT for Fx [min]	Peak width for Fx [min]	RT for neighbour peaks [min]	Peak width for neighbour peaks [min]	Average resolution for Fx peak
1 (Op-12)	Ethanol	6.625 ± 0.645	0.375 ± 0.041	6.100 ± 0.450, 7.442 ± 0.623	0.424 ± 0.015, 0.388 ± 0.050	1.728 ± 0.064
2 (Op-18)	Ethanol	7.908 ± 0.645	0.457 ± 0.041	7.000 ± 0.450, 8.688 ± 0.623	0.423 ± 0.015, 0.488 ± 0.050	1.857 ± 0.064
3 (Op-3)	Ethanol	7.383 ± 0.645	0.423 ± 0.041	6.575 ± 0.450, 8.092 ± 0.623	0.397 ± 0.015, 0.442 ± 0.050	1.805 ± 0.064
Mean value		7.305 ± 0.645	0.418 ± 0.041	6.558 ± 0.450, 8.074 ± 0.623	0.415 ± 0.015, 0.439 ± 0.050	1.797 ± 0.064
4 (Op-7)	Ethanol	7.267 ± 0.482	0.413 ± 0.031	6.500 ± 0.386, 7.967 ± 0.555	0.389 ± 0.027, 0.467 ± 0.046	1.752 ± 0.098
5 (Op-8)	Ethanol	6.325 ± 0.482	0.353 ± 0.031	5.742 ± 0.386, 6.883 ± 0.555	0.342 ± 0.027, 0.375 ± 0.046	1.605 ± 0.098
6 (Op-15)	Ethanol	6.975 ± 0.482	0.396 ± 0.031	6.250 ± 0.386, 7.633 ± 0.555	0.344 ± 0.027, 0.416 ± 0.046	1.790 ± 0.098
Mean value		6.856 ± 0.482	0.387 ± 0.031	6.164 ± 0.386, 7.494 ± 0.555	0.358 ± 0.027, 0.419 ± 0.046	1.716 ± 0.098
7 (Op-16)	Methanol	7.417 ± 0.466	0.360 ± 0.023	6.617 ± 0.367, 8.113 ± 0.515	0.414 ± 0.098, 0.411 ± 0.023	1.936 ± 0.236
8 (Op-4)	Methanol	8.017 ± 0.466	0.386 ± 0.023	7.083 ± 0.367, 8.800 ± 0.515	0.341 ± 0.098, 0.404 ± 0.023	2.276 ± 0.236
9 (Op-9)	Methanol	7.100 ± 0.466	0.341 ± 0.023	6.358 ± 0.367, 7.792 ± 0.515	0.535 ± 0.098, 0.368 ± 0.023	1.823 ± 0.236
Mean value		7.511 ± 0.466	0.362 ± 0.023	6.686 ± 0.367, 8.235 ± 0.515	0.430 ± 0.098, 0.394 ± 0.023	2.012 ± 0.236

10 (Op-5)	Methanol	7.575 ± 0.428	0.364 ± 0.021	6.734 ± 0.461, 8.296 ± 0.460	0.318 ± 0.066, 0.400 ± 0.007	2.177 ± 0.336
11 (Op-17)	Methanol	7.458 ± 0.428	0.360 ± 0.021	6.996 ± 0.461, 8.163 ± 0.460	0.439 ± 0.066, 0.401 ± 0.007	1.505 ± 0.336
12 (Op-13)	Methanol	6.783 ± 0.428	0.325 ± 0.021	6.100 ± 0.461, 7.442 ± 0.460	0.424 ± 0.066, 0.388 ± 0.007	1.836 ± 0.336
Mean value		7.272 ± 0.428	0.350 ± 0.021	6.610 ± 0.461, 7.967 ± 0.460	0.394 ± 0.066, 0.396 ± 0.007	1.839 ± 0.336
13 (Op-14)	2-propanol	6.942 ± 0.492	0.490 ± 0.032	6.208 ± 0.380, 7.608 ± 0.577	0.469 ± 0.093, 0.516 ± 0.029	1.427 ± 0.056
14 (Op-2)	2-propanol	7.829 ± 0.492	0.549 ± 0.032	6.904 ± 0.380, 8.650 ± 0.577	0.635 ± 0.093, 0.562 ± 0.029	1.520 ± 0.056
15 (Op-11)	2-propanol	7.017 ± 0.492	0.499 ± 0.032	6.292 ± 0.380, 7.700 ± 0.577	0.479 ± 0.093, 0.509 ± 0.029	1.419 ± 0.056
Mean value		7.263 ± 0.492	0.513 ± 0.032	6.468 ± 0.380, 7.986 ± 0.577	0.528 ± 0.093, 0.529 ± 0.029	1.455 ± 0.056
16 (Op-6)	2-propanol	7.458 ± 0.430	0.524 ± 0.027	6.642 ± 0.335, 8.167 ± 0.454	0.480 ± 0.045, 0.507 ± 0.050	1.500 ± 0.039
17 (Op-10)	2-propanol	6.917 ± 0.430	0.495 ± 0.027	6.208 ± 0.335, 7.617 ± 0.454	0.424 ± 0.045, 0.600 ± 0.050	1.470 ± 0.039
18 (Op-1)	2-propanol	7.767 ± 0.430	0.548 ± 0.027	6.867 ± 0.335, 8.517 ± 0.454	0.514 ± 0.045, 0.524 ± 0.050	1.547 ± 0.039
Mean value		7.381 ± 0.430	0.522 ± 0.027	6.572 ± 0.335, 8.100 ± 0.454	0.473 ± 0.045, 0.544 ± 0.050	1.506 ± 0.039

The extracts used in the study were all determined within a period of three weeks at the most, and were stored in the dark at 4 °C. There was some variation of the resolution for the extracts, which was to be expected considering that the extracts had different matrixes. Re-runs of experiments Op-2, Op-5, Op-16, Op-17, and Op-18 were done to increase the confidence of the mean for the factor combination. Op-16, Op-17 and Op-18 were rerun to verify the mean because of extraordinary conditions at the time of the run. The disposable guard column filter was clogged between Op-17 and Op-18, whilst Op-16 was included because of high back pressure before the clogging. The filter was replaced, and the reruns were done with a low back pressure.

The determination method was developed with a methanol extract, so it was not surprising to see a superior resolution for the methanol extracts. The worst resolution was for the 2-

propanol extracts. The resolution in general ranged from 1.419 to 2.276, and the range was considered acceptable for a comparison.

Calculation of the response variable

The concentration of extraction number 1 was calculated using equation # from the calibration curve for ethanol extracts:

$$X_{concentration,1} = \frac{Y_{signal,1} - 7.3266}{1.6951} = \frac{11.3936 - 7.3266}{1.6951}$$

$$= 2.399268 \frac{mg Fx}{L} \sim 2.3993 \frac{mg Fx}{L}$$

To standardize the concentration with regards to the dilution (different STSRs) it was divided by the dry weight of the extract:

$$\frac{\left(\frac{mg Fx}{L}\right)}{g DW} = \frac{2.399268 \frac{mg Fx}{L}}{9.9986 g DW} = 0.239960 \sim 0.2400 \frac{mg Fx}{g DW}$$

With reference to table 32 below, extraction number 1 through 6 were ethanol extracts, extraction number 7 through 12 were methanol extracts, and extraction number 13 through 18 were 2-propanol extracts.

Table 32 - Peak area, weight (DW), concentration of Fx extracted, and standardized concentration of Fx extracted in optimization study

Extraction number	Peak area [mAU*min]	Weight (DW) [g]	Concentration of Fucoxanthin extracted [$\frac{mg Fx}{L}$]	Standardized concentration of Fucoxanthin extracted [$\frac{\left(\frac{mg Fx}{L}\right)}{g DW}$]
1 (Op-12)	11.3936 ± 2.3697	9,9986 ±0.0001	2.399268 ~ 2.3993 ± 1.3980	0.239960 ~ 0.2400 ± 0.1398
2 (Op-18)	14.7828 ± 2.3697	9,9983 ±0.0001	4.398679 ~ 4.3987 ± 1.3980	0.439943 ~ 0.4399 ± 0.1398
3 (Op-3)	10.2191 ± 2.3697	10,0012 ±0.0001	1.706389 ~ 1.7064 ± 1.3980	0.170618 ~ 0.1706 ± 0.1398
Mean value	12.1318 ± 2.3697	9.9994 ±0.0001	2.834779 ~ 2.8348 ± 1.3980	0.283507 ~ 0.2835 ± 0.1398
4 (Op-7)	7.6734 ± 0.2630	6.6759 ±0.0001	0.204590 ~ 0.2046 ± 0.1551	0.030646 ~ 0.0306 ± 0.0232
5 (Op-8)	7.2463 ± 0.2630	6,6809 ±0.0001	-0.047372 ~ -0.0474 ± 0.1551	-0.007091 ~ -0.0071 ± 0.0232

6 (Op-15)	7.1941 ± 0.2630	6,6736 ±0.0001	-0.078166 ~ - 0.0782 ± 0.1551	-0.011713 ~ -0.0117 ± 0.0232
Mean value	7.3713 ± 0.2630	6.6768 ±0.0001	0.026351 ~ 0.0264 ± 0.1551	-0.003947 ~ -0.0039 ± 0.0232
7 (Op-16)	18.4206 ± 0.4485	10,0031 ±0.0001	10.104306 ~ 10.1043 ± 0.4915	1.010117 ~ 1.0101 ± 0.0461
8 (Op-4)	17.6596 ± 0.4485	9,9992 ±0.0001	9.270516 ~ 9.2705 ± 0.4915	0.927126 ~ 0.9271 ± 0.0461
9 (Op-9)	18.4515 ± 0.4485	10,0040 ±0.0001	10.138162 ~ 10.1382 ± 0.4915	1.003415 ~ 1.0034 ± 0.0461
Mean value	18.1772 ± 0.4485	10.0021 ±0.0001	9.83766 ~ 9.8377 ± 0.4915	0.980219 ~ 0.9802 ± 0.0461
10 (Op-5)	13.4965 ± 0.5741	6,6642 ±0.0001	4.709214 ~ 4.7092 ± 0.6290	0.706644 ~ 0.7066 ± 0.0948
11 (Op-17)	12.8454 ± 0.5741	6,6729 ±0.0001	3.995837 ~ 3.9958 ± 0.6290	0.598816 ~ 0.5988 ± 0.0948
12 (Op-13)	12.3520 ± 0.5741	6,6750 ±0.0001	3.455243 ~ 3.4552 ± 0.6290	0.517639 ~ 0.5176 ± 0.0948
Mean value	12.8980 ± 0.5741	6.6707 ±0.0001	4.053431 ~ 4.0534 ± 0.6290	0.607700 ~ 0.6077 ± 0.0948
13 (Op-14)	11.6949 ± 0.4443	9,9949 ±0.0001	6.919319 ~ 6.9193 0.3440	0.692285 ~ 0.6923 ± 0.0352
14 (Op-2)	10.8064 ± 0.4443	10.0213 ±0.0001	6.231359 ~ 6.2314 0.3440	0.621811 ~ 0.6218 ± 0.0352
15 (Op-11)	11.2376 ± 0.4443	10,0070 ±0.0001	6.565234 ~ 6.5652 0.3440	0.656064 ~ 0.6561 ± 0.0352
Mean value	11.2463 ± 0.4443	10.0077 ±0.0001	6.571971 ~ 6.5720 ± 0.3440	0.656720 ~ 0.6567 ± 0.0352
16 (Op-6)	6.6815 ± 0.6871	6,6638 ±0.0001	3.037476 ~ 3.0375 ± 0.5320	0.455817 ~ 0.4558 ± 0.0802
17 (Op-10)	7.6818 ± 0.6871	6,6657 ±0.0001	3.812002 ~ 3.8120 ± 0.5320	0.571883 ~ 0.5719 ± 0.0802
18 (Op-1)	6.3657 ± 0.6871	6,6828 ±0.0001	2.792954 ~ 2.7930 ± 0.5320	0.417932 ~ 0.4179 ± 0.0802
Mean value	6.9097 ± 0.6871	6.6708 ±0.0001	3.214144 ~ 3.2144 ± 0.5320	0.481877 ~ 0.4819 ± 0.0802

Analysis of optimization study

A plot of the standardized concentration of extracted Fx for the experiments in the optimization study can be found in figure 25 below.

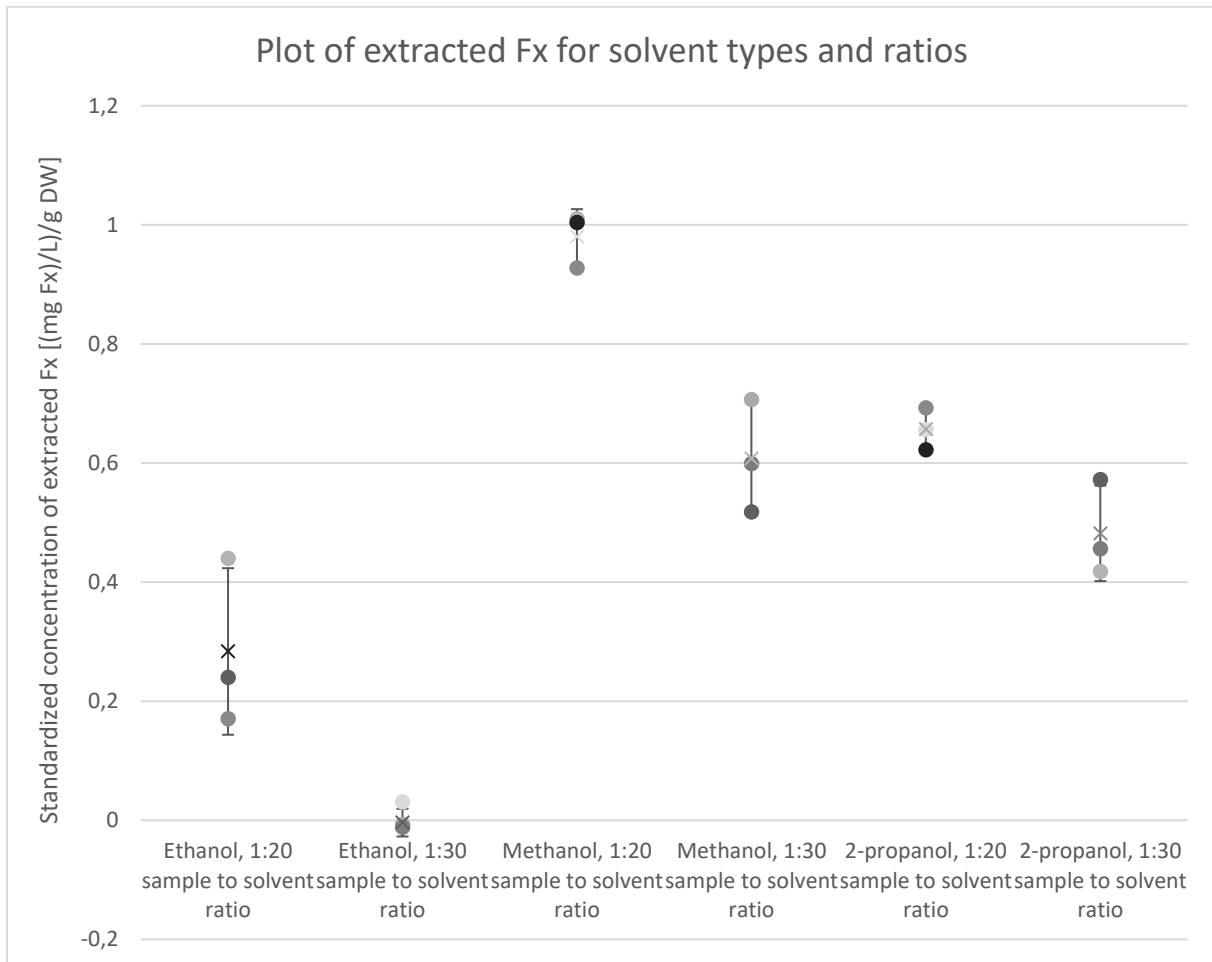


Figure 25 - Plot of standardized concentration of extracted Fx for the different factors in the optimization study, with mean values (marked as x in the plot) and error bars (standard deviation)

From figure 25 it was observed that methanol with a STSR of 1:20 provided the highest levels of extracted Fx, and ethanol provided the lowest levels. Furthermore, the levels of extracted Fx were reduced for all solvents with a STSR of 1:30. This could indicate that the optimal point of STSR was lower than 1:30 and having such a high ratio diluted the extracts rather than increasing the extraction of Fx.

Factorial analysis

General formula for main effect of a solvent:

Main effect of solvent

$$= \left(\text{Mean of solvent extracts} - \frac{\text{Sum of the other solvent extract means}}{2} \right)$$

Main effect of ethanol with a 1:20 sample to solvent ratio:

$$\begin{aligned} \text{Main effect of ethanol (1:20)} &= \left(0.283507 - \frac{(0.980219 + 0.656720)}{2} \right) \frac{\left(\frac{\text{mg Fx}}{\text{L}} \right)}{\text{g DW}} \\ &= -0.534963 \sim -0.5350 \frac{\left(\frac{\text{mg Fx}}{\text{L}} \right)}{\text{g DW}} \end{aligned}$$

Table 33 - Main effects of the solvent types sorted by STSR

Solvent type	Main effects 1:20 sample to solvent ratio $\left[\frac{\left(\frac{\text{mg Fx}}{\text{L}} \right)}{\text{g DW}} \right]$	Main effects 1:30 sample to solvent ratio $\left[\frac{\left(\frac{\text{mg Fx}}{\text{L}} \right)}{\text{g DW}} \right]$
Ethanol	-0.534963	-0.548736
Methanol	0.510106	0.368735
2-propanol	0.024857	0.180001

A plot for main effects on standardized concentration of Fx in the extracts can be seen in figure 26 below.

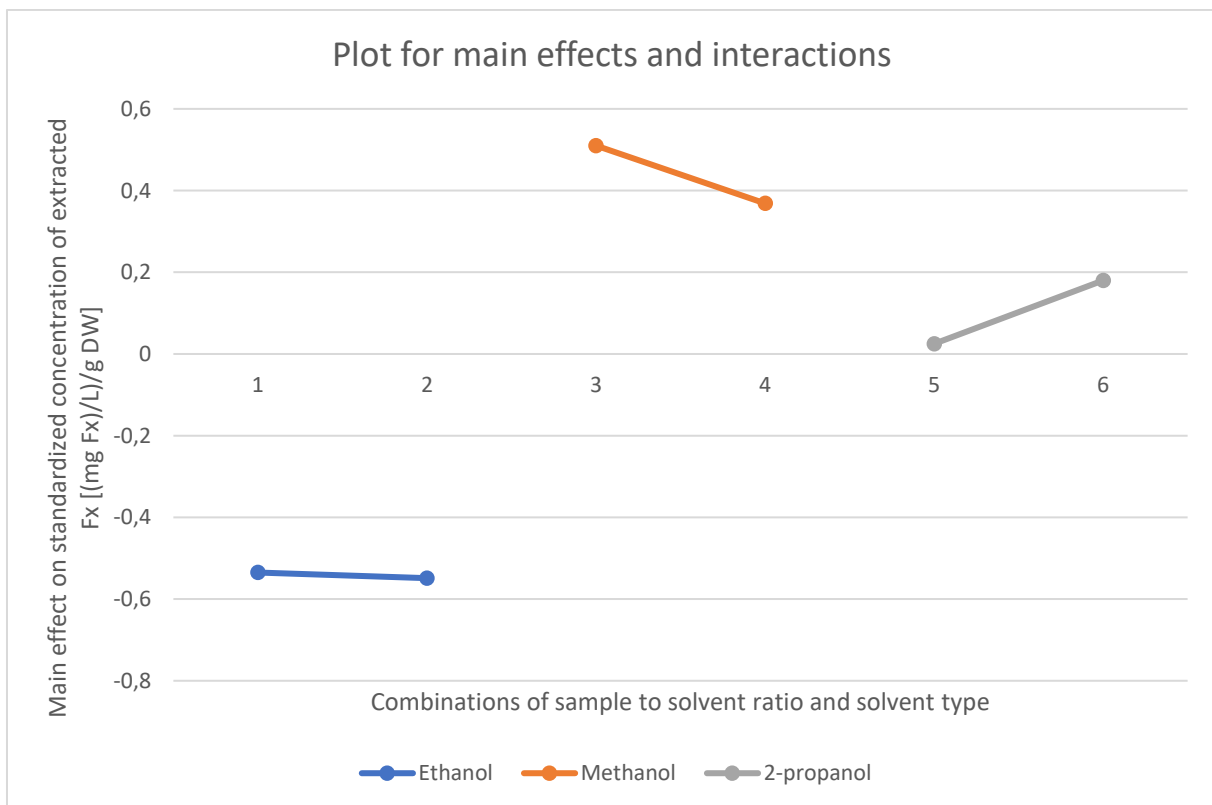


Figure 26 - A plot for main effects on standardized concentration of Fx in the extracts. Points 1, 3 and 5 had STSRs of 1:20, and points 2, 4 and 6 had STSRs of 1:30

As seen by figure 26 methanol had the highest main effect, and ethanol had the lowest main effect. For the ethanol extracts there was a minimal interaction involving increased sample to

solvent ratio, for the methanol extracts an increase of ratio had a detrimental effect, and for the 2-propanol extracts an increase had a positive effect. This may have been an indication that the ideal sample to solvent ratio for methanol was lower than for ethanol and 2-propanol, especially in comparison to the latter solvent. Hence, the diluting effect was worse for the methanol extracts.

Relationship between temperature and Fx concentration

The optimization study was run on a Soxhlet-system without the use of vacuum to lower the boiling points of the solvents (Source), so there was a need to investigate a possible correlation between the boiling points and the standardized concentration of extracted Fx. A plot of the boiling points of the solvents (<https://onlinelibrary.wiley.com/doi/pdf/10.1002/9783527632220.app1>) and the standardized concentration of Fx can be found in figures 27 and 28 below.

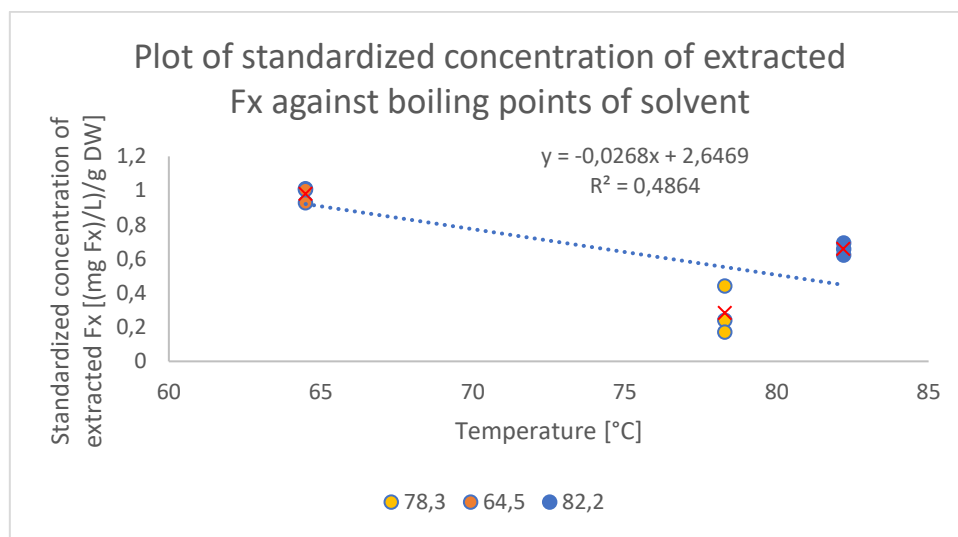


Figure 27 - A plot of standardized concentration of Fx against the boiling temperature of the solvent type with a STSR of 1:20. Orange points are for methanol extracts, yellow points are for ethanol extracts, and blue points are for 2-propanol extracts

As seen by figure 27 there was a negative correlation between the concentration of Fx and the boiling point of the solvent with a R^2 of 0,4864. Methanol had the highest yield of Fx and the lowest boiling point, but this trend did not extend to ethanol and 2-propanol. Alginor will use a vacuum to lower the boiling point and might therefore get higher yields with 2-propanol than with a conventional Soxhlet-setup used in this study.

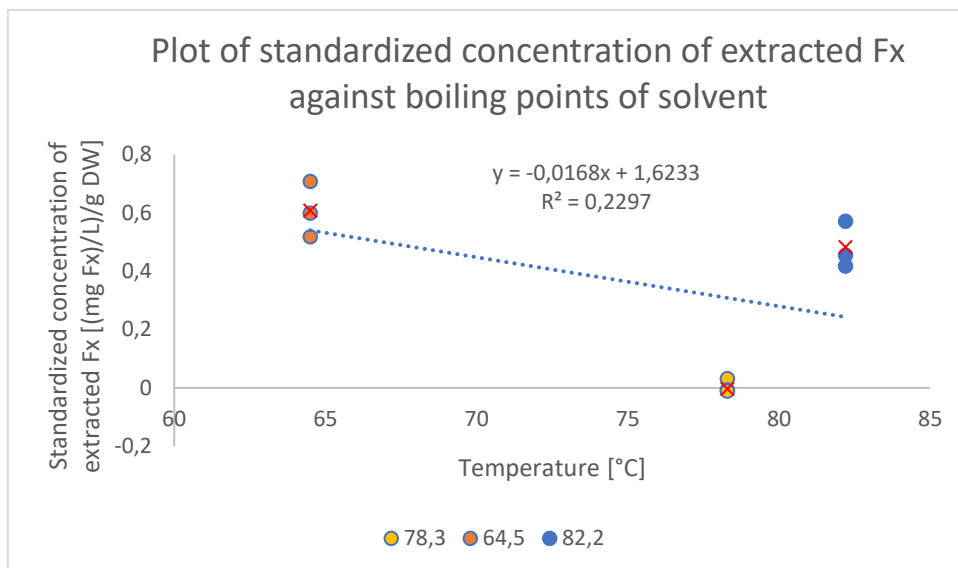


Figure 28 - A plot of standardized concentration of Fx against the boiling temperature of the solvent type with a STSR of 1:30. Orange points are for methanol extracts, yellow points are for ethanol extracts, and blue points are for 2-propanol extracts

As seen by figure 28 the negative correlation factor was lower for extracts with a sample to solvent ratio of 1:30, reduced from 0,4864 to 0,2297. Overall, the effect of a negative correlation with an increased boiling point should be taken into account along with the results of a ANOVA-test.

ANOVA analysis

A one-sided ANOVA for the means with 1:20 sample to solvent ratio was performed to check significance in the variation. The means with 1:30 sample to solvent ratio were not included to make a two-way ANOVA because the interactions found in figure 26 indicate that the variables are dependent, and one of the requirements for a two-way ANOVA is that the factors are independent of each other. The means with a 1:30 STSR were so low compared to the mean with a 1:20 STSR that they were not considered for significance with a second one-way ANOVA.

Variation within the samples

The measurements from different extraction conditions in the optimization study, the means of these measurements, and an overall mean can be found in table 34 below.

The null hypothesis, H_0 , is that the variance within the samples is not significantly different from the variance between the samples. The test hypothesis, H_1 , is that there is a significant difference between the sources of variation.

Table 34 - The measurements from different extraction conditions in the optimization study, the means of these measurements, and an overall mean

	Standardized concentration of Fx extracted, $\left[\frac{\text{mg Fx}}{\text{L}}\right]$ g DW			Mean
Ethanol, 1:20 STSR	0.2400	0.4399	0.1706	0.2835
Methanol, 1:20 STSR	1.0101	0.9271	1.0034	0.9802
2- propanol, 1:20 STSR	0.6923	0.6218	0.6561	0.6567
Overall mean = 0.6401				

As seen by table 34 the number of measurements, n , was 3, and the number of groups, h , was 3.

Null hypothesis: The within-sample variation = The between-sample variation

Test hypothesis: The within-sample variation < The between-sample variation

Calculation of the variance for the ethanol extracts was done as an example below with formula 13:

$$\begin{aligned} \sum \frac{(X_i - \bar{X})^2}{(n-1)} &= \frac{(0.2400 - 0.2835)^2 + (0.4399 - 0.2835)^2 + (0.1706 - 0.2835)^2}{3-1} \\ &= \frac{0.03909962}{2} = 0.01954981 \sim 0.0195 \frac{\left(\frac{\text{mg Fx}}{\text{L}}\right)}{\text{g DW}} \end{aligned}$$

The variation for the methanol and 2-propanol extracts were done in the same way.

An estimate of the variation within the samples, σ_0^2 , was calculated with formula 14:

$$\begin{aligned} \sigma_0^2 &= \sum_i \sum_j \frac{(X_{ij} - \bar{X}_i)^2}{h(n-1)} = \frac{0.01954981 + 0.00212593 + 0.001242865}{3} \\ &= 0.007639535 \sim 0.0076 \frac{\left(\frac{\text{mg Fx}}{\text{L}}\right)}{\text{g DW}} \end{aligned}$$

Variation between the samples

An estimate of the variation between the samples, σ_0^2 , is calculated with formula 15:

$$\begin{aligned}\sigma_0^2 &= n \times \sum_i \frac{(\bar{X}_i - \bar{X})^2}{(h-1)} \\ &= 3 \times \frac{(0.2835 - 0.6401)^2 + (0.9802 - 0.6401)^2 + (0.6567 - 0.6401)^2}{(3-1)} \\ &= 0.364660695 \sim 0.3647 \frac{\left(\frac{\text{mg Fx}}{\text{L}}\right)}{\text{g DW}}\end{aligned}$$

The F-value for the F-test was calculated by formula 16 and compared to the critical F-values found for a one-tailed test.

$$F - \text{value} = \frac{\sigma_0^2 \text{ between samples}}{\sigma_0^2 \text{ within samples}} = \frac{0.364660695}{0.007639535} = 47.7333627 \sim \mathbf{47.73}$$

A summary of the variation within and between samples and the resulting f-value can be found below in table 35.

Table 35 - ANOVA-table with sums of squares and a resulting F-value

Source of variation	Sum of variation	F-value
Within-sample	0.007639535	47.73
Between-sample	0.364660695	

The degrees of freedom were six for the variation within the samples ($h(n-1)$) and two for the variation between the samples ($n-1$), and with a p-value of 0.05 the critical value was found using a table (p. 280, stat): $F_{critical} = \mathbf{5.143}$

The null hypothesis was discarded, there was a significant difference between the extracted concentration of Fx from the different solvent types.

The least significant difference method was used to confirm that there was a significant difference between the methanol and 2-propanol extracts, considering the much lower values for the ethanol extracts. The test value was calculated from formula 17:

$$\begin{aligned}\text{least significant difference} &= s \times \sqrt{\left(\frac{2}{n}\right) \times t_{h(n-1)}} = \sqrt{0.007639535} \times \sqrt{\frac{2}{3}} \times 2.45 \\ &= 0.174845 \sim \mathbf{0.1748} \frac{\left(\frac{\text{mg Fx}}{\text{L}}\right)}{\text{g DW}}\end{aligned}$$

The difference between the means of the methanol and 2-propanol extracts was 0.3235, almost twice the difference needed for significance.

The least significant difference method confirmed a significant difference between the methanol and 2-propanol extracts, proving that methanol was the superior solvent for Fx.

Analytes other than Fucoxanthin

As seen by figure 29 below there were large differences in the color of the extracts, indicating that the solvents extracted compounds with a significantly different efficiency. The color of the extracts solved with 2-propanol (Op-1, Op-2, and Op-6) were brown, indicating that the predominant pigment extracted was fucoxanthin which are brown in color, not chlorophylls which are green in color. The extracts solved with ethanol (Op-3) and methanol (Op-5 and Op-6) were green, indicating a predominant presence of chlorophyll pigments. One other difference between the extracts in color was that the methanol extracts looked richer in color than the ethanol extracts, even diluted with a STSR of 1:30. These trends observed for the first six extracts were consistent for all the 18 extractions in the optimization study. The color of the extracts could not be used to determine the best solvent for any of the analytes, it only served to indicate the presence of fucoxanthin or chlorophylls.

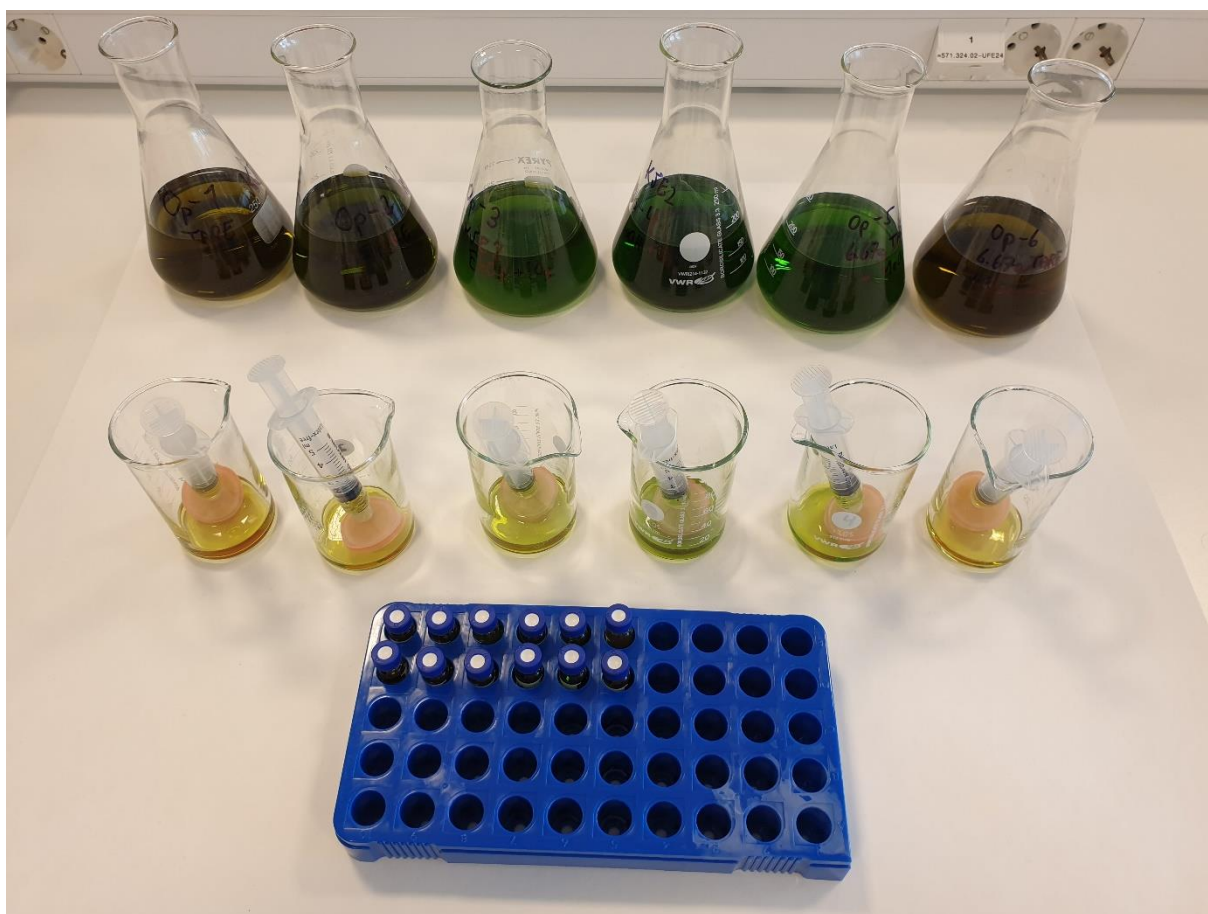


Figure 29 - Sample preparation of the extracts from Op-1 to Op-6

Figure: Sample preparation of the extracts from Op-1 to Op-6.

To get an identification of analytes like polyphenols, chlorophylls and β -carotene in the extracts standards were co-eluted along with extraction number 12 (Op-13). Extraction number 12 was chosen because of its middling resolution and numerous chromatograms from repeatability measurements in the method validation for comparison at 448 nm. First the bandwidth for the maximum absorption of the standards had to be found.

Phloroglucinol has a maximum absorption at 246 - 261 nm according to literature (<https://spectrabase.com/spectrum/7XHLcY0R211>,

<https://pubchem.ncbi.nlm.nih.gov/compound/Phloroglucinol#section=UV-Spectra>) and 100 mg/L of the standard in methanol was injected with a recording at 240 nm, 247 nm, 254 nm, and at 265 nm. With the contour plot given in attachment 6 the maximum absorption with the gradient program developed was measured at 231 nm. There was difficulty in finding absorption in this range because of the absorbance of ethyl acetate in the mobile phase.

Chlorophyll a has a maximum absorption at 405 nm according to literature (https://www.researchgate.net/publication/51909710_Ab_Initio_Calculation_of_UV-Vis_Absorption_Spectra_of_a_Single_Molecule_Chlorophyll_a_Comparison_Study_between_RHFCIS_TDDFT_and_Semi-Empirical_Methods), and at 418 nm in other sources (<https://omlc.org/spectra/PhotochemCAD/html/122.html>). 50 mg/L of the standard in methanol was injected with a recording at 405 nm, 410 nm, 415 nm, and at 420 nm. With the contour plot given in attachment 6 the maximum absorption with the gradient program developed was measured at 431 nm.

β -carotene has a maximum absorbance at 451 nm in hexane (<https://omlc.org/spectra/PhotochemCAD/html/041.html>), and somewhere in the range of 440 – 457 nm in hexane according to another source (<https://pubchem.ncbi.nlm.nih.gov/compound/beta-Carotene>). 100 mg/L of the standard in methanol was injected with a recording at 440 nm, 446 nm, 452 nm, and at 458 nm. With the contour plot given in attachment 6 the maximum absorption with the gradient program developed was measured at 451 nm.

A mixture of extraction number 12 (Op-13), chlorophyll a, phloroglucinol, and β -carotene was made with a 100 μ L of each. 20 μ L of this mixture was injected, and the chromatograms are given with a comparison to an injection of 20 μ L of extraction 12 in figures 30-33.

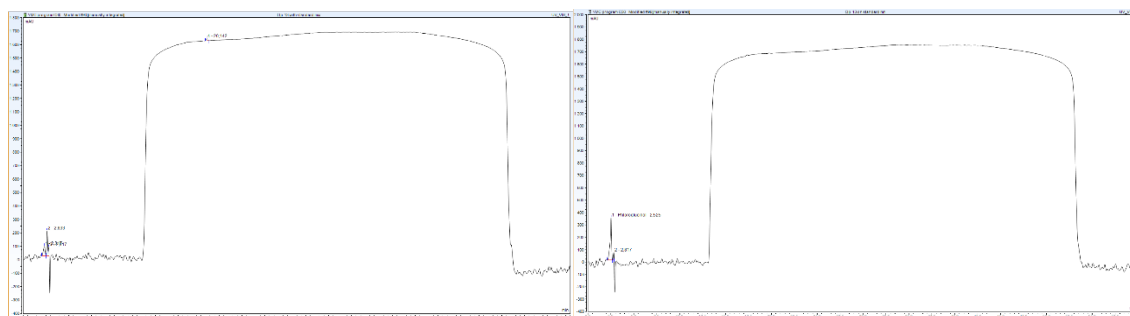


Figure 30 - A chromatogram of a standard-extract-mixture at 231 nm on the left compared to extract number 12 (Op-13) on the right at 231 nm, the maximum absorption point of phloroglucinol

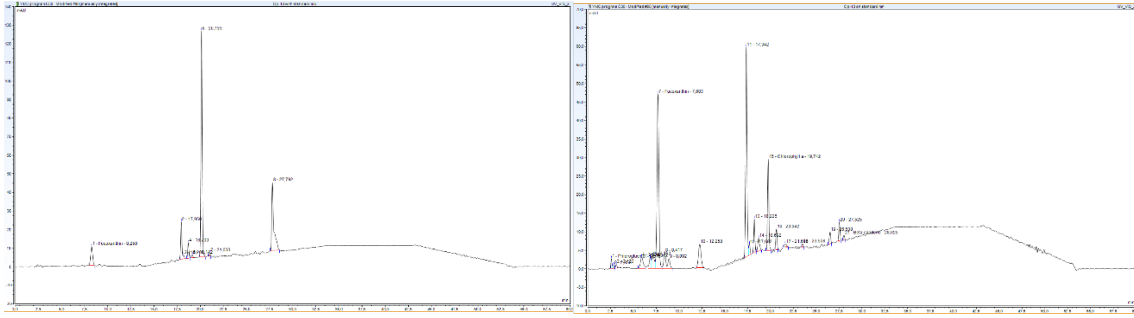


Figure 31 - A chromatogram of a standard-extract-mixture at 431 nm on the left compared to extract number 12 (Op-13) on the right at 431 nm, the maximum absorption point of chlorophyll a

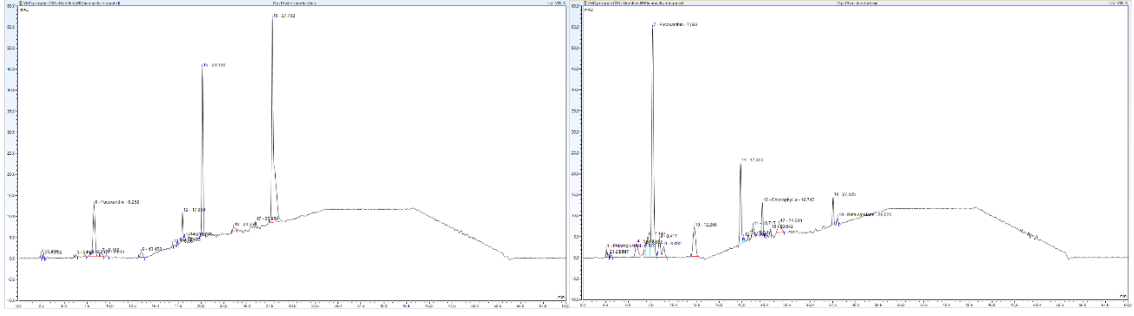


Figure 32 - A chromatogram of a standard-extract-mixture at 448 nm on the left compared to extract number 12 (Op-13) on the right at 448 nm, the maximum absorption point of fucoxanthin

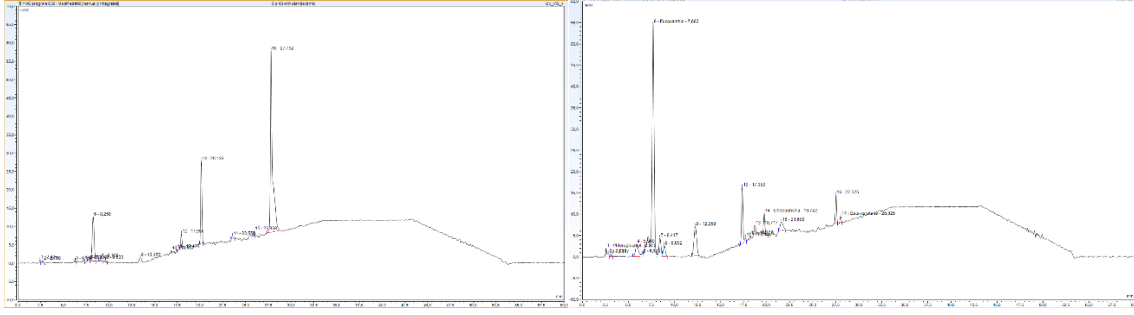


Figure 33 - A chromatogram of a standard-extract-mixture at 451 nm on the left compared to extract number 12 (Op-13) on the right at 451 nm, the maximum absorption point of β -carotene

Conclusion

The significant factors for the extraction conditions were found to be solvent type, sample to solvent ratio, and extraction time. Previous work done at the behest of Alginor had found the optimal extraction time to be five cycles. The solvent types that were suitable with regards to greenness were ethanol, methanol, and 2-propanol. The sample to solvent ratios that were tested were 1:20 and 1:30. A factorial design with 18 experiments was set up to find the optimal extraction conditions, but first, the determination method had to be developed. The column used was YMC Carotenoid (250 mm x 4.6 mm I.D., 5 μ m particle size) with a temperature set at 36 °C, and the injection volume for the samples was 20 μ L. The mobile phases used were water (A), Methanol (B), and Ethyl acetate (C), and the gradient program (A%:B%:C%) was made up by the following linear gradients: 3:94:3 from start to 10 minutes, 3:62:35 at 15 minutes, 3:47:50 at 22 minutes, 3:7:90 at 30 minutes, 3:7:90 at 40 minutes, 3:94:3 at 50 minutes, and 3:94:3 at 60 minutes. The resolutions for the extracts varied from 1.455 ± 0.056 for the 2-propanol extracts to 2.012 ± 0.236 for the methanol extracts, suitable for quantification. The linearity coefficients varied from 0.96675 to 0.98577, which was acceptable for this comparison. A factorial analysis showed that methanol with a sample to solvent ratio of 1:20 was the optimal extraction conditions. A plot of the main effects revealed that there were interaction effects between the solvent type and sample to solvent ratio factors, and that methanol had a decrease in extracted Fucoxanthin, whilst 2-propanol had a slight increase. The results for the optimal extraction conditions were confirmed by a significant variance by a one-way ANOVA-test, and a least significant difference test between the methanol and 2-propanol extracts. The ethanol extracts had a very low concentration of Fucoxanthin compared to the other solvent extracts. The concentration of Fx divided by DW for the ethanol extracts with a 1:20 STSR was 0.2835 ± 0.1398 (mg/l)/g DW, and with a 1:30 STSR -0.0039 ± 0.0232 (mg/l)/g DW. The concentration of Fx divided by DW for the methanol extracts with a 1:20 STSR was 0.9802 ± 0.0461 (mg/l)/g DW, and with a 1:30 STSR 0.6077 ± 0.0948 (mg/l)/g DW. The concentration of Fx divided by DW for the 2-propanol extracts with a 1:20 STSR was 0.6567 ± 0.0352 (mg/l)/g DW, and with a 1:30 STSR 0.4819 ± 0.0802 (mg/l)/g DW.

Future work

There should be a full optimization study on the extraction conditions for Fucoxanthin from *Laminaria hyperborea* using response surface methods to find the optimal STSR for solvents methanol and 2-propanol, and then compare the yields of Fucoxanthin. Ethanol gave much lower yields and can probably be discounted. There should be a study comparing yields of Fucoxanthin with and without additives like ascorbic acid in the extractions. Ascorbic acid has been shown to reduce the trans-cis isomerization of Fucoxanthin (Source).

References

1. ASA A. About us 2022 [Available from: <https://alginor.no/about-us/>].
2. ASA A. Homepage. 2022.
3. ASA A. A major green deal for Alginor 2022 [Available from: <https://alginor.no/2021/07/a-major-green-deal-for-alginor/>].
4. ASA A. Biorefining 2022 [Available from: <https://alginor.no/solutions/biorefining/>].
5. Registry AFTSaD. Formaldehyde and Your Health 2022 [Available from: <https://www.atsdr.cdc.gov/formaldehyde/>].
6. ASA A. Nutraceuticals - Carotenoids 2022 [Available from: <https://alginor.no/products/nutraceuticals/>].
7. ASA A. Pharmaceuticals - Polyphenols 2022 [Available from: <https://alginor.no/products/pharmaceuticals/>].
8. ASA A. Our raw material 2022 [Available from: <https://alginor.no/about-us/our-raw-material/>].
9. Poojary MM, Barba FJ, Aliakbarian B, Dons F, Pataro G, Dias DA, et al. Innovative alternative technologies to extract carotenoids from microalgae and seaweeds. *Mar Drugs*. 2016;14(11):214.
10. Gebregziabher BS, Zhang S, Qi J, Azam M, Ghosh S, Feng Y, et al. Simultaneous determination of carotenoids and chlorophylls by the hplc-uv-vis method in soybean seeds. *Agronomy (Basel)*. 2021;11(4):758.
11. Derrien MI, Badr A, Gosselin A, Desjardins Y, Angers P. Optimization of a green process for the extraction of lutein and chlorophyll from spinach by-products using response surface methodology (RSM). *Food science & technology*. 2017;79:170-7.
12. ASA A. Sustainability 2022 [Available from: <https://alginor.no/sustainability/>].
13. Rodr?guez-Bernaldo de Quir?s A, Frecha-Ferreiro S, Vidal-P?rez AM, L?pez-Hern?ndez J. Antioxidant compounds in edible brown seaweeds. *European food research & technology*. 2010;231(3):495-8.
14. Yal??n S, Karaka z, Okudan Ek, Ba?kan KSz, eki SD, Apak Ra. HPLC Detection and Antioxidant Capacity Determination of Brown, Red and Green Algal Pigments in Seaweed Extracts. *J Chromatogr Sci*. 2021;59(4):325-37.
15. Grodowska K, Parczewski A. Organic solvents in the pharmaceutical industry. *Acta Pol Pharm*. 2010;67(1):3-12.
16. Zaharieva MM, Zheleva-Dimitrova D, Rusinova-Videva S, Ilieva Y, Brachkova A, Balabanova V, et al. Antimicrobial and Antioxidant Potential of *Scenedesmus obliquus* Microalgae in the Context of Integral Biorefinery Concept. *Molecules*. 2022;27(2):519.
17. Hynstova V, Sterbova D, Klejdus B, Hedbavny J, Huska D, Adam V. Separation, identification and quantification of carotenoids and chlorophylls in dietary supplements containing *Chlorella vulgaris* and *Spirulina platensis* using High Performance Thin Layer Chromatography. *J Pharm Biomed Anal*. 2018;148:108-18.
18. Rodr?guez-Bernaldo de Quir?s A, Costa HS. Analysis of carotenoids in vegetable and plasma samples: A review. *Journal of food composition and analysis*. 2006;19(2):97-111.
19. Simonovska B, Vovk I, Glavnik V, erneli K. Effects of extraction and high-performance liquid chromatographic conditions on the determination of lutein in spinach. *J Chromatogr A*. 2013;1276:95-101.
20. Gleize Ba, Steib Mn, Andr M, Reboul E. Simple and fast HPLC method for simultaneous determination of retinol, tocopherols, coenzyme Q10 and carotenoids in complex samples. *Food chemistry*. 2012;134(4):2560-4.

21. Ponder A, Hallmann E. Phenolics and carotenoid contents in the leaves of different organic and conventional raspberry (*Rubus idaeus* L.) cultivars and their in vitro activity. *Antioxidants*. 2019;8(10):458.
22. Machu L, Misurcova L, Ambrozova JV, Orsavova J, Mlcek J, Sochor J, et al. Phenolic content and antioxidant capacity in algal food products. *Molecules*. 2015;20(1):1118-33.
23. Yalçın S, Uzun M, Karakaş Z, Şözen Başkan K, Okudan Ek, Apak MRa. Determination of Total Antioxidant Capacities of Algal Pigments in Seaweed by the Combination of High-Performance Liquid Chromatography (HPLC) with A Cupric Reducing Antioxidant Capacity (CUPRAC) Assay. *Analytical letters*. 2021;54(14):2239-58.
24. Dewick PM. *Medicinal Natural Products: A Biosynthetic Approach*. 3rd ed. ed. West Sussex, UK: John Wiley & Sons Ltd; 2009.
25. Airanthi MKW-A, Hosokawa M, Miyashita K. Comparative Antioxidant Activity of Edible Japanese Brown Seaweeds. *J Food Sci*. 2011;76(1):C104-C11.
26. Sibel Yalçın ÖK, Emine Şükran Okudan, Kevser Sözen Başkan, Sema Demirci Çekiş, Reşat Apak. HPLC Detection and Antioxidant Capacity Determination of Brown, Red and Green Algal Pigments in Seaweed Extracts. *Journal of Chromatographic Science*. 2021;59(4):325-37.
27. Koivikko R, Loponen J, Pihlaja K, Jormalainen V. High-performance liquid chromatographic analysis of phlorotannins from the brown alga *Fucus Vesiculosus*. *Phytochem Anal*. 2007;18(4):326-32.
28. Ford L, Theodoridou K, Sheldrake GN, Walsh PJ. A critical review of analytical methods used for the chemical characterisation and quantification of phlorotannin compounds in brown seaweeds. *Phytochem Anal*. 2019;30(6):587-99.
29. Miller JM. *Chromatography : concepts and contrasts*. 2nd ed. Hoboken, N.J: Wiley; 2005.
30. Pun Creso MO, Lage Yusty MA. Comparison of supercritical fluid extraction and Soxhlet extraction for the determination of PCBs in seaweed samples. *Chemosphere*. 2005;59(10):1407-13.
31. Harris DC, Lucy CA. *Quantitative chemical analysis*. 9th ed. New York: Freeman; 2016.
32. YMC. YMC Carotenoid 2022 [Available from: https://www.ymc.co.jp/en/columns/ymc_carotenoid/].
33. Otto M. *Chemometrics : statistics and computer application in analytical chemistry*. Weinheim, Germany: Wiley-VCH; 2017.
34. Glasgow Uo. Coding categorical predictor variables in factorial designs 2019 [Available from: <https://talklab.psy.gla.ac.uk/tvw/catpred/>].
35. Kumar LRG, Treasa Paul P, Anas KK, Tejpal CS, Chatterjee NS, Anupama TK, et al. Screening of effective solvents for obtaining antioxidant-rich seaweed extracts using principal component analysis. *Journal of food processing and preservation*. 2020;44(9):n/a.
36. Fabrowska J, Messyas B, Szyling J, Walkowiak J, Ska Ba. Isolation of chlorophylls and carotenoids from freshwater algae using different extraction methods. *Phycological research*. 2018;66(1):52-7.
37. Yoshie Y, Wang W, Petillo D, Suzuki T. Distribution of catechins in Japanese seaweeds. *Fisheries science*. 2000;66(5):998-1000.
38. Saini RK, Keum Y-S. Carotenoid extraction methods: A review of recent developments. *Food Chem*. 2018;240:90-103.
39. Repaji M, Cegledi E, Zori Z, Pedisi S, Garofuli IE, Radman S, et al. Bioactive compounds in wild nettle (*Urtica dioica* L.) leaves and stalks: Polyphenols and pigments upon seasonal and habitat variations. *Foods*. 2021;10(1):190.

40. Maeda H, Fukuda S, Izumi H, Saga N. Anti-oxidant and fucoxanthin contents of brown alga ishimozuku (*Sphaerotrichia divaricata*) from the west coast of aomori, Japan. *Mar Drugs*. 2018;16(8):255.
41. Reichardt C, Welton T. *Solvents and Solvent Effects in Organic Chemistry: Fourth Edition* 2010.
42. Dembek Ma, Bocian S. Pure water as a mobile phase in liquid chromatography techniques. *TrAC, Trends in analytical chemistry (Regular ed)*. 2020;123:115793.

Attachments

Attachment 1 – Calculations of uncertainty

- Concentration of the between standard for Fucoxanthin
 - Weight: $\mp 0.1 \text{ mg}$
 - Volume: Measured with a measuring flask, 10 ml $\mp 0.04 \text{ ml}$

p. 170-171 Quality Assurance in Analytical Chemistry

Concentration of between standard solutions

Standard uncertainties:

- Weight, $u(w) = \pm 0.1 \text{ mg}$
- Volume, $u(V) = \pm 0.00004 \text{ L}$

Using formula #, the standard uncertainty of the concentration was:

$$u(\text{concentration}) = 100 \frac{\text{mg}}{\text{L}} \times \sqrt{\left(\frac{0.1 \text{ mg}}{1 \text{ mg}}\right)^2 + \left(\frac{0.00004 \text{ L}}{0.01 \text{ L}}\right)^2} = \pm 10.0080 \text{ mg/L}$$

Concentration of standard solutions for calibration curves

- Uncertainty of the between standard: $\pm 10.0080 \text{ mg/L}$
- Thermoscientific: <https://static.thermoscientific.com/images/D20949~.pdf>
- Finnpiquette F1
 - 100 μl : $\mp 1.0000 \mu\text{l}$
 - using a 20 - 200 μl pipette
 - The five measurements for the standard solutions were weighted to ensure that the volumes were the same in every standard solution
 - 650 μl , 900 μl , 1150 μl , 1400 μl , 1650 μl , 5350 μl , 6900 μl
- Interpolation for the solvent fraction of the standard solutions using a 0.5 - 5 ml pipette
 - 650 μl
 - 2500 μl : $\mp 17.5 \mu\text{l}$
 - 500 μl : $\mp 10.0 \mu\text{l}$
 - $\pm \mu\text{l} = 10 \mu\text{l} + \frac{(650 - 500)(17.5 - 10.0)}{(2500 - 500)} \mu\text{l} = \pm 10.5625 \mu\text{l}$
 - 900 μl
 - 2500 μl : $\mp 17.5 \mu\text{l}$
 - 500 μl : $\mp 10.0 \mu\text{l}$
 - $\pm \mu\text{l} = 10 \mu\text{l} + \frac{(900 - 500)(17.5 - 10.0)}{(2500 - 500)} \mu\text{l} = \pm 11.5000 \mu\text{l}$
 - 1150 μl

- 2500 μl : $\bar{\pm}17.5 \mu\text{l}$
- 500 μl : $\bar{\pm}10.0 \mu\text{l}$
- $\pm\mu\text{l} = 10 \mu\text{l} + \frac{(1150-500)(17,5-10.0)}{(2500-500)}\mu\text{l} = \pm 12.4375 \mu\text{l}$
- 1400 μl
 - 2500 μl : $\bar{\pm}17.5 \mu\text{l}$
 - 500 μl : $\bar{\pm}10.0 \mu\text{l}$
 - $\pm\mu\text{l} = 10 \mu\text{l} + \frac{(1400-500)(17,5-10.0)}{(2500-500)}\mu\text{l} = \pm 13.3750 \mu\text{l}$
- 1650 μl
 - 2500 μl : $\bar{\pm}17.5 \mu\text{l}$
 - 500 μl : $\bar{\pm}10.0 \mu\text{l}$
 - $\pm\mu\text{l} = 10 \mu\text{l} + \frac{(1650-500)(17,5-10.0)}{(2500-500)}\mu\text{l} = \pm 14.3125 \mu\text{l}$
- 2100 μl
 - 2500 μl : $\bar{\pm}17.5 \mu\text{l}$
 - 500 μl : $\bar{\pm}10.0 \mu\text{l}$
 - $\pm\mu\text{l} = 10 \mu\text{l} + \frac{(2100-500)(17,5-10.0)}{(2500-500)}\mu\text{l} = \pm 16.0000 \mu\text{l}$
- 3780 μl
 - 5000 μl : $\bar{\pm}25.0 \mu\text{l}$
 - 2500 μl : $\bar{\pm}17.5 \mu\text{l}$
 - $\pm\mu\text{l} = 17.5 \mu\text{l} + \frac{(3780-2500)(25.0-17,5)}{(5000-2500)}\mu\text{l} = \pm 21.3400 \mu\text{l}$
- Labsystems finnpipette 4500 series 2-10 ml
 - Imprecision: <https://americanlaboratorytrading.com/lab-equipment-products/labsystems-finnpipette-4500-series-2-10-ml-pippette-17884>
 - 10000 μL : $\bar{\pm} 20 \mu\text{L}$
 - 5000 μL : $\bar{\pm} 15 \mu\text{L}$
 - 2000 μL : $\bar{\pm} 6 \mu\text{L}$
- Interpolation for the solvent fraction of the standard solutions using a 2 - 10 ml pipette
 - 5300 μl
 - 10000 μL : $\bar{\pm} 20 \mu\text{L}$
 - 5000 μL : $\bar{\pm} 15 \mu\text{L}$
 - $\pm\mu\text{l} = 15 \mu\text{l} + \frac{(5300-5000)(20.0-15.0)}{(10000-5000)}\mu\text{l} = \pm 15.3000 \mu\text{l}$
 - 6900 μl
 - 10000 μL : $\bar{\pm} 20 \mu\text{L}$
 - 5000 μL : $\bar{\pm} 15 \mu\text{L}$
 - $\pm\mu\text{l} = 15 \mu\text{l} + \frac{(6900-5000)(20.0-10.0)}{(10000-5000)}\mu\text{l} = \pm 16.9000 \mu\text{l}$
 - <https://tools.thermofisher.com/content/sfs/brochures/D21222.pdf>

- Confirmed the imprecision

- Using formula #, the standard uncertainty of the concentration of the standard solution for concentration level 1 was:
 - Concentration of between standard: 100 mg/L
 - Standard uncertainty of between standard: $\pm 10.0080 \text{ mg/L}$
 - Dilution factor fraction: $\frac{100 \mu\text{l } Fx}{(100 \mu\text{l}+650 \mu\text{l})} = 0.133333$
 - Standard uncertainty in dilution factor fraction, calculated using formula #:

$$u_{fraction}(\text{concentration}) = 0.133333 \frac{\text{mg}}{\text{L}} \times \sqrt{\left(\frac{1.000000}{100}\right)^2 + \left(\frac{10.609732}{750}\right)^2}$$

$$= \pm 0.002310 \frac{\text{mg}}{\text{L}}$$

Where, standard uncertainty for the total volume in the fraction (the denominator) was calculated using formula #:

$$u_{denominator}(\text{total volume}) = \sqrt{(1.0000)^2 + (10.5625)^2} = \pm 10.609732 \mu\text{l}$$

$$u_{level 1}(\text{concentration}) = 13.3333 \frac{\text{mg}}{\text{L}} \times \sqrt{\left(\frac{10.0080}{100}\right)^2 + \left(\frac{0.002310}{0.133333}\right)^2}$$

$$= \pm 1.354247 \frac{\text{mg}}{\text{L}} \sim \pm 1.3542 \frac{\text{mg}}{\text{L}}$$

- Using formula #, the standard uncertainty of the concentration of the standard solution for concentration level 2 was:
 - Concentration of between standard: 100 mg/L
 - Standard uncertainty of between standard: $\pm 10.0080 \text{ mg/L}$
 - Dilution factor fraction: $\frac{100 \mu\text{l } Fx}{(100 \mu\text{l}+900 \mu\text{l})} = 0.100000$
 - Standard uncertainty in dilution factor fraction, calculated using formula #:

$$u_{fraction}(\text{concentration}) = 0.1000 \frac{\text{mg}}{\text{L}} \times \sqrt{\left(\frac{1.000000}{100}\right)^2 + \left(\frac{11.543396}{1000}\right)^2}$$

$$= \pm 0.001573 \frac{\text{mg}}{\text{L}}$$

Where, standard uncertainty for the total volume in the fraction (the denominator) was calculated using formula #:

$$u_{denominator}(\text{total volume}) = \sqrt{(1.0000)^2 + (11.5000)^2} = \pm 11.543396 \mu\text{l}$$

$$u_{level\ 2} (concentration) = 10.0000 \frac{mg}{L} \times \sqrt{\left(\frac{10.008000}{100}\right)^2 + \left(\frac{0.001573}{0.100000}\right)^2}$$

$$= \pm 1.013086 \frac{mg}{L} \sim \pm 1.0131 \frac{mg}{L}$$

- Using formula #, the standard uncertainty of the concentration of the standard solution for concentration level 3 was:
 - Concentration of between standard: 100 mg/L
 - Standard uncertainty of between standard: $\pm 10.0080\ mg/L$
 - Dilution factor fraction: $\frac{100\ \mu l\ Fx}{(100\ \mu l + 900\ \mu l)} = 0.080000$
 - Standard uncertainty in dilution factor fraction, calculated using formula #:

$$u_{fraction} (concentration) = 0.0800 \frac{mg}{L} \times \sqrt{\left(\frac{1.000000}{100}\right)^2 + \left(\frac{11.543396}{1250}\right)^2}$$

$$= \pm 0.001089 \frac{mg}{L}$$

Where, standard uncertainty for the total volume in the fraction (the denominator) was calculated using formula #:

$$u_{denominator} (total\ volume) = \sqrt{(1.0000)^2 + (11.5000)^2} = \pm 11.543396\ \mu l$$

$$u_{level\ 3} (concentration) = 8.0000 \frac{mg}{L} \times \sqrt{\left(\frac{10.008000}{100}\right)^2 + \left(\frac{0.001089}{0.080000}\right)^2}$$

$$= \pm 0.808012 \frac{mg}{L} \sim \pm 0.8080 \frac{mg}{L}$$

- Using formula #, the standard uncertainty of the concentration of the standard solution for concentration level 4 was:
 - Concentration of between standard: 100 mg/L
 - Standard uncertainty of between standard: $\pm 10.0080\ mg/L$
 - Dilution factor fraction: $\frac{100\ \mu l\ Fx}{(100\ \mu l + 1400\ \mu l)} = 0.066667$
 - Standard uncertainty in dilution factor fraction, calculated using formula #:

$$u_{fraction} (concentration) = 0.066667 \frac{mg}{L} \times \sqrt{\left(\frac{1.000000}{100}\right)^2 + \left(\frac{13.412331}{1500}\right)^2}$$

$$= \pm 0.000894 \frac{mg}{L}$$

Where, standard uncertainty for the total volume in the fraction (the denominator) was calculated using formula #:

$$u_{denominator} (total\ volume) = \sqrt{(1.0000)^2 + (13.3750)^2} = \pm 13.412331\ \mu l$$

$$u_{level\ 4} (concentration) = 6.666667 \frac{mg}{L} \times \sqrt{\left(\frac{10.008000}{100}\right)^2 + \left(\frac{0.000894}{0.066667}\right)^2}$$

$$= \pm 0.673163 \frac{mg}{L} \sim \pm 0.6732 \frac{mg}{L}$$

- Using formula #, the standard uncertainty of the concentration of the standard solution for concentration level 5 was:

- Concentration of between standard: 100 mg/L
- Standard uncertainty of between standard: $\pm 10.0080\ mg/L$
- Dilution factor fraction: $\frac{100\ \mu l\ Fx}{(100\ \mu l + 1650\ \mu l)} = 0.057143$
- Standard uncertainty in dilution factor fraction, calculated using formula #:

$$u_{fraction} (concentration) = 0.057143 \frac{mg}{L} \times \sqrt{\left(\frac{1.000000}{100}\right)^2 + \left(\frac{14.347392}{1650}\right)^2}$$

$$= \pm 0.000757 \frac{mg}{L}$$

Where, standard uncertainty for the total volume in the fraction (the denominator) was calculated using formula #:

$$u_{denominator} (total\ volume) = \sqrt{(1.0000)^2 + (14.3125)^2} = \pm 14.347392\ \mu l$$

$$u_{level\ 5} (concentration) = 5.714286 \frac{mg}{L} \times \sqrt{\left(\frac{10.008000}{100}\right)^2 + \left(\frac{0.000757}{0.057143}\right)^2}$$

$$= \pm 0.576874 \frac{mg}{L} \sim \pm 0.5769 \frac{mg}{L}$$

- Using formula #, the standard uncertainty of the concentration of the altered standard solution for concentration level 2 was:

- Concentration of between standard: 100 mg/L
- Standard uncertainty of between standard: $\pm 10.0080\ mg/L$
- Dilution factor fraction: $\frac{100\ \mu l\ Fx}{(100\ \mu l + 2100\ \mu l)} = 0.045454$
- Standard uncertainty in dilution factor fraction, calculated using formula #:

$$u_{fraction} (concentration) = 0.045454 \frac{mg}{L} \times \sqrt{\left(\frac{1.000000}{100}\right)^2 + \left(\frac{16.031220}{2200}\right)^2}$$

$$= \pm 0.000562 \frac{mg}{L}$$

Where, standard uncertainty for the total volume in the fraction (the denominator) was calculated using formula #:

$$u_{denominator} (total\ volume) = \sqrt{(1.0000)^2 + (16.0000)^2} = \pm 16.031220\ \mu l$$

$$u_{level\ 2*} (concentration) = 4.545454 \frac{mg}{L} \times \sqrt{\left(\frac{10.008000}{100}\right)^2 + \left(\frac{0.000562}{0.045454}\right)^2}$$

$$= \pm 0.458367 \frac{mg}{L} \sim \pm 0.4584 \frac{mg}{L}$$

- Using formula #, the standard uncertainty of the concentration of the altered standard solution for concentration level 3 was:
 - Concentration of between standard: 100 mg/L
 - Standard uncertainty of between standard: $\pm 10.0080\ mg/L$
 - Dilution factor fraction: $\frac{100\ \mu l\ Fx}{(100\ \mu l + 3780\ \mu l)} = 0.025773$
 - Standard uncertainty in dilution factor fraction, calculated using formula #:

$$u_{fraction} (concentration) = 0.025773 \frac{mg}{L} \times \sqrt{\left(\frac{1.000000}{100}\right)^2 + \left(\frac{21.363442}{3780}\right)^2}$$

$$= \pm 0,000296 \frac{mg}{L}$$

Where, standard uncertainty for the total volume in the fraction (the denominator) was calculated using formula #:

$$u_{denominator} (total\ volume) = \sqrt{(1.0000)^2 + (21.3400)^2} = \pm 21,363442\ \mu l$$

$$u_{level\ 3*} (concentration) = 4.545454 \frac{mg}{L} \times \sqrt{\left(\frac{10.008000}{100}\right)^2 + \left(\frac{0.000296}{0.025773}\right)^2}$$

$$= \pm 0.457895 \frac{mg}{L} \sim \pm 0.4579 \frac{mg}{L}$$

- Using formula #, the standard uncertainty of the concentration of the altered standard solution for concentration level 4 was:
 - Concentration of between standard: 100 mg/L
 - Standard uncertainty of between standard: $\pm 10.0080\ mg/L$
 - Dilution factor fraction: $\frac{100\ \mu l\ Fx}{(100\ \mu l + 5300\ \mu l)} = 0.018519$
 - Standard uncertainty in dilution factor fraction, calculated using formula #:

$$u_{fraction} (concentration) = 0.018519 \frac{mg}{L} \times \sqrt{\left(\frac{1.000000}{100}\right)^2 + \left(\frac{15.332645}{5300}\right)^2}$$

$$= \pm 0.000193 \frac{mg}{L}$$

Where, standard uncertainty for the total volume in the fraction (the denominator) was calculated using formula #:

$$u_{denominator} (total\ volume) = \sqrt{(1.0000)^2 + (15.3000)^2} = \pm 15.332645\ \mu l$$

$$u_{level\ 4*} (concentration) = 1.851852 \frac{mg}{L} \times \sqrt{\left(\frac{10.008000}{100}\right)^2 + \left(\frac{0.00019}{0.018519}\right)^2}$$

$$= \pm 0.186305 \frac{mg}{L} \sim \pm 0.1863 \frac{mg}{L}$$

- Using formula #, the standard uncertainty of the concentration of the altered standard solution for concentration level 5 was:
 - Concentration of between standard: 100 mg/L
 - Standard uncertainty of between standard: $\pm 10.0080\ mg/L$
 - Dilution factor fraction: $\frac{100\ \mu l\ Fx}{(100\ \mu l + 6900\ \mu l)} = 0.014286$
 - Standard uncertainty in dilution factor fraction, calculated using formula #:

$$u_{fraction} (concentration) = 0.014286 \frac{mg}{L} \times \sqrt{\left(\frac{1.000000}{100}\right)^2 + \left(\frac{16.929560}{7000}\right)^2}$$

$$= \pm 0.000147 \frac{mg}{L}$$

Where, standard uncertainty for the total volume in the fraction (the denominator) was calculated using formula #:

$$u_{denominator} (total\ volume) = \sqrt{(1.0000)^2 + (16,9000)^2} = \pm 16.929560\ \mu l$$

$$u_{level\ 5*} (concentration) = 1.428571 \frac{mg}{L} \times \sqrt{\left(\frac{10.008000}{100}\right)^2 + \left(\frac{0.000147}{0.014286}\right)^2}$$

$$= \pm 0.143725 \frac{mg}{L} \sim \pm 0.1437 \frac{mg}{L}$$

Concentration of the sample

- Weight: $\mp 0.1\ mg$
- Volume: Measuring syylinder, 250 ml. 200 ml $\mp 2\ ml$ -> $0.2000\ l \mp 0.0020\ l$

Uncertainty in injection volume for HPLC

- Assumed no uncertainty in injection volume

Attachment 2 – Calculations for modified mobile phases

Calculations for alternative #1:

Relative polarity:

A: Water = 1,000, Acetic acid = 0,648 ->

$$\text{Relative polarity} = (0,99 \cdot 1,000 + 0,01 \cdot 0,648) = 0,9965$$

B: Water = 1,000, Acetonitrile = 0,460, Acetic acid = 0,648 ->

$$\text{Relative polarity} = (0,67 \cdot 1,000 + 0,32 \cdot 0,460 + 0,01 \cdot 0,648) = 0,8237$$

Ethyl acetate was the most suitable green substitute for acetonitrile, relative polarity = 0,228. Ethyl acetate is not miscible in water though

(<https://www.sigmaaldrich.com/NO/en/technical-documents/technical-article/analytical-chemistry/purification/solvent-miscibility-table>), so water and acetonitrile was exchanged with methanol with acetic acid.

Methanol has a relative polarity of 0,762 and acetic acid has a relative polarity of 0,648:

$$\text{Relative polarity} = (0,99 \cdot 0,762 + 0,01 \cdot 0,648) = 0,761$$

The relative polarity of the modified mobile phase was a bit lower, but still close to the original mobile phase.

Relative polarity in relation to retention time in unmodified gradient program #1

RT (min)	Relative polarity:
0	0,9729
10	0,9729
16	0,9494
20	0,9022
25	0,8787
27	0,9022
35	0,9729
45	0,9729

Relative polarity in relation to retention time in modified gradient program #1

RT (min)	Relative polarity:
0	0,9792
10	0,9792
16	0,9619
20	0,9274
25	0,9101

27	0,9274
35	0,9792
45	0,9792

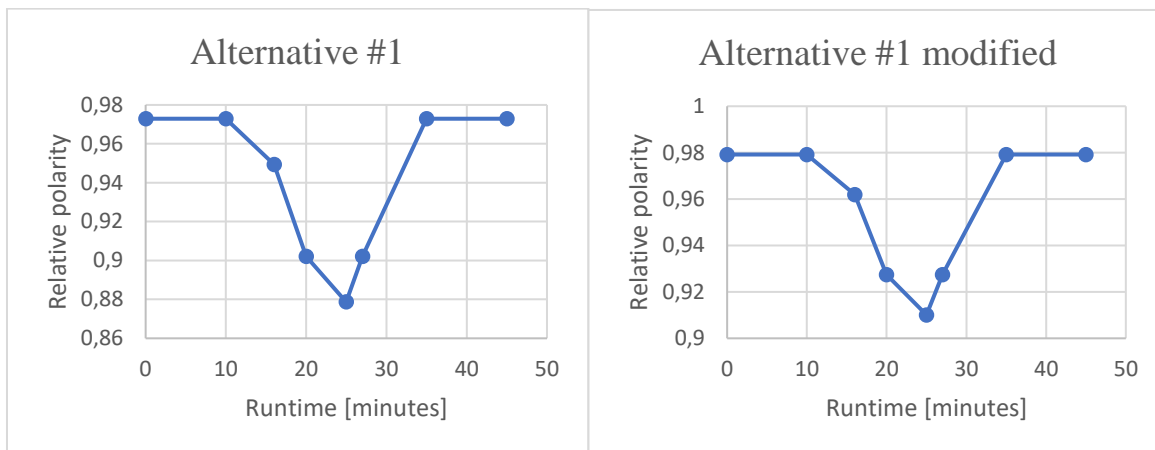


Figure - Plot of relative polarity in relation to retention time for unmodified and modified gradient programs for alternative #1

Calculation of the viscosity of the mobile phases:

A: Viscosity = $(0,99 \cdot 1,00 + 0,01 \cdot 1,31)$ cp = 1,0031 cp \sim 1,00 cp

B_{unmodified}: Viscosity = $(0,67 \cdot 1,00 + 0,32 \cdot 0,37 + 0,01 \cdot 1,31)$ cp = 0,8015 cp \sim 0,80 cp

B_{modified}: Viscosity = $(0,77 \cdot 1,00 + 0,22 \cdot 0,46 + 0,01 \cdot 1,31)$ cp = 0,8843 cp \sim 0,88 cp

There was an increase in viscosity, but the change was not considered to be enough to justify having to increase the flow rate for a starting point.

Calculations for alternative #2:

Relative polarity:

A: MeOH = 0,762, Acetonitrile = 0,460 Triethylamine = 0,043 ->

$$\text{Relative polarity} = (0,50 \cdot 0,762 + 0,50 \cdot 0,460) + (0,001 \cdot 0,043) = 0,6110 + 0,000043 = 0,6110$$

B: Relative polarity of acetone = 0,3550

The most suitable substitution for mobile phase A was methanol-ethyl acetate, where the volume fraction of ethyl acetate was set to Y. The impact of TEA on the relative polarity was neglected considering the small volume fraction.

Formula 1: $X \cdot \text{MeOH} \cdot 0,762 + Y \cdot 0,228 = 0,611$

Formula 2: $X \cdot \text{MeOH} + Y = 1,00$

2: $Y = 1,00 - X \cdot \text{MeOH}$, inserted into 1:

1: $X \cdot \text{MeOH} \cdot 0,762 + 1,00 - X \cdot \text{MeOH} \cdot 0,228 = 0,611$

$$0,762X_{\text{MeOH}} - 0,228X_{\text{MeOH}} = 0,611 - 0,228$$

$$0,534X_{\text{MeOH}} = 0,383$$

$$X_{\text{MeOH}} = 0,383 / 0,534 = 0,7172 \sim 0,72, \text{ inserted into 2:}$$

$$Y = 1,00 - 0,72 = 0,28$$

Control:

Relative polarity = $(0,72 * 0,762 + 0,28 * 0,228) = 0,61248$, considered to be close enough to 0,611.

Tweaking the volume fractions showed that the original fractions came the closest while still holding the variation in the the second decimal place:

$$\underline{X_{\text{MeOH}} = 0,72, Y_{\text{Ethyl acetate}} = 0,28 \text{ and } Z_{\text{TBA}} = 0,001}$$

B: Mobile phase must be modified because of Acetone, with a relative polarity of 0,355. The closest possible substitute is Ethyl acetate with a relative polarity of 0,228.

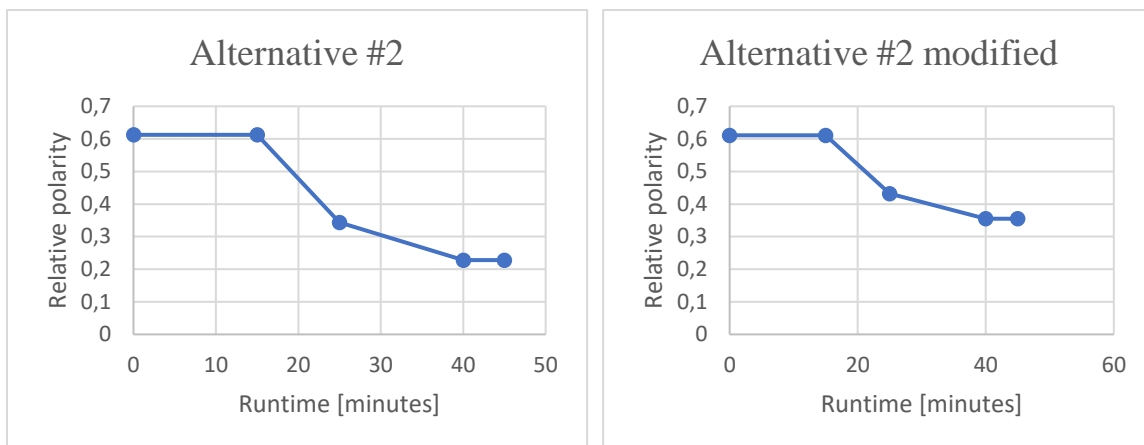
$$B = 0,228$$

Relative polarity in relation to retention time in unmodified gradient program #2

RT (min)	Relative polarity:
0	0,6125
15	0,6125
25	0,3433
40	0,228
45	0,228

Relative polarity in relation to retention time in modified gradient program #2

RT (min)	Relative polarity:
0	0,611
15	0,611
25	0,4318
40	0,355
45	0,355



Plot of relative polarity in relation to retention time for unmodified and modified gradient programs for alternative #2

Calculation of the viscosity of the mobile phases:

$$A_{\text{unmodified}}: \text{Viscosity} = (0,50 \cdot 0,55 + 0,50 \cdot 0,37) \text{ cp} = 0,46 \text{ cp}$$

$$A_{\text{modified}}: \text{Viscosity} = (0,72 \cdot 0,55 + 0,28 \cdot 0,46) \text{ cp} = 0,5248 \text{ cp} \sim 0,52 \text{ cp}$$

The volume fraction of TEA was considered to be negligible.

$$B_{\text{unmodified}}: \text{Viscosity} = 0,32 \text{ cp}$$

$$B_{\text{modified}}: \text{Viscosity} = 0,46 \text{ cp}$$

There was an increase in viscosity, but not enough to justify having to increase the flow rate for a starting point.

Calculations for alternative #3:

Relative polarity:

$$A: \text{MeOH} = 0,7620$$

$$B: \text{Water} = 1,0000$$

$$C: \text{Dichloromethane} = 0,309, \text{ hexane} = 0,009.$$

$$\text{Relative polarity} = (0,50 \cdot 0,309 + 0,50 \cdot 0,009) = 0,1590$$

The closest possible substitute is Ethyl acetate with a relative polarity of 0,228.

$$C = 0,228$$

Ethyl acetate is not miscible in water, but as seen in table # the gradient program separated stages using water from the phases with mobile phase C. Neither DCM nor hexane are miscible in water, making the consideration already accounted for in the original gradient program.

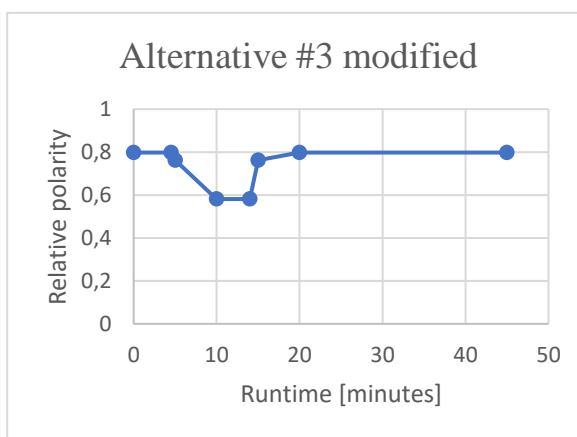
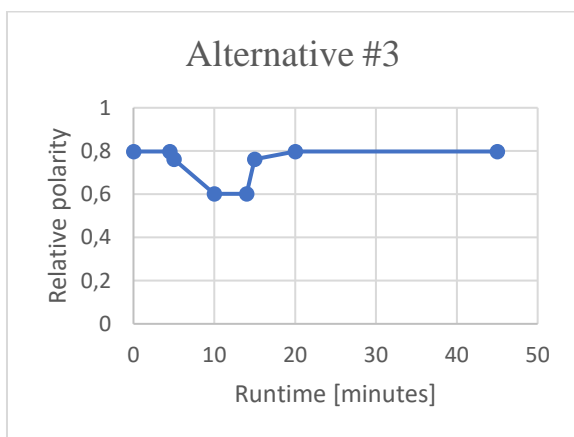
Relative polarity in relation to retention time in unmodified gradient program #3

RT (min)	Relative polarity:
0	0,7977
4,5	0,7977
5	0,762

10	0,6018
14	0,6018
15	0,762
20	0,7977
45	0,7977

Relative polarity in relation to retention time in modified gradient program #3

RT (min)	Relative polarity:
0	0,7977
4,5	0,7977
5	0,762
10	0,5811
14	0,5811
15	0,762
20	0,7977
45	0,7977



Plot of relative polarity in relation to retention time for unmodified and modified gradient programs for alternative #3

Calculation of the viscosity of the mobile phases:

A: Viscosity = 0,55 cp

B: Viscosity = 1,00 cp

$C_{\text{unmodified}}$: Viscosity = $(0,50 \cdot 0,45 + 0,50 \cdot 0,31)$ cp = 0,38 cp

C_{modified} : Viscosity = 0,46 cp

There was an increase in viscosity, but not enough to justify having to increase the flow rate for a starting point.

Attachment 3 – Screening test runs

Experiment 1 (14 in experimental design)

- C30 column with alternative #2

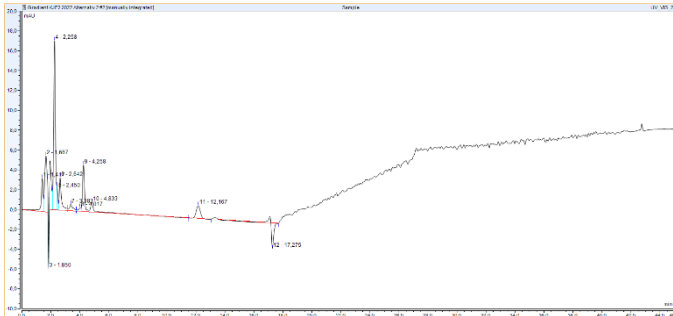


Figure: Experiment 1 measured at 450 nm

Experiment 2 (13 in experimental design)

- C30 column with alternative #2

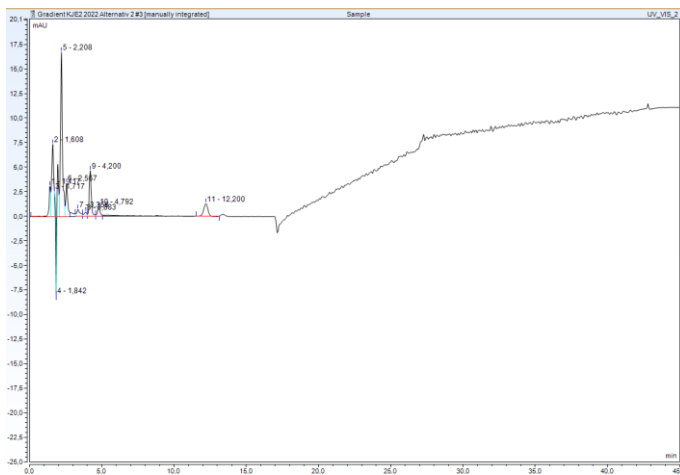


Figure: Experiment 2 measured at 450 nm

Experiment 3 (4 in experimental design)

- C18 column with alternative #2

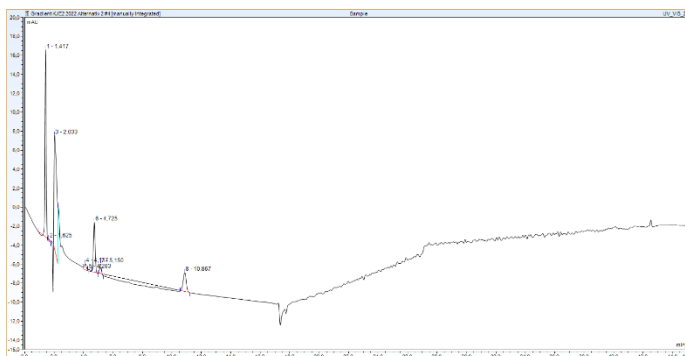


Figure: Experiment 3 measured at 450 nm

Experiment 4 (2 in experimental design)

- C18 column with alternative #1

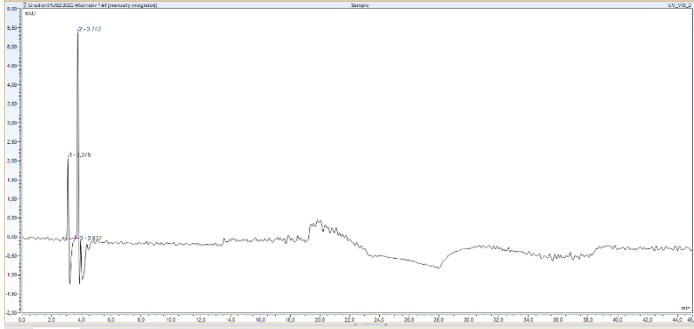


Figure: Experiment 4 measured at 450 nm

Experiment 5 (16 in experimental design)

- C30 column with alternative #3

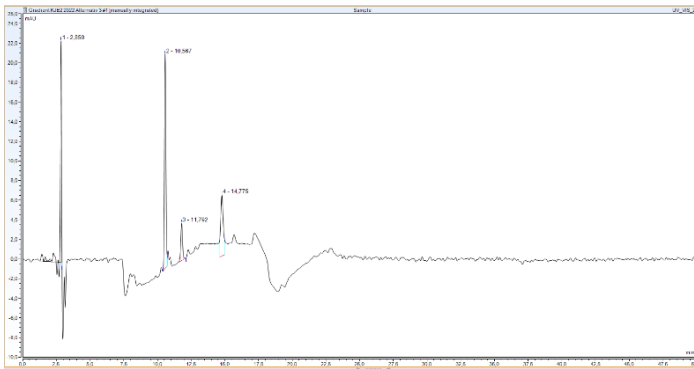


Figure: Experiment 5 measured at 450 nm

Attachment 4 – YMC modified runs

The matrix of extract #3, methanol, was run to help separate it from the peak of Fucoxanthin.

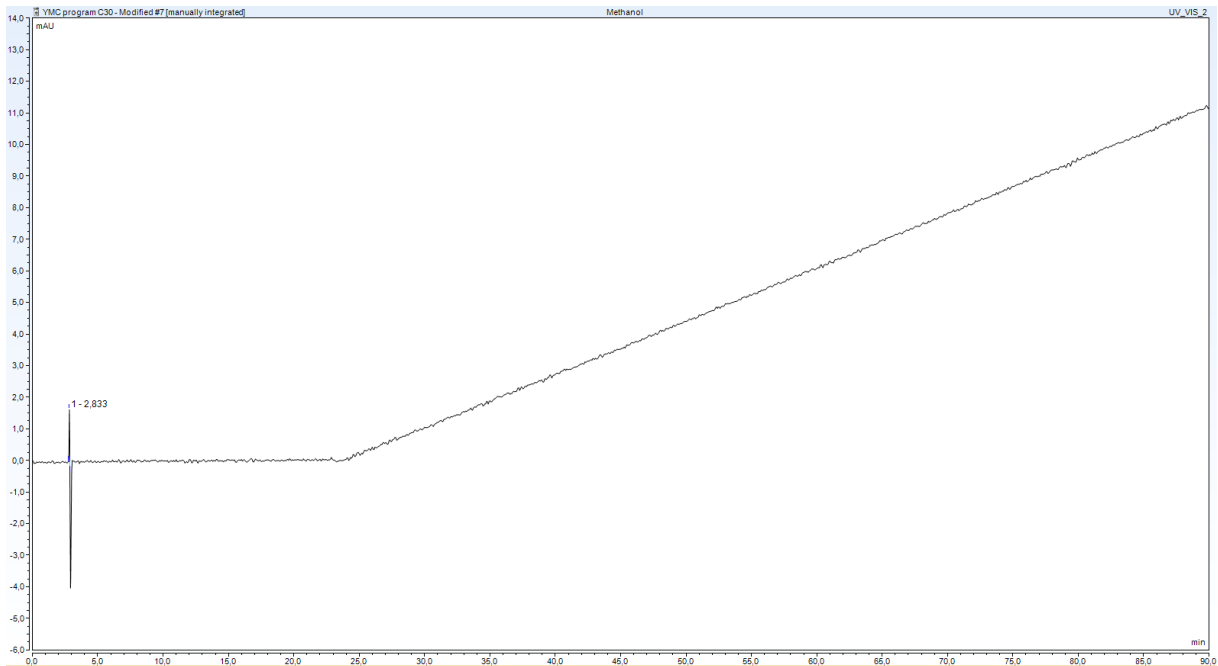


Figure: Chromatogram of 20 µl of methanol with gradient program #3 at 450 nm

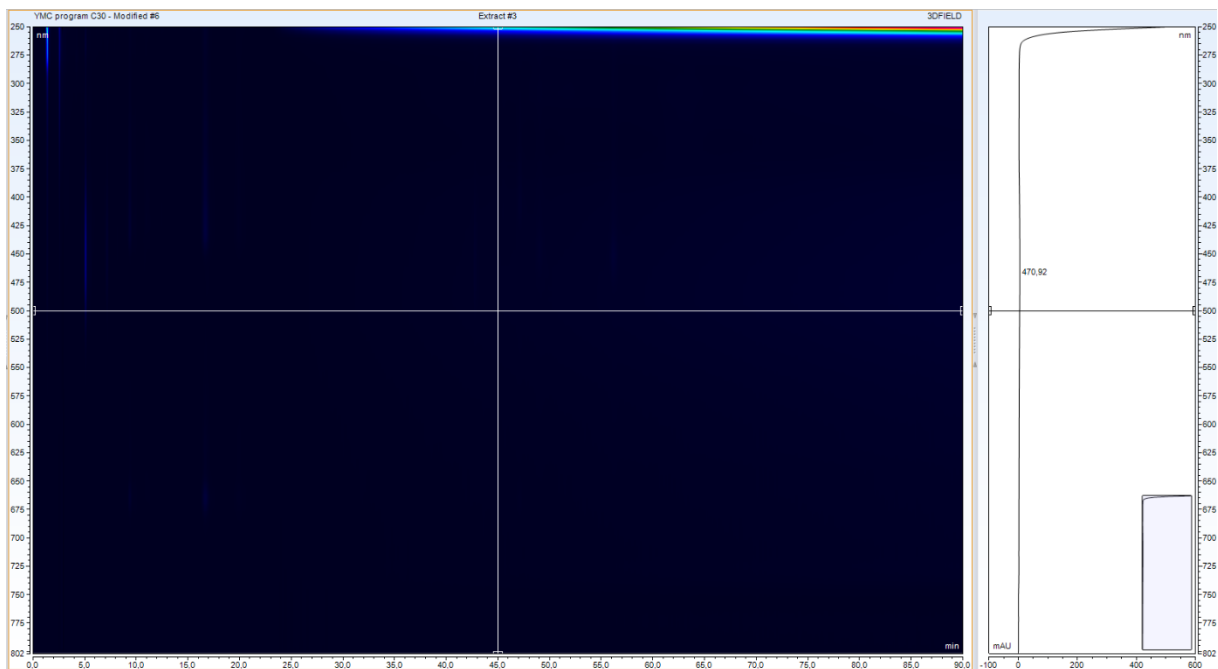


Figure: Contour plot of the run with gradient program #3 with 20 µl of extract #3 from 250 to 800 nm

Identification of Fucoxanthin:

Mobile phases:

- A: Methanol
- B: Ethyl acetate

Table: A precursor to the modified YMC gradient program #4:

Stages in gradient program [min]:	Mobile phase composition [%]:
0	97:3 A-B
20	97:3 A-B
25	70:30 A-B
45	50:50 A-B
50	10:90 A-B
60	10:90 A-B
65	97:3 A-B
90	97:3 A-B

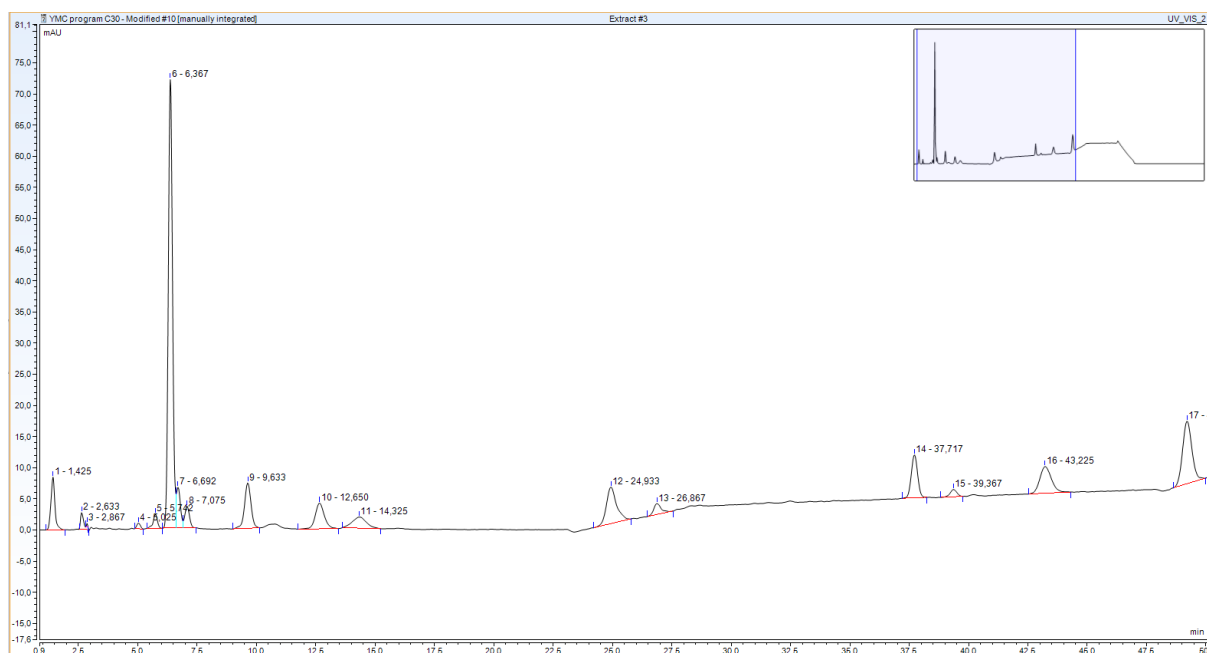


Figure: Chromatogram of precursor to modified YMC gradient program #4 with 20 µl of extract #3 at 450 nm

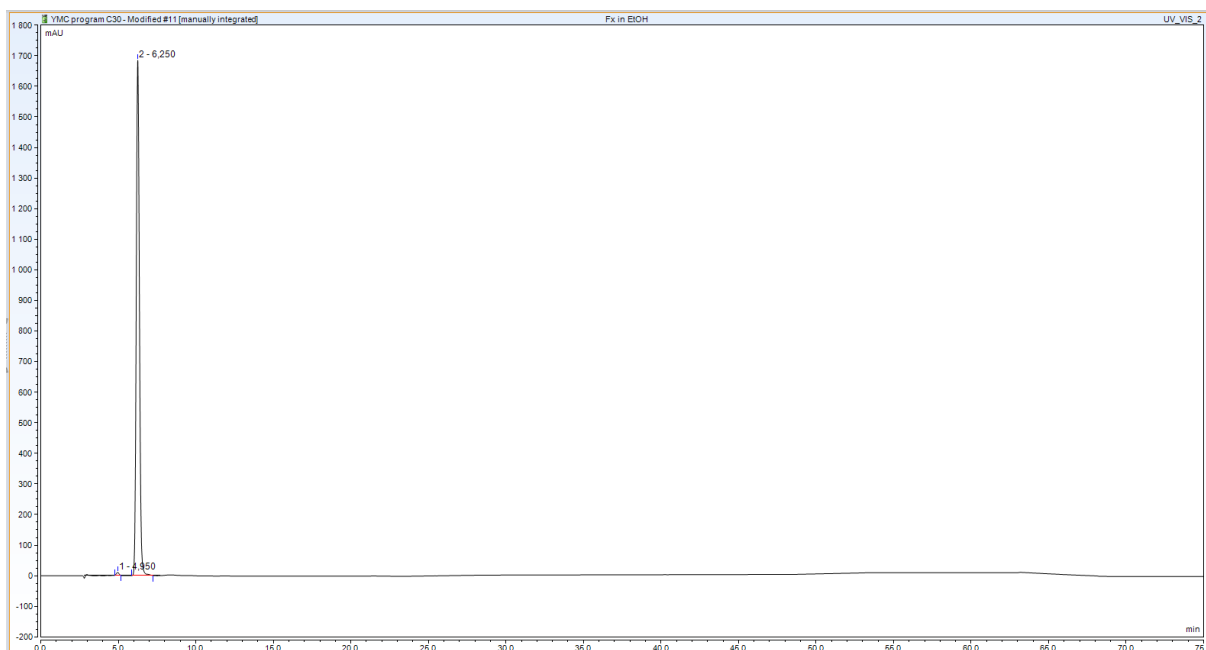


Figure: Chromatogram of precursor to modified YMC gradient program #4 with 20 μ l of Fucoxanthin standard in ethanol at 450 nm.

The HPLC vial with the standard used in the chromatogram given in figure # above was left out in room temperature and some light for two days by mistake and was partially degraded. This vial of standard was only used for identification purposes for a while.

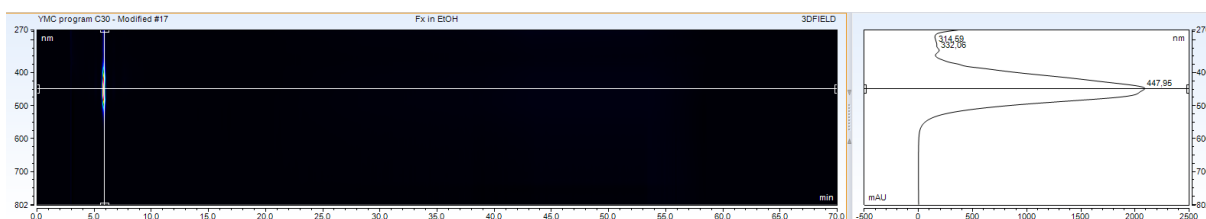


Figure: Contour plot of 20 μ l of Fucoxanthin standard in ethanol in gradient program #4, with PDA limits of 270 nm to 800 nm.

Continued modification of YMC program:

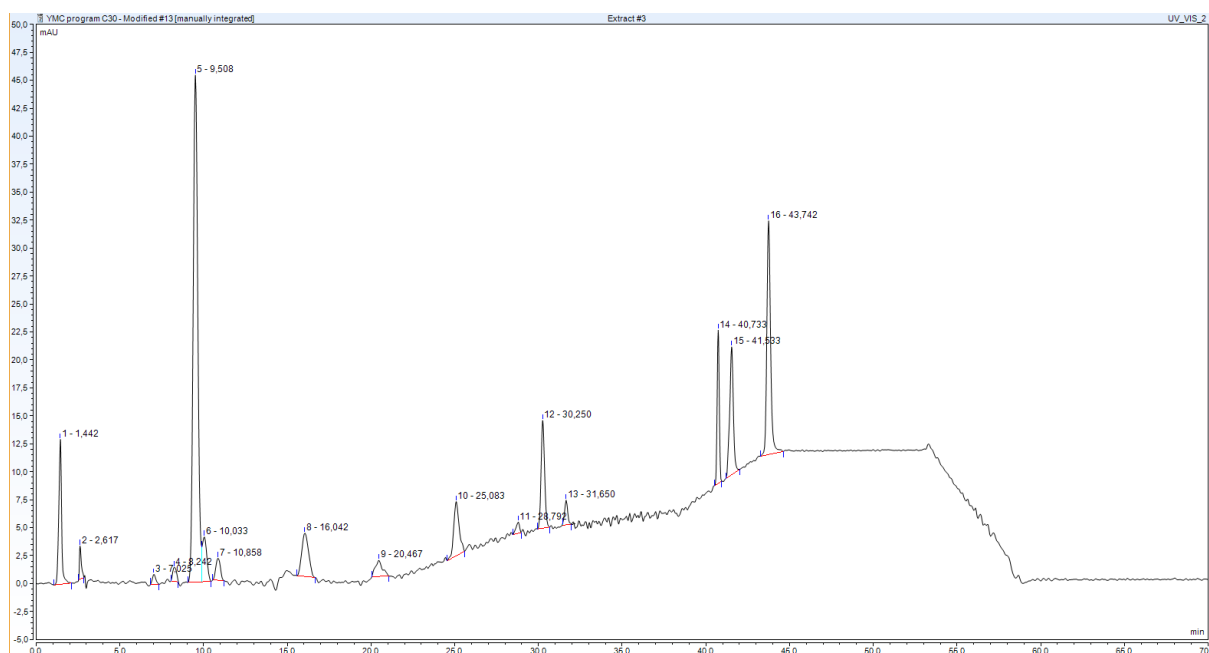


Figure: Zoom of a chromatogram of modified YMC gradient program #4 with 20 µl of extract #3 at 450 nm

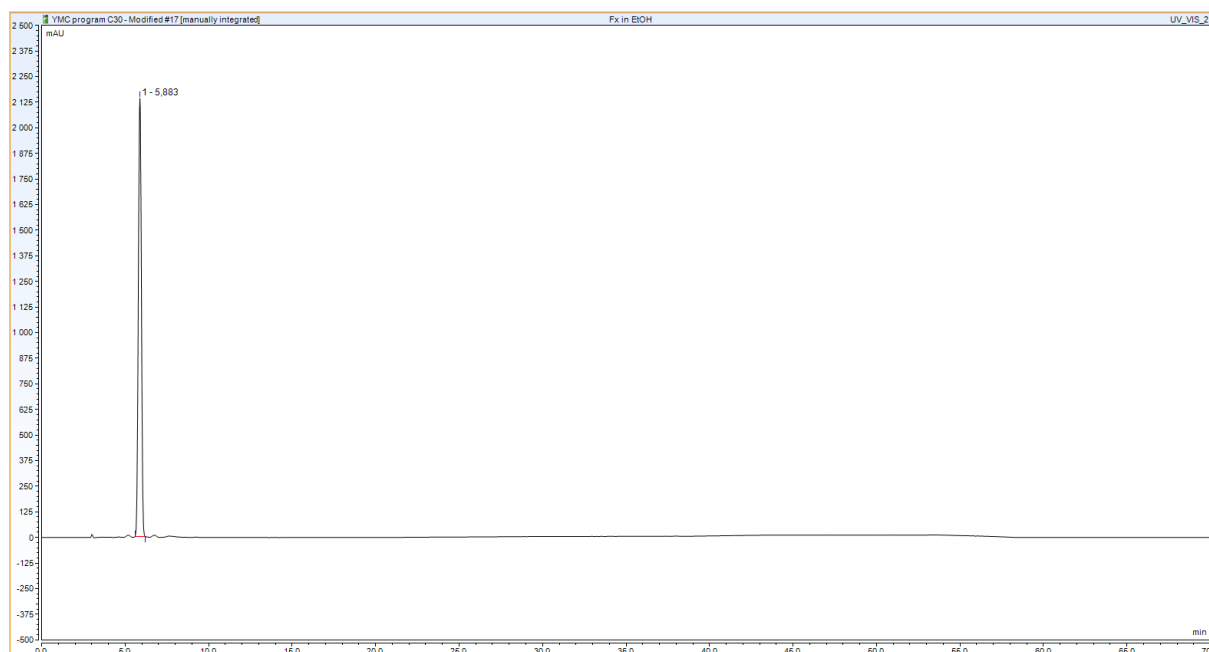


Figure: A chromatogram of modified YMC gradient program #4 with 20 µl of Fucoxanthin standard in ethanol at 450 nm, with a flow rate of 0.9 ml/min, 50 °C and with a runtime of 70 minutes

Property Name	Property Value
No.	1
Peakname	
Ret.Time	5,883 min
Peak Width	0,338 min
Type	BMB*
Height	2142,131 mAU
Area	453,3130 mAU*min

Figure: Peak properties of Fucoxanthin in gradient program #4 at 448 nm

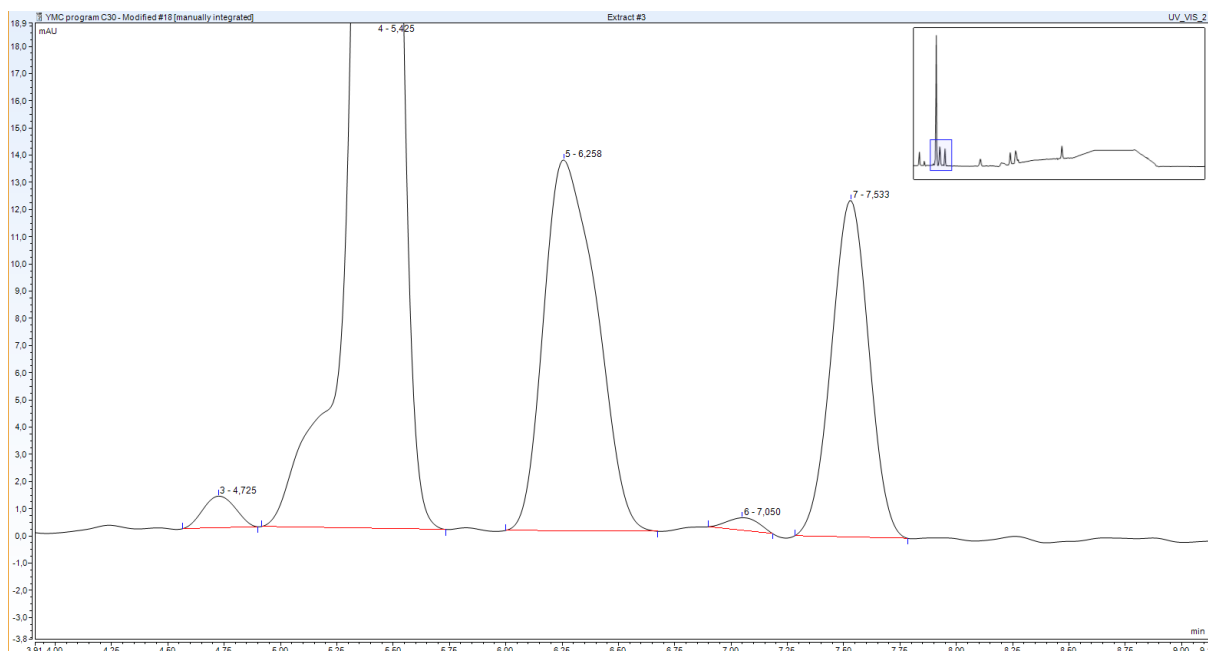
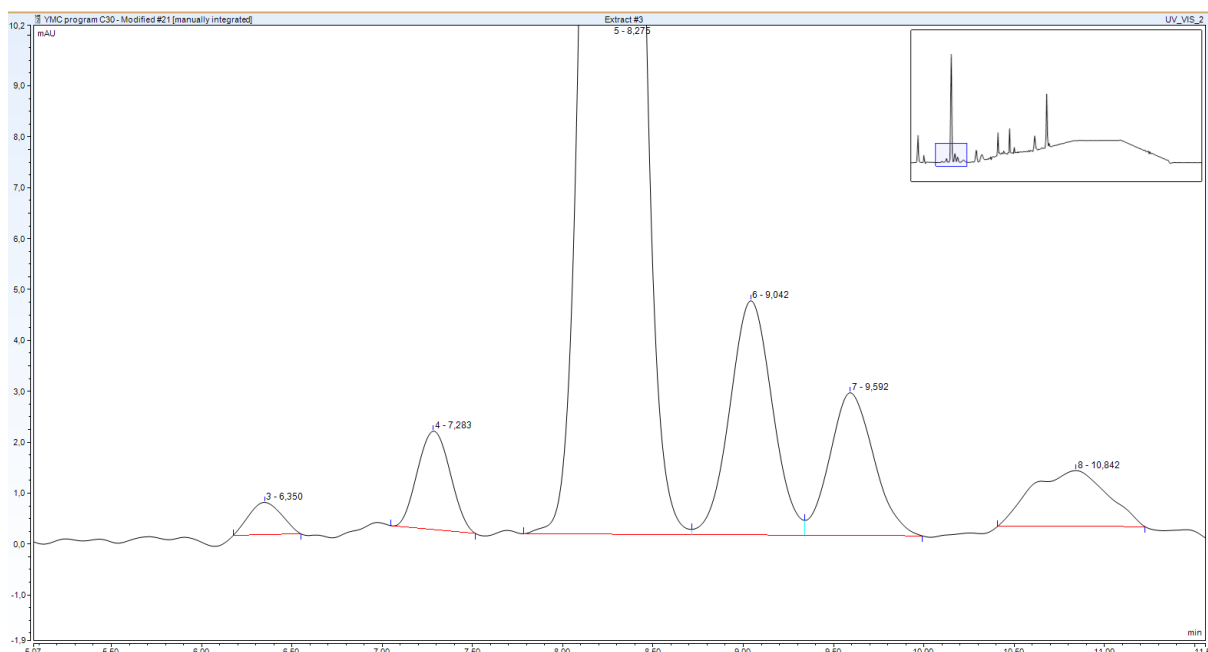
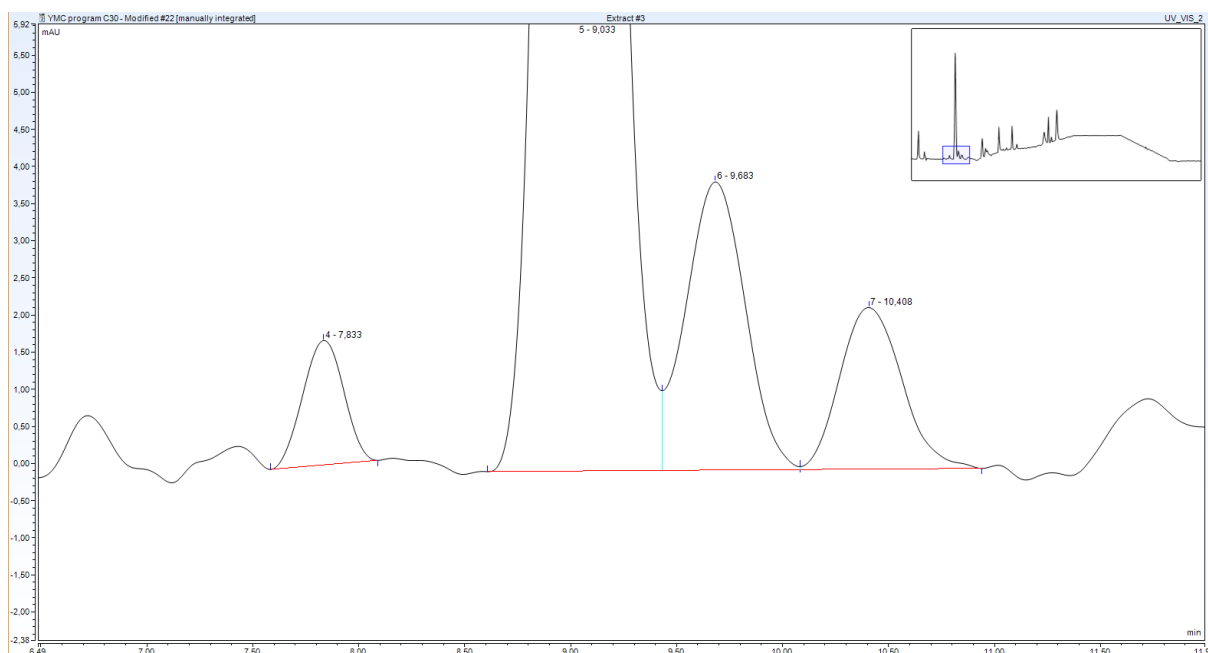


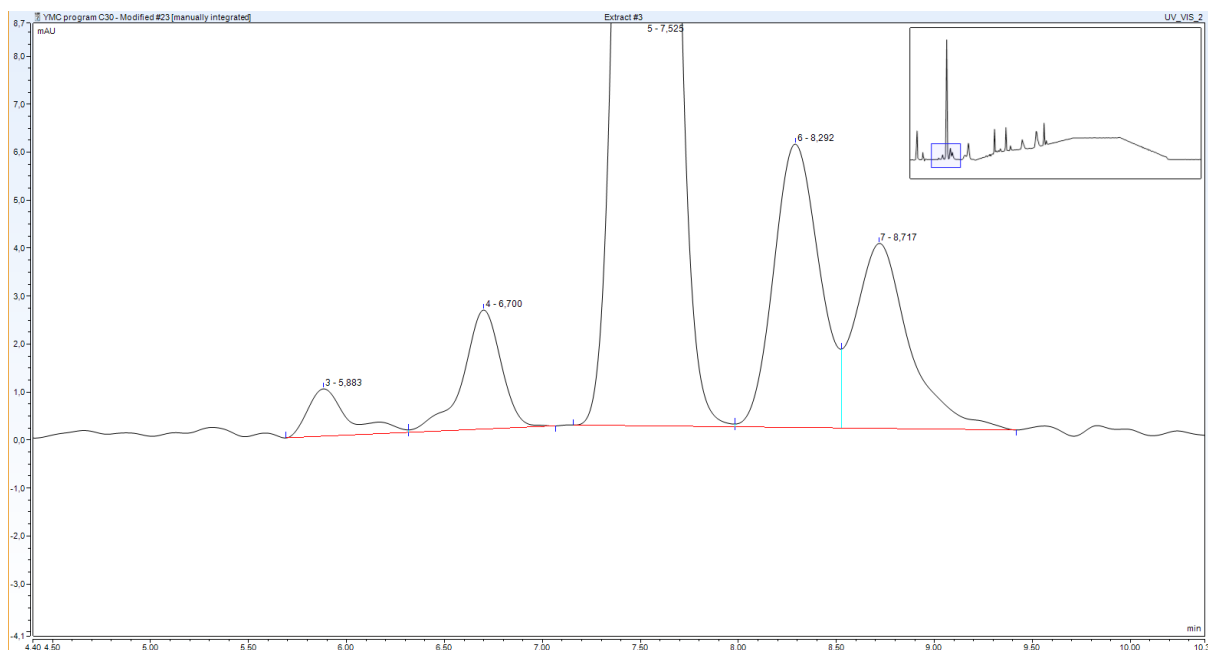
Figure: Zoom of a chromatogram of modified YMC gradient program #4 with 20 µl of extract #3 at 450 nm, with a flow rate of 1.0 ml/min, 50 °C and with a runtime of 70 minutes



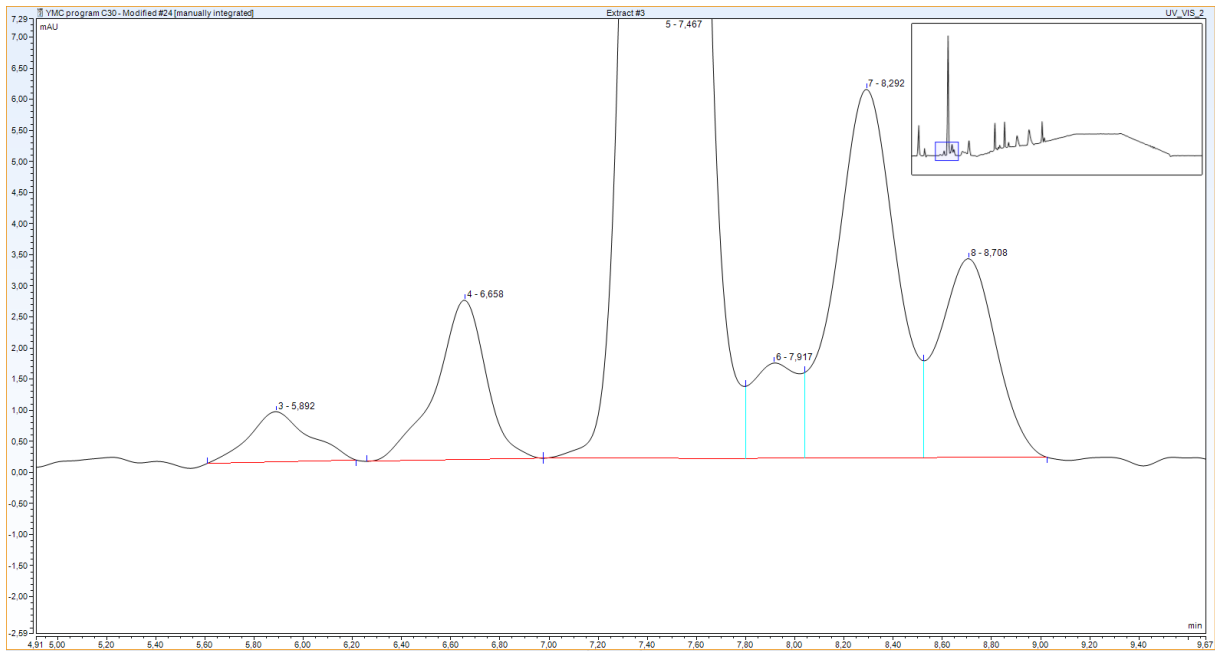
Zoom of a chromatogram of modified YMC gradient program #5 with 20 μ l of extract #3 at 450 nm, with a flow rate of 1.0 ml/min, 35 $^{\circ}$ C on the column



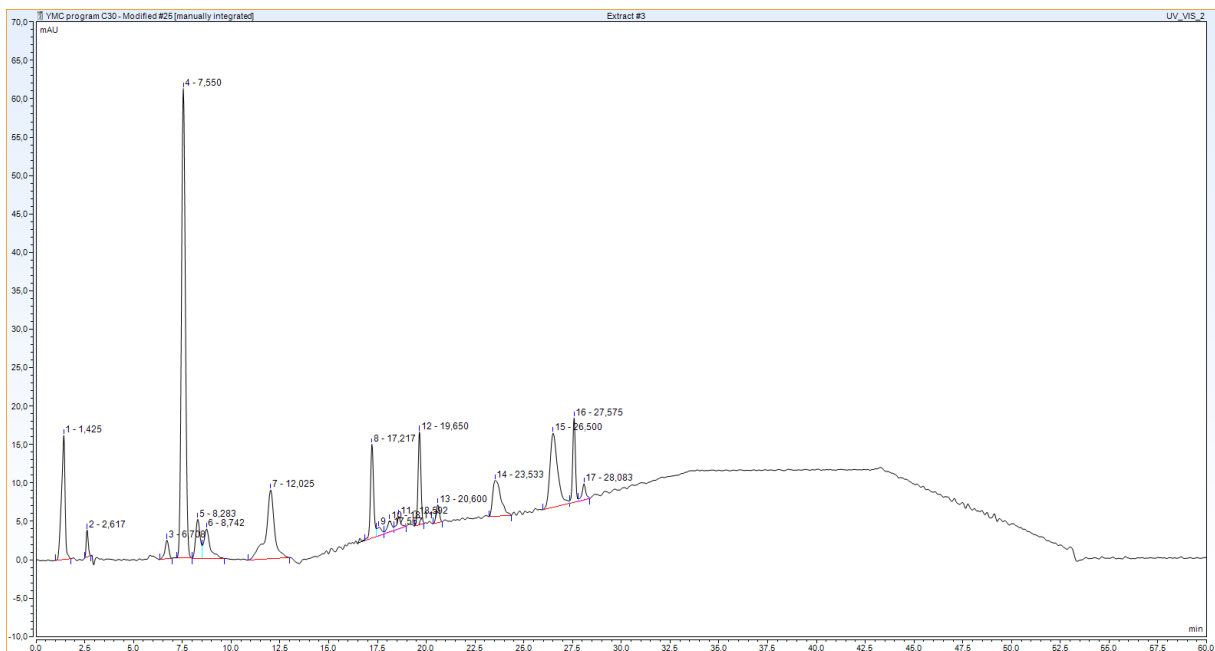
Zoom of a chromatogram of modified YMC gradient program #5 with 20 μ l of extract #3 at 450 nm, with a flow rate of 1.0 ml/min, 30 $^{\circ}$ C on the column



Zoom of a chromatogram of modified YMC gradient program #5 with 20 μ l of extract #3 at 450 nm, with a flow rate of 1.0 ml/min, 37 $^{\circ}$ C on the column



Zoom of a chromatogram of modified YMC gradient program #5 with 20 μ l of extract #3 at 450 nm, with a flow rate of 1.0 ml/min, 39 $^{\circ}$ C on the column



Zoom of a chromatogram of modified YMC gradient program #5 with 20 μ l of extract #3 at 450 nm, with a flow rate of 1.0 ml/min, 36 $^{\circ}$ C on the column

Attachment 5 – Method validation

Linearity

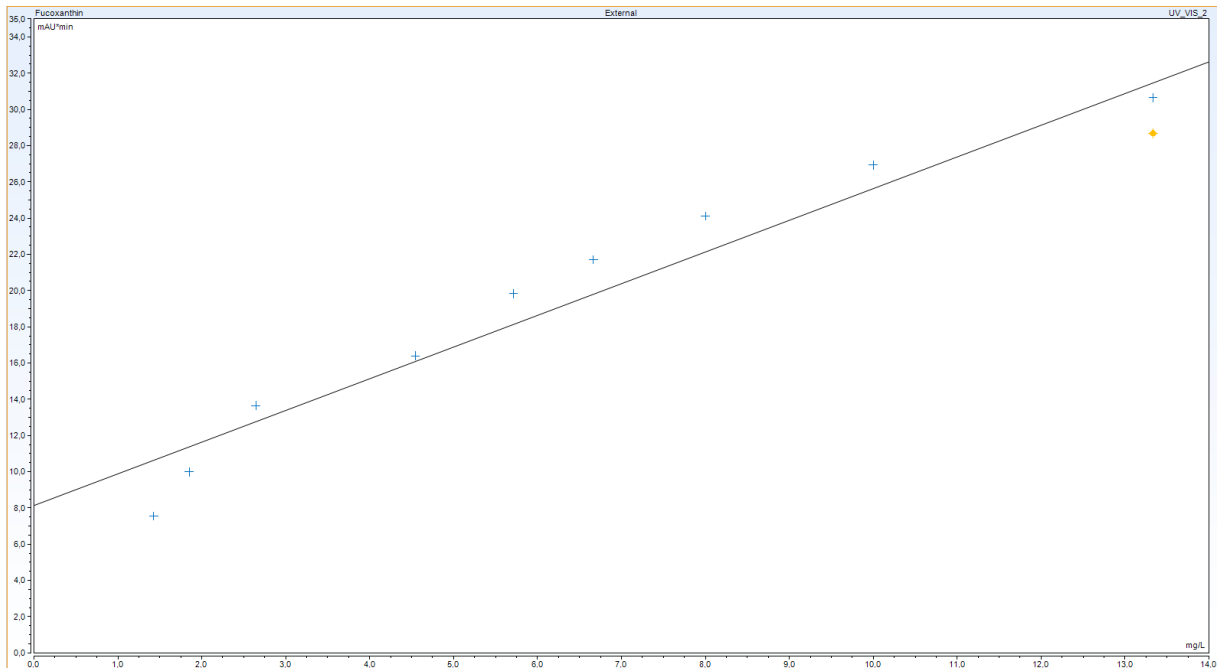


Figure: Calibration curve for ethanol extracts, ten measurements on nine concentration levels, four of which were altered to accommodate the lower peak areas

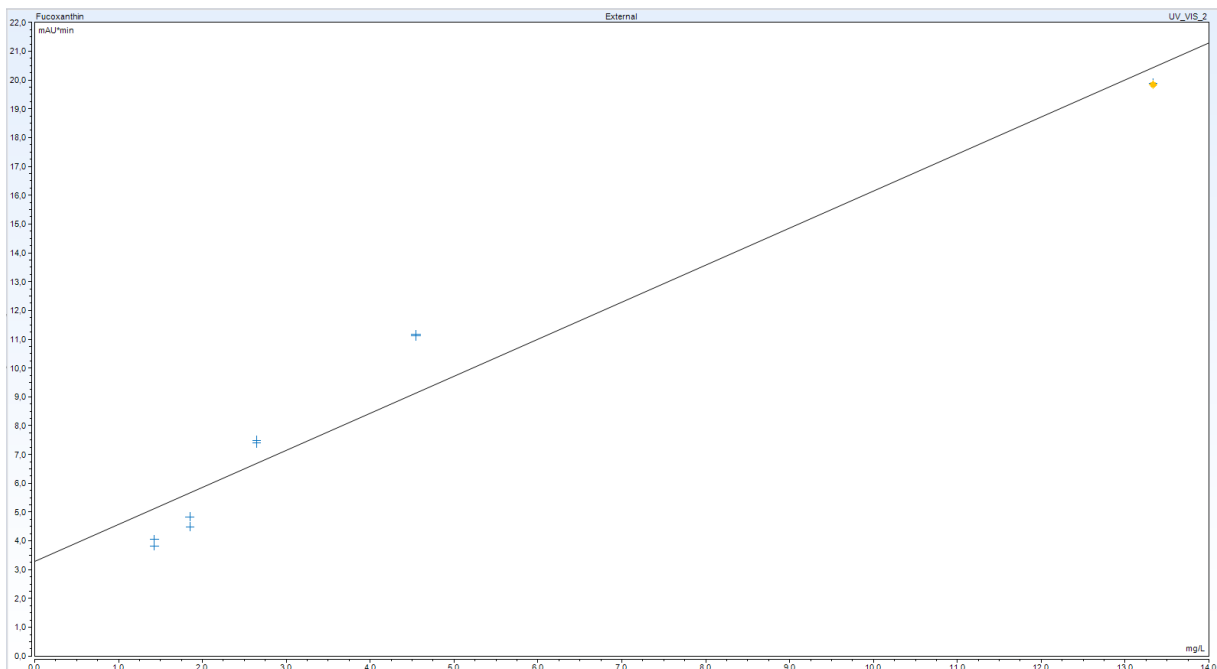


Figure: Calibration curve for 2-propanol extracts, ten measurements on five concentration levels

Peak No.	Peak Name	Ret.Time min	Cal.Type	Eval.Type	Number of Points	Rel.Std.Dev. %	Coeff.of Determination	C0 (Offset)	C1 (Slope)	C2 (Curve)
1	Fucoxanthin	8,000	Lin, WithOffset	Area	10	2,9843	0,96675	9,1984	0,9127	0,0000
Maximum						2,9843	0,96675			
Minimum						2,9843	0,96675			

Figure: Calibration curve data for the methanol extracts

Peak Name	Ret.Time min	Cal.Type	Eval.Type	Number of Points	Rel.Std.Dev. %	Coeff.of Determination	C0 (Offset)	C1 (Slope)	C2 (Curve)
Fucoxanthin	7,933	Lin, WithOffset	Area	6	9,8586	0,97366	7,3266	1,6951	0,0000
					9,8586	0,97366			
					9,8586	0,97366			

Figure: Calibration curve data for the ethanol extracts

Peak Name	Ret.Time min	Cal.Type	Eval.Type	Number of Points	Rel.Std.Dev. %	Coeff.of Determination	C0 (Offset)	C1 (Slope)	C2 (Curve)
Fucoxanthin	8,033	Lin, WithOffset	Area	8	9,8565	0,98577	2,7586	1,2915	0,0000
					9,8565	0,98577			
					9,8565	0,98577			

Figure: Calibration curve data for the 2-propanol extracts

Repeatability

6 consecutive measurements of Op-13

Property Name	Property Value
No.	6
Peakname	Fucoxanthin
Ret.Time	7,792 min
Peak Width	0,383 min
Type	BM *
Height	54,229 mAU
Area	13,6377 mAU*min

Property Name	Property Value
No.	6
Peakname	Fucoxanthin
Ret.Time	8,250 min
Peak Width	0,409 min
Type	BM *
Height	54,043 mAU
Area	14,4858 mAU*min

Property Name	Property Value
No.	8
Peakname	Fucoxanthin
Ret.Time	8,042 min
Peak Width	0,387 min
Type	M *
Height	53,341 mAU
Area	13,2770 mAU*min

Property Name	Property Value
No.	7
Peakname	Fucoxanthin
Ret.Time	7,900 min
Peak Width	0,386 min
Type	M *
Height	53,178 mAU
Area	13,1733 mAU*min

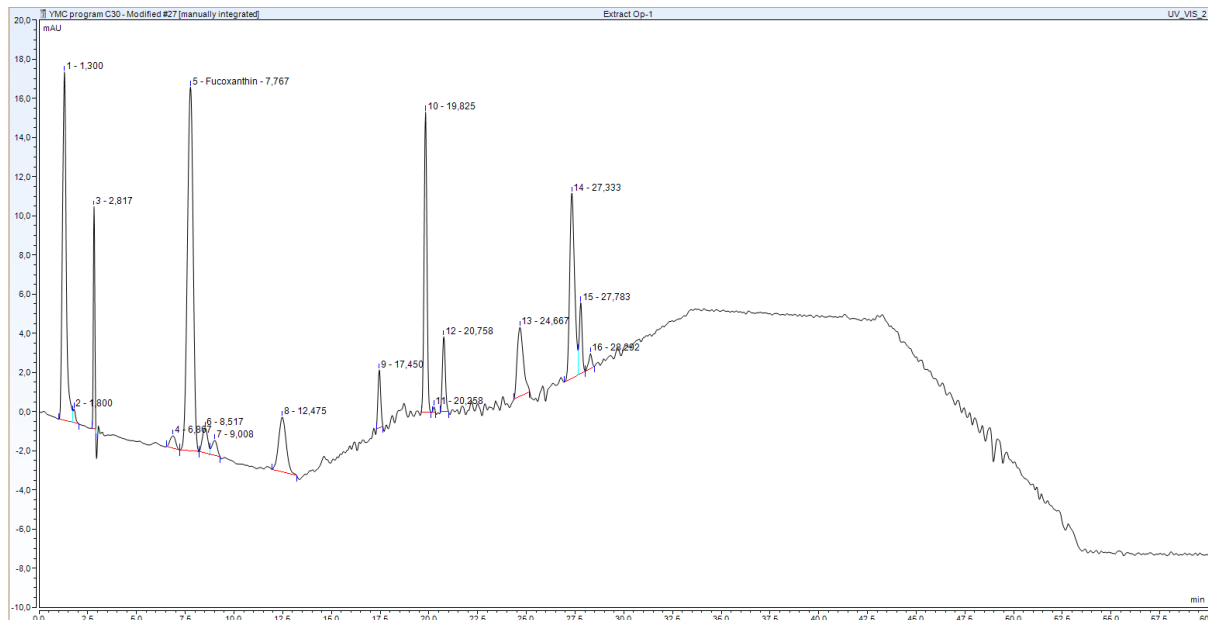
Property Name	Property Value
No.	7
Peakname	Fucoxanthin
Ret.Time	7,850 min
Peak Width	0,382 min
Type	M *
Height	53,619 mAU
Area	13,1521 mAU*min

Property Name	Property Value
No.	8
Peakname	Fucoxanthin
Ret.Time	7,858 min
Peak Width	0,383 min
Type	M *
Height	53,551 mAU
Area	13,1427 mAU*min

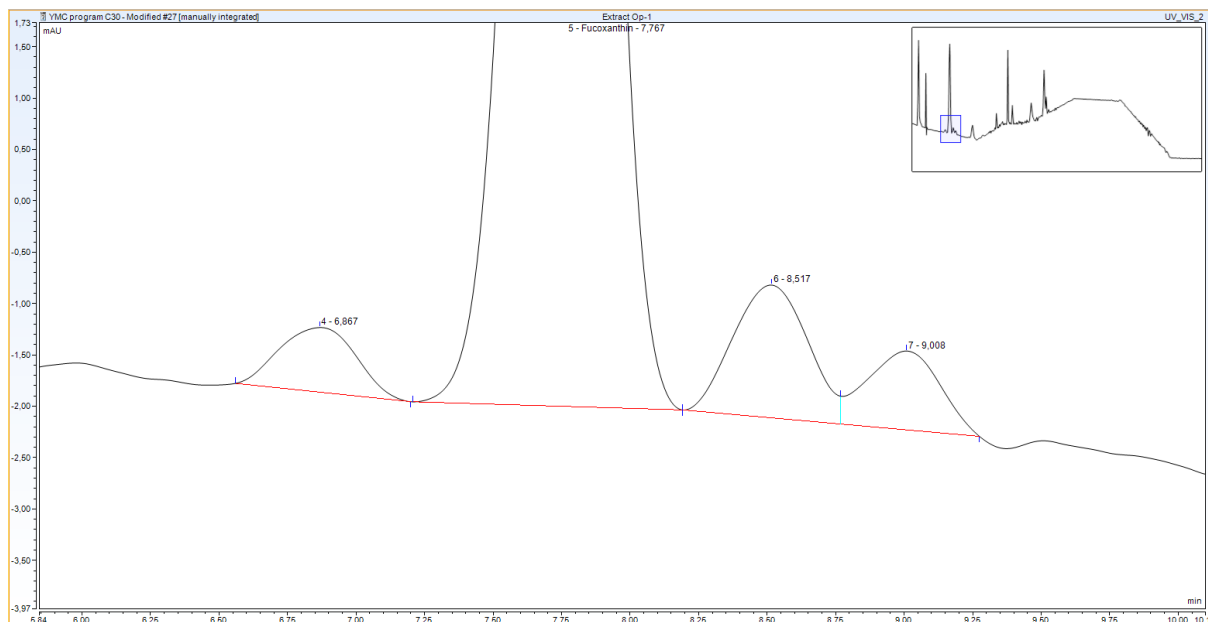
Attachment 6 – HPLC data from the optimization study

Extraction number (Op-1)

448 nm



Zoom



Peak properties Fucoxanthin

Property Name	Property Value
No.	5
Peakname	Fucoxanthin
Ret.Time	7,767 min
Peak Width	0,548 min
Type	BMb*
Height	18,584 mAU
Area	6,3657 mAU*min

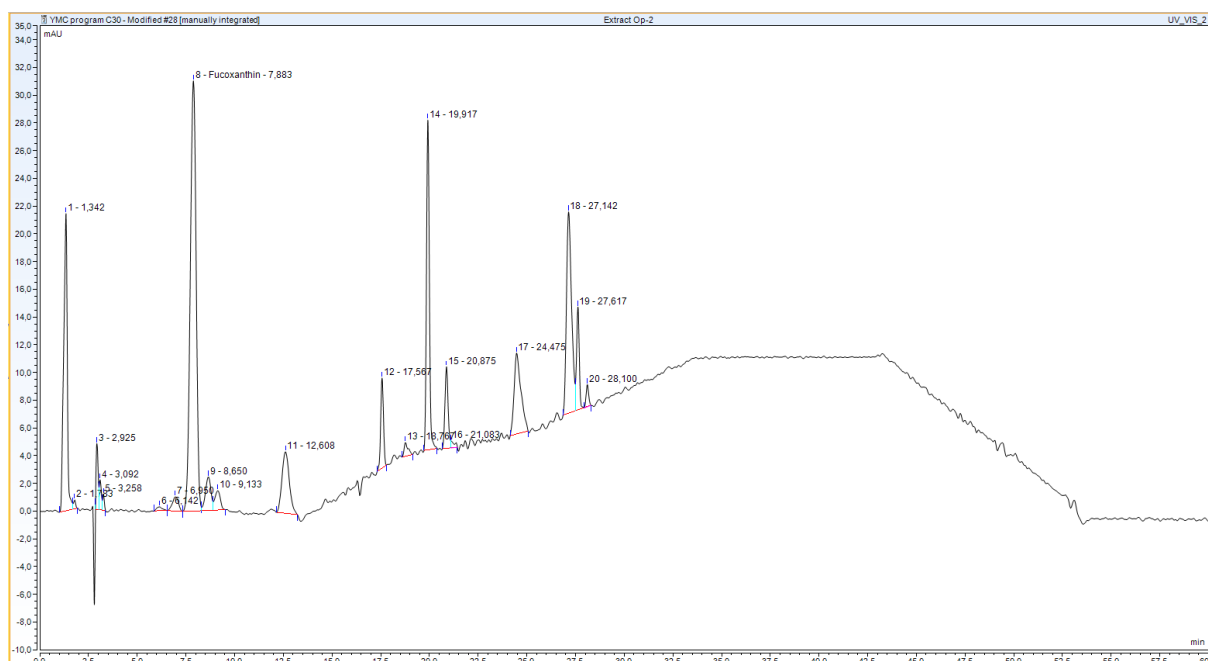
Peak properties for neighboring peaks

Property Name	Property Value
No.	4
Peakname	
Ret.Time	6,867 min
Peak Width	0,514 min
Type	BMB*
Height	0,630 mAU
Area	0,2038 mAU*min

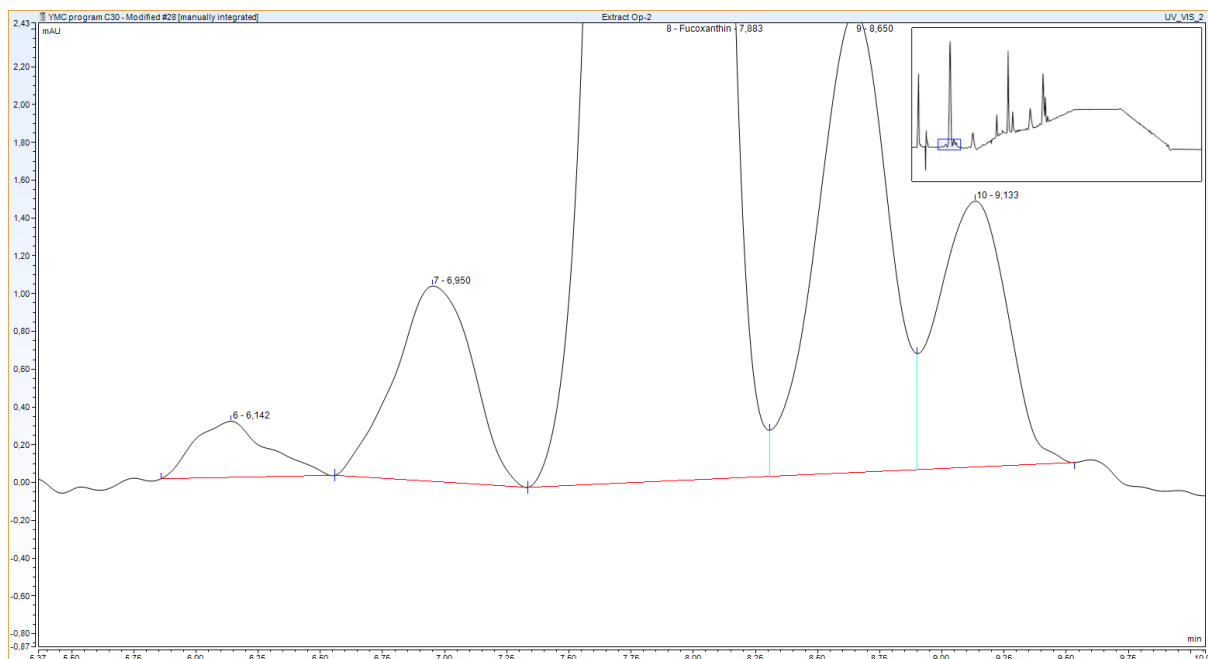
Property Name	Property Value
No.	6
Peakname	
Ret.Time	8,517 min
Peak Width	0,524 min
Type	bM *
Height	1,294 mAU
Area	0,4080 mAU*min

Extraction number (Op-2)

448 nm



Zoom



Peak properties Fucoxanthin

Property Name	Property Value
No.	8
Peakname	Fucoxanthin
Ret.Time	7,883 min
Peak Width	0,557 min
Type	bM *
Height	31,035 mAU
Area	10,7855 mAU*min

Peak properties for neighboring peaks

Property Name	Property Value
No.	7
Peakname	
Ret.Time	6,950 min
Peak Width	0,549 min
Type	bMb*
Height	1,034 mAU
Area	0,3753 mAU*min

Property Name	Property Value
No.	9
Peakname	
Ret.Time	8,650 min
Peak Width	0,528 min
Type	M *
Height	2,435 mAU
Area	0,8017 mAU*min

Rerun: Op-2

Peak properties Fucoxanthin

Property Name	Property Value
No.	5
Peakname	Fucoxanthin
Ret.Time	7,775 min
Peak Width	0,541 min
Type	bM *
Height	32,014 mAU
Area	10,8272 mAU*min

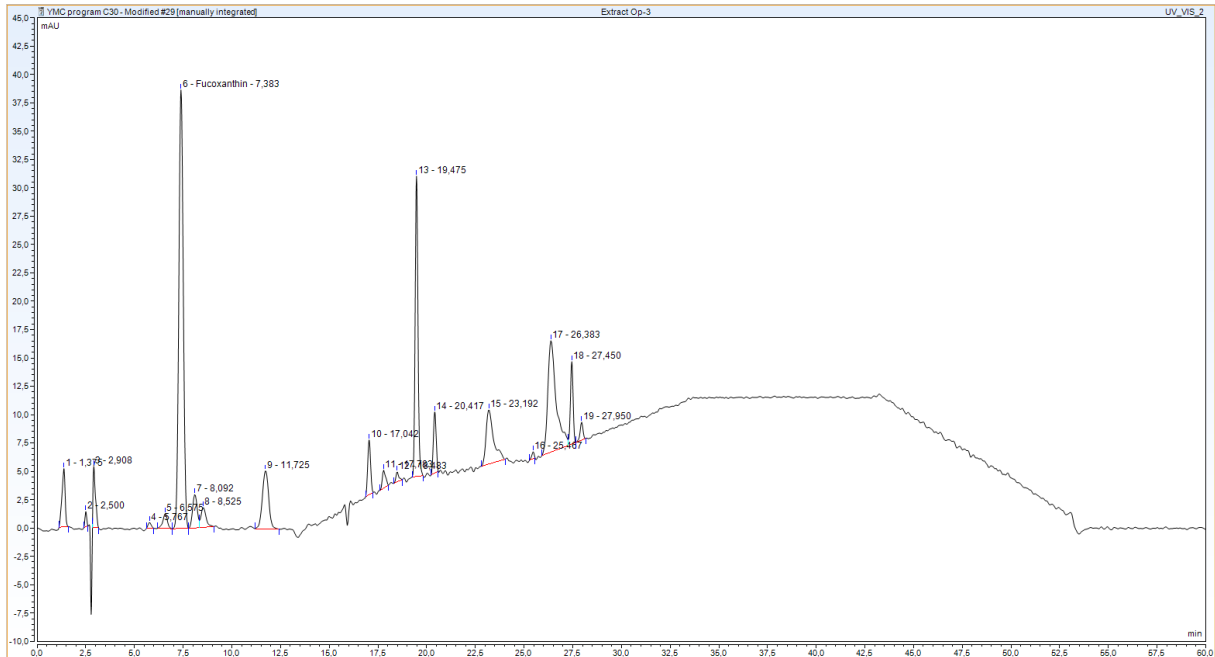
Peak properties for neighboring peaks

Property Name	Property Value
No.	4
Peakname	
Ret.Time	6,858 min
Peak Width	0,720 min
Type	Mb*
Height	1,120 mAU
Area	0,3624 mAU*min

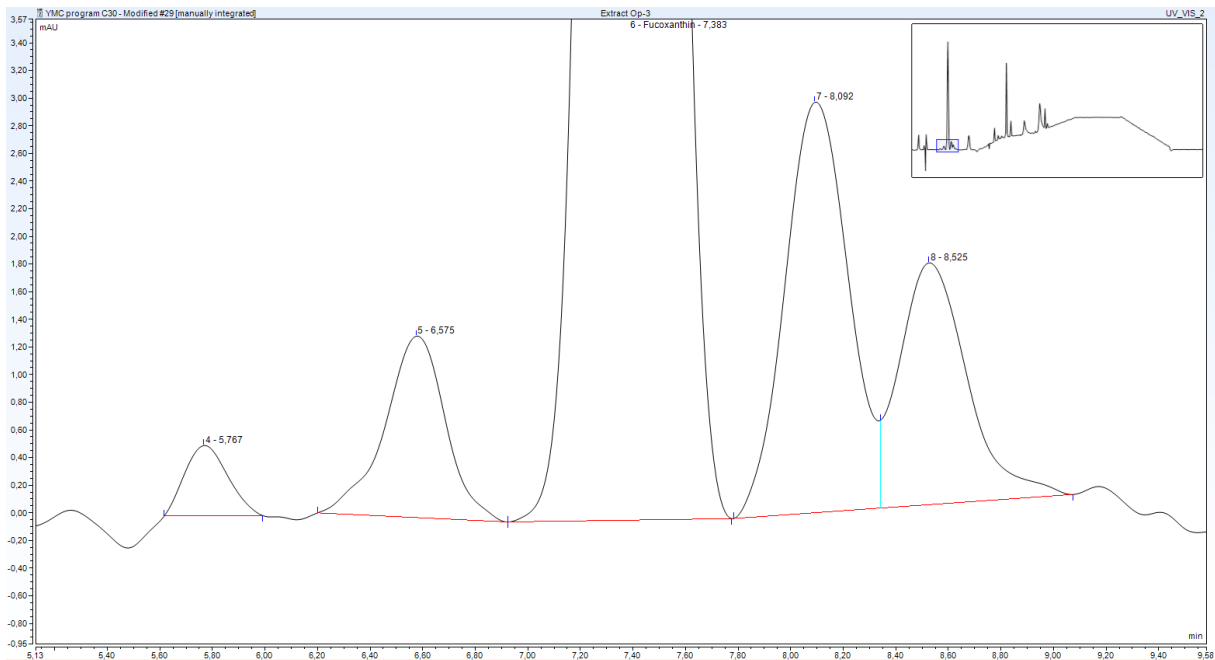
Property Name	Property Value
No.	6
Peakname	
Ret.Time	8,508 min
Peak Width	0,596 min
Type	M *
Height	2,241 mAU
Area	0,8008 mAU*min

Experiment number (Op-3)

448 nm



Zoom



Peak properties Fucoxanthin

Property Name	Property Value
No.	6
Peakname	Fucoxanthin
Ret.Time	7,383 min
Peak Width	0,423 min
Type	BMB
Height	38,707 mAU
Area	10,2191 mAU*min

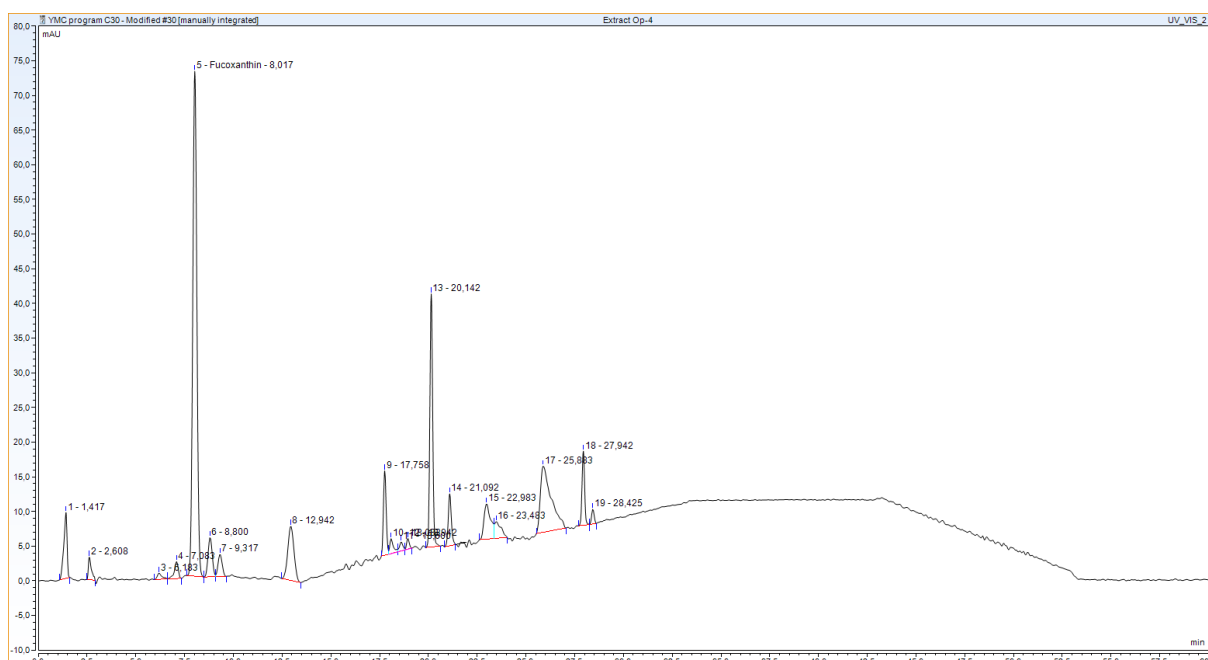
Peak properties for neighboring peaks

Property Name	Property Value
No.	5
Peakname	
Ret.Time	6,575 min
Peak Width	0,397 min
Type	BMB*
Height	1,313 mAU
Area	0,3506 mAU*min

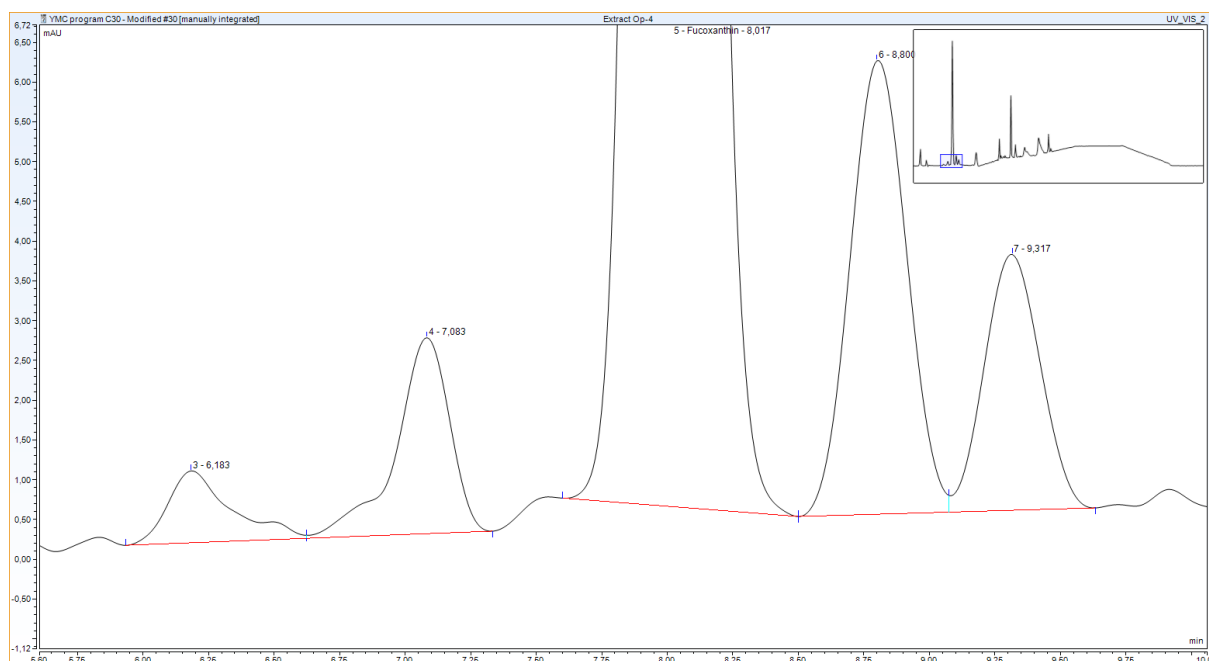
Property Name	Property Value
No.	7
Peakname	
Ret.Time	8,092 min
Peak Width	0,442 min
Type	BM
Height	2,970 mAU
Area	0,8301 mAU*min

Experiment number (Op-4)

448 nm



Zoom



Peak properties Fucoxanthin

Property Name	Property Value
No.	5
Peakname	Fucoxanthin
Ret.Time	8,017 min
Peak Width	0,386 min
Type	BMB
Height	72,842 mAU
Area	17,6596 mAU*min

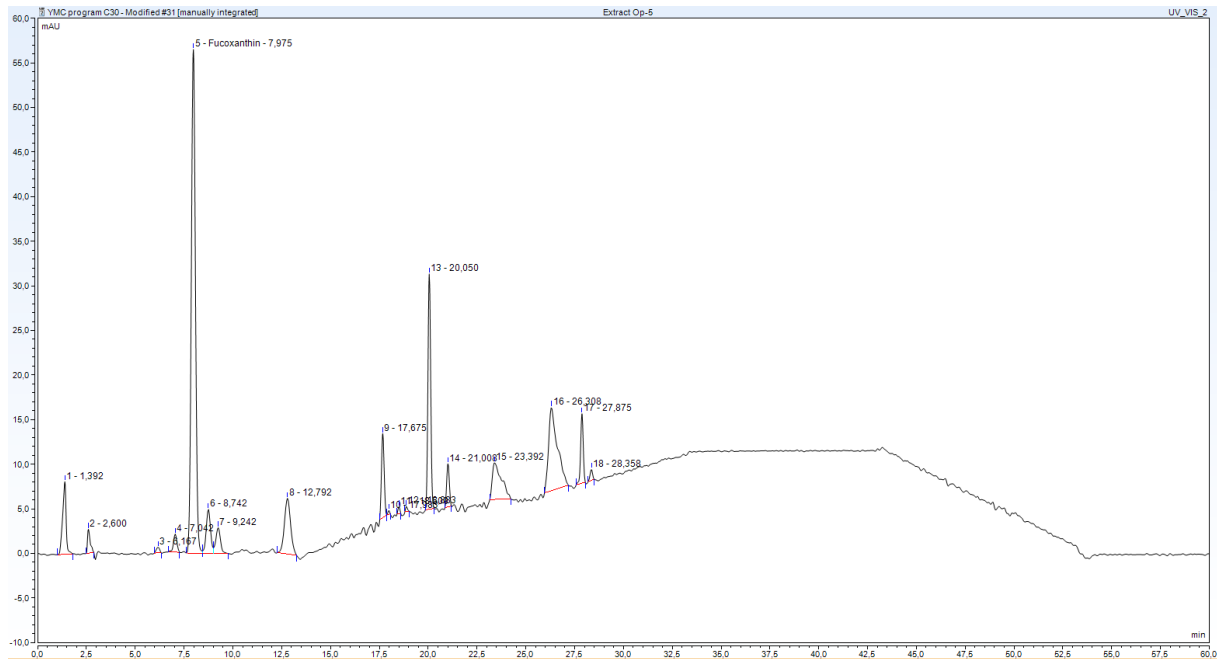
Peak properties for neighboring peaks

Property Name	Property Value
No.	4
Peakname	
Ret.Time	7,083 min
Peak Width	0,341 min
Type	MB
Height	2,465 mAU
Area	0,5856 mAU*min

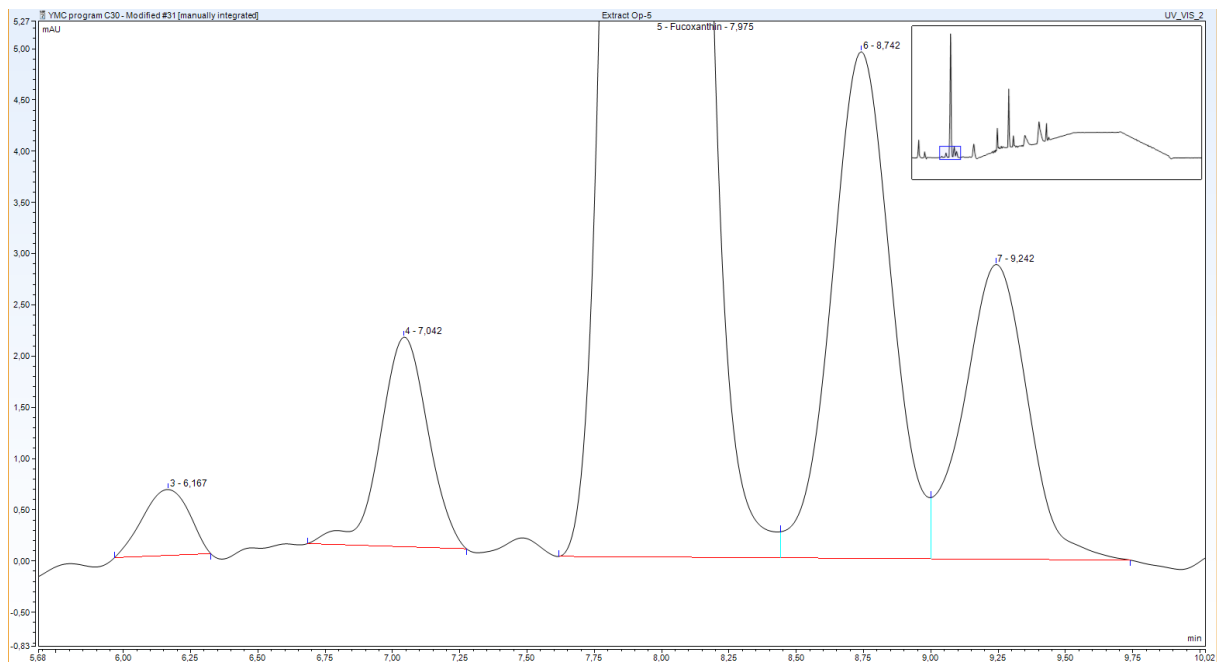
Property Name	Property Value
No.	6
Peakname	
Ret.Time	8,800 min
Peak Width	0,404 min
Type	BM
Height	5,704 mAU
Area	1,4262 mAU*min

Experiment number (Op-5)

448 nm



Zoom



Peak properties Fucoxanthin

Property Name	Property Value
No.	5
Peakname	Fucoxanthin
Ret.Time	7,975 min
Peak Width	0,386 min
Type	BM *
Height	56,467 mAU
Area	13,7570 mAU*min

Peak properties for neighboring peaks

Property Name	Property Value
No.	4
Peakname	
Ret.Time	7,042 min
Peak Width	0,321 min
Type	BMB*
Height	2,047 mAU
Area	0,4242 mAU*min

Property Name	Property Value
No.	6
Peakname	
Ret.Time	8,742 min
Peak Width	0,406 min
Type	M *
Height	4,946 mAU
Area	1,2729 mAU*min

Rerun: Op-5

Peak properties Fucoxanthin

Property Name	Property Value
No.	5
Peakname	Fucoxanthin
Ret.Time	7,175 min
Peak Width	0,342 min
Type	BM *
Height	61,333 mAU
Area	13,2360 mAU*min

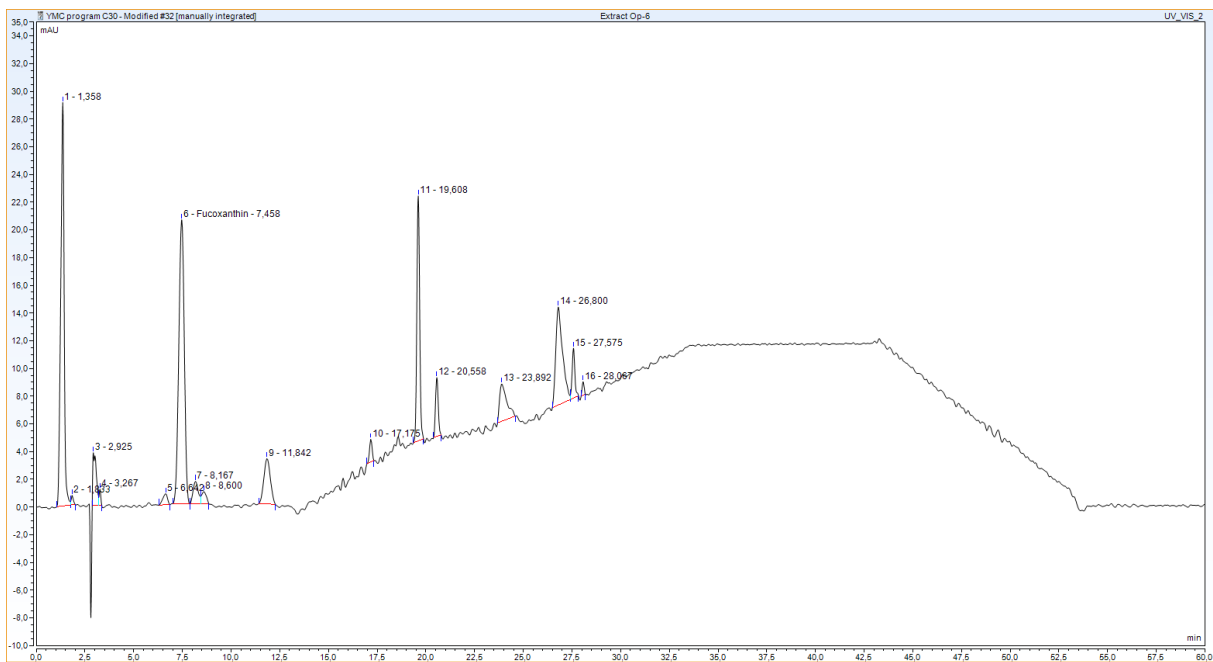
Peak properties for neighboring peaks

Property Name	Property Value
No.	4
Peakname	
Ret.Time	6,425 min
Peak Width	0,315 min
Type	BMB*
Height	2,445 mAU
Area	0,5284 mAU*min

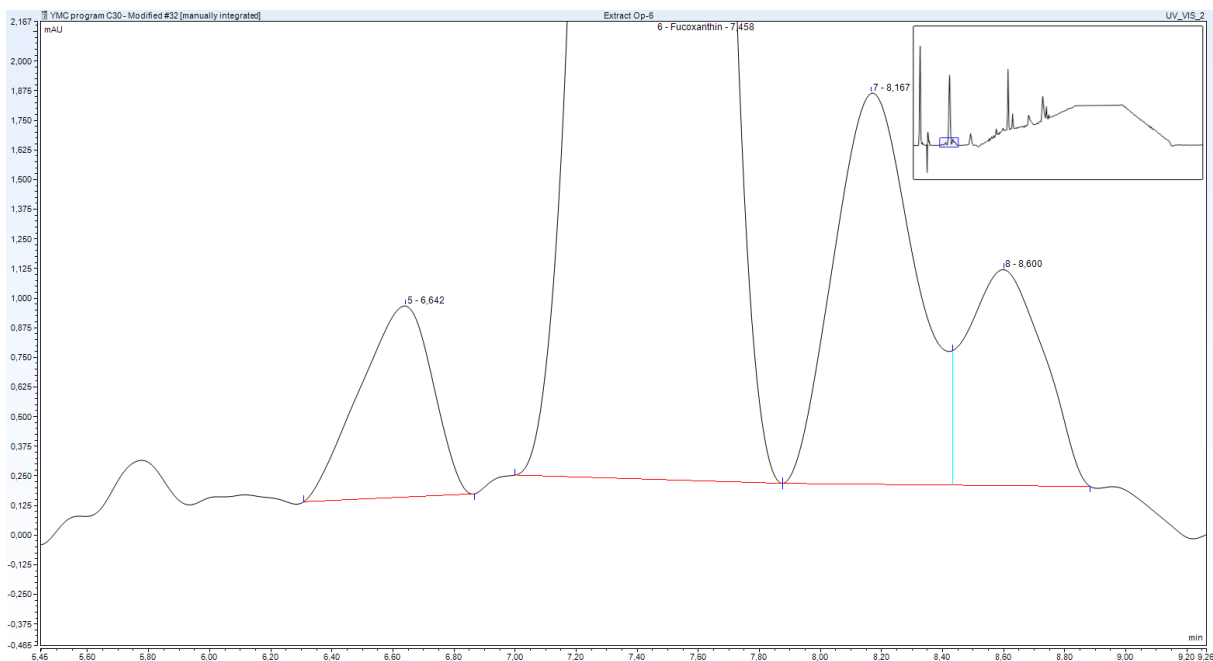
Property Name	Property Value
No.	6
Peakname	Fucoxanthin
Ret.Time	7,850 min
Peak Width	0,393 min
Type	M *
Height	5,166 mAU
Area	1,3311 mAU*min

Experiment number (Op-6)

448 nm



Zoom



Peak properties Fucoxanthin

Property Name	Property Value
No.	6
Peakname	Fucoxanthin
Ret.Time	7,458 min
Peak Width	0,524 min
Type	BMb*
Height	20,499 mAU
Area	6,6815 mAU*min

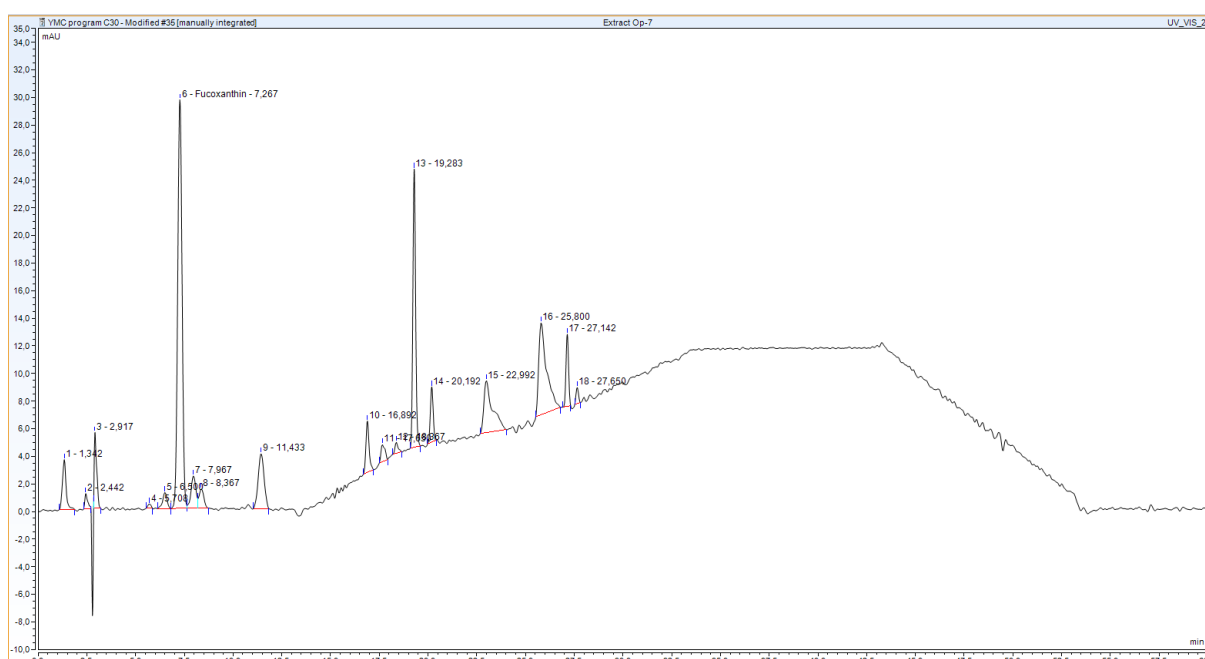
Peak properties for neighboring peaks

Property Name	Property Value
No.	5
Peakname	
Ret.Time	6,642 min
Peak Width	0,480 min
Type	BMB*
Height	0,806 mAU
Area	0,2222 mAU*min

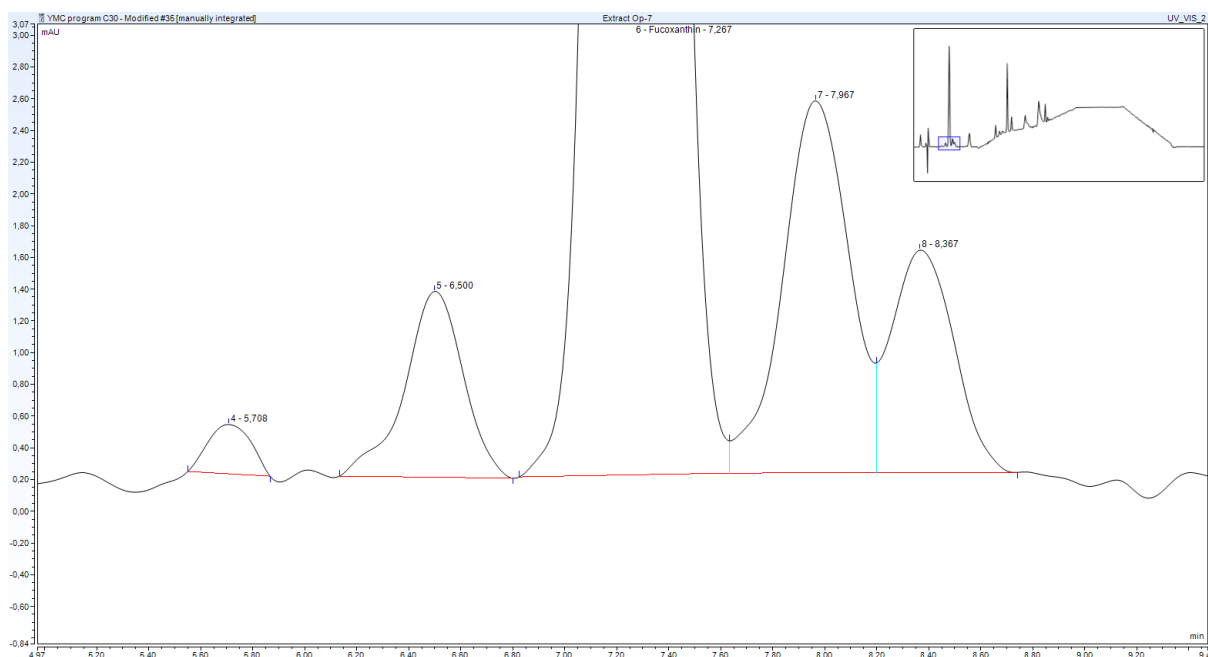
Property Name	Property Value
No.	7
Peakname	
Ret.Time	8,167 min
Peak Width	0,507 min
Type	bM *
Height	1,651 mAU
Area	0,5088 mAU*min

Experiment number (Op-7)

448 nm



Zoom



Peak properties Fucoxanthin

Property Name	Property Value
No.	6
Peakname	Fucoxanthin
Ret.Time	7,267 min
Peak Width	0,413 min
Type	BM *
Height	29,615 mAU
Area	7,6734 mAU*min

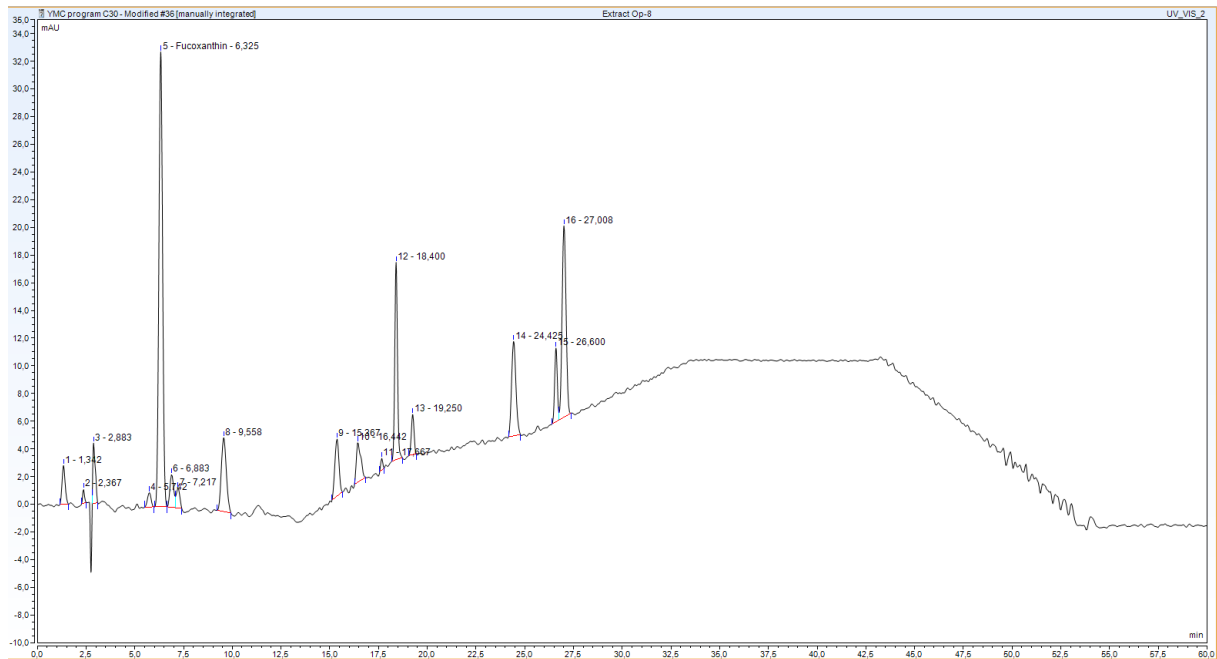
Peak properties for neighboring peaks

Property Name	Property Value
No.	5
Peakname	
Ret.Time	6,500 min
Peak Width	0,389 min
Type	BMB*
Height	1,172 mAU
Area	0,3060 mAU*min

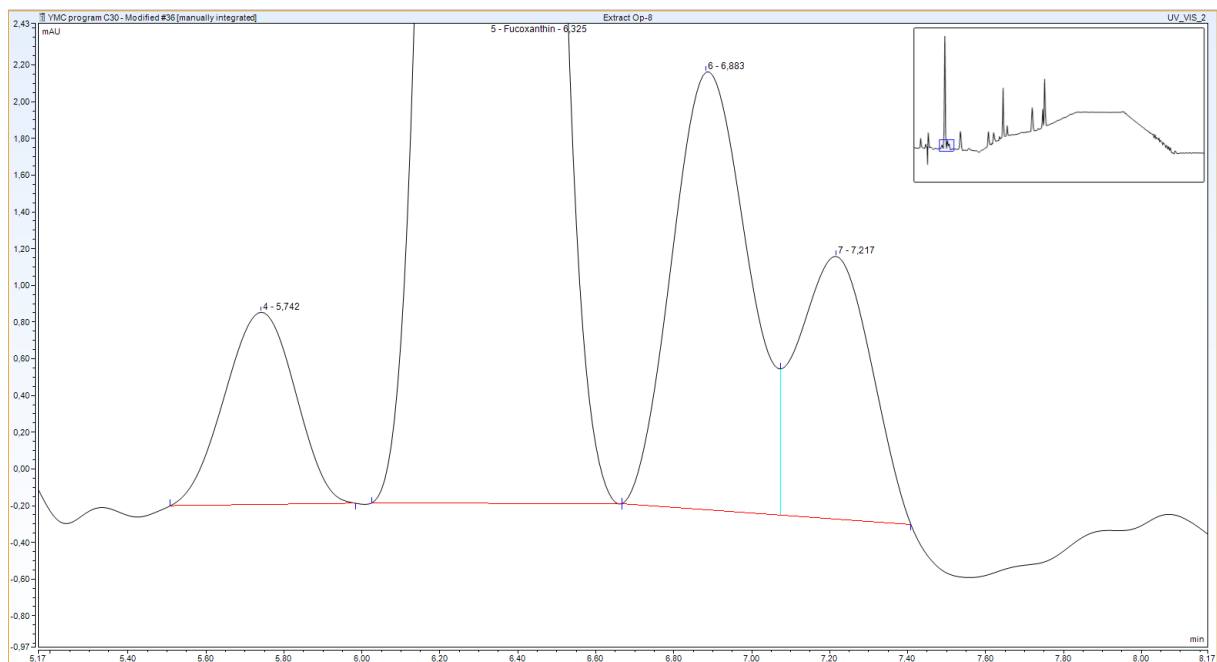
Property Name	Property Value
No.	7
Peakname	
Ret.Time	7,967 min
Peak Width	0,467 min
Type	M *
Height	2,345 mAU
Area	0,6994 mAU*min

Experiment number (Op-8)

448 nm



Zoom



Peak properties Fucoxanthin

Property Name	Property Value
No.	5
Peakname	Fucoxanthin
Ret.Time	6,325 min
Peak Width	0,353 min
Type	BMb*
Height	32,879 mAU
Area	7,2463 mAU*min

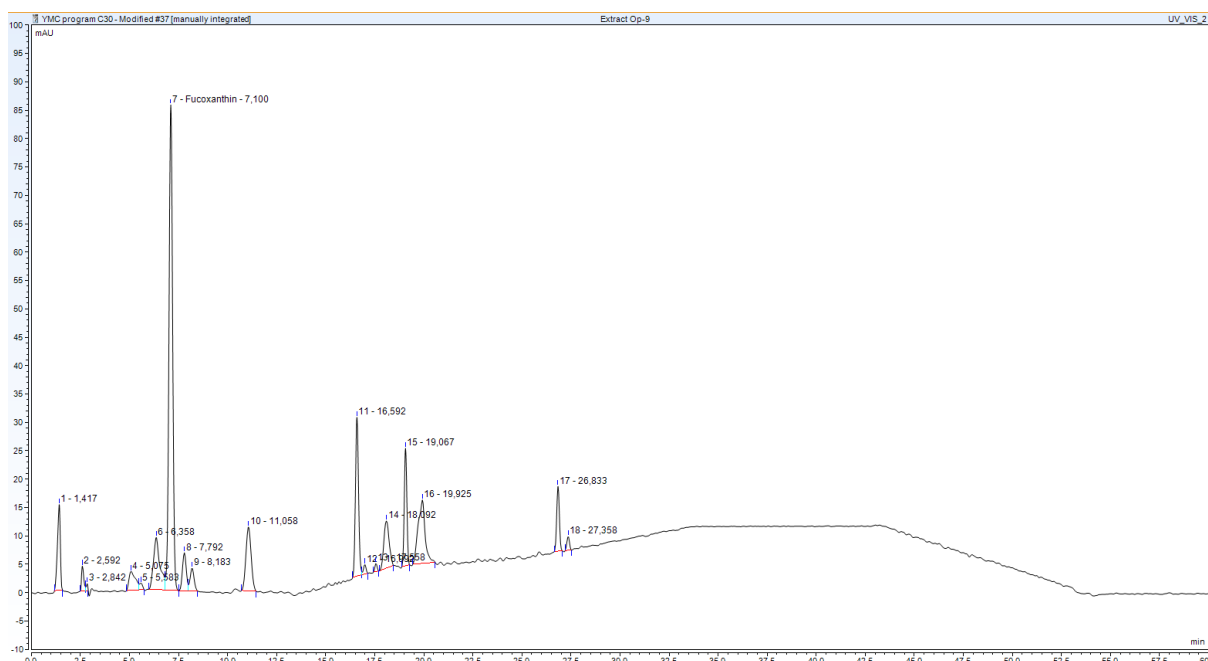
Peak properties neighboring peaks

Property Name	Property Value
No.	4
Peakname	
Ret.Time	5,742 min
Peak Width	0,342 min
Type	BMB*
Height	1,047 mAU
Area	0,2195 mAU*min

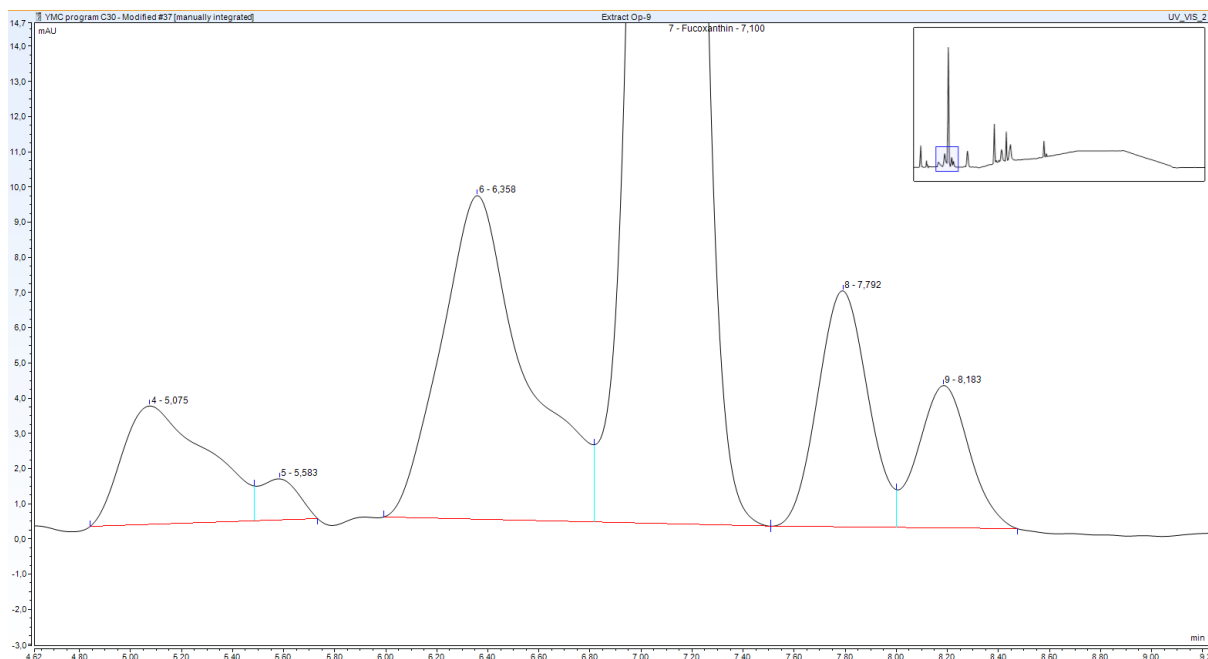
Property Name	Property Value
No.	6
Peakname	
Ret.Time	6,883 min
Peak Width	0,375 min
Type	bM *
Height	2,384 mAU
Area	0,5399 mAU*min

Experiment number (Op-9)

448 nm



Zoom



Peak properties Fucoxanthin

Property Name	Property Value
No.	7
Peakname	Fucoxanthin
Ret.Time	7,100 min
Peak Width	0,341 min
Type	Mb*
Height	85,495 mAU
Area	18,4515 mAU*min

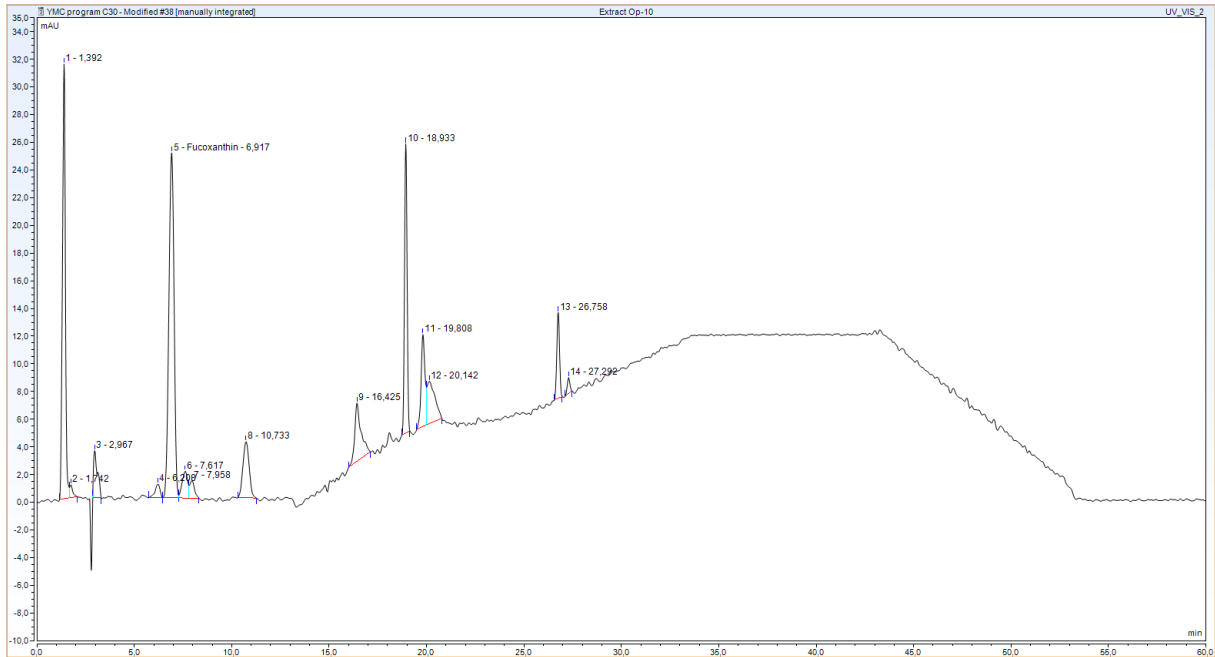
Peak properties neighboring peaks

Property Name	Property Value
No.	6
Peakname	
Ret.Time	6,358 min
Peak Width	0,535 min
Type	BM *
Height	9,195 mAU
Area	3,5364 mAU*min

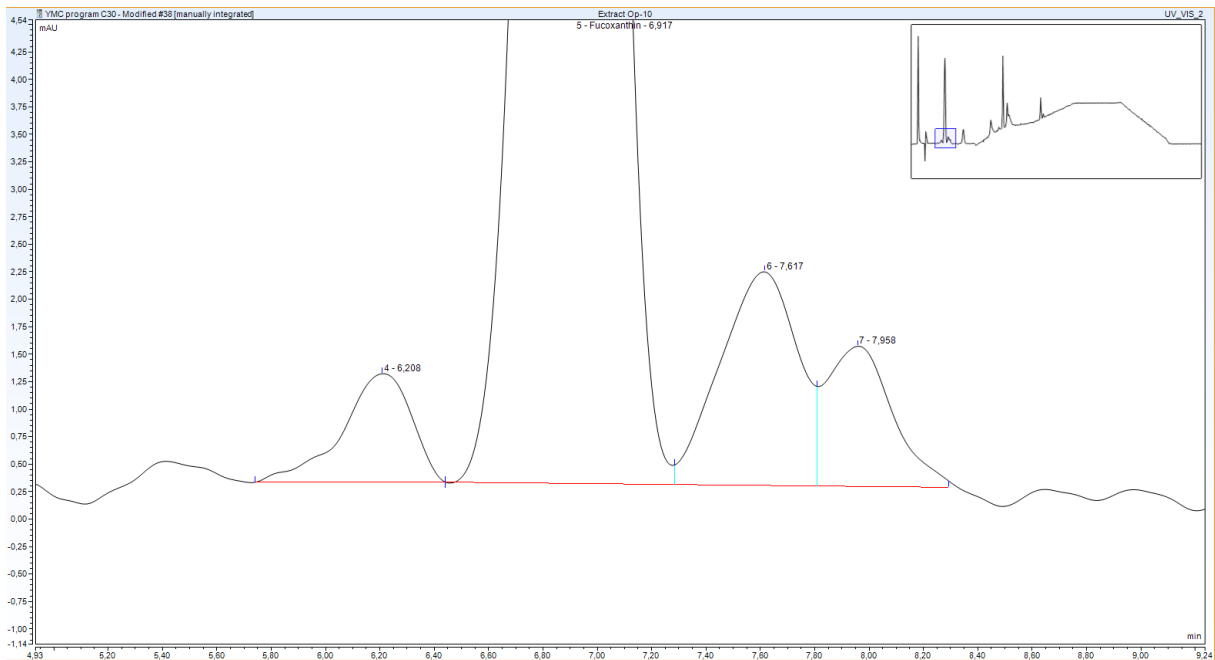
Property Name	Property Value
No.	8
Peakname	
Ret.Time	7,792 min
Peak Width	0,368 min
Type	bM *
Height	6,710 mAU
Area	1,5261 mAU*min

Experiment number (Op-10)

448 nm



Zoom



Peak properties Fucoxanthin

Property Name	Property Value
No.	5
Peakname	Fucoxanthin
Ret.Time	6,917 min
Peak Width	0,495 min
Type	bM *
Height	24,919 mAU
Area	7,6818 mAU*min

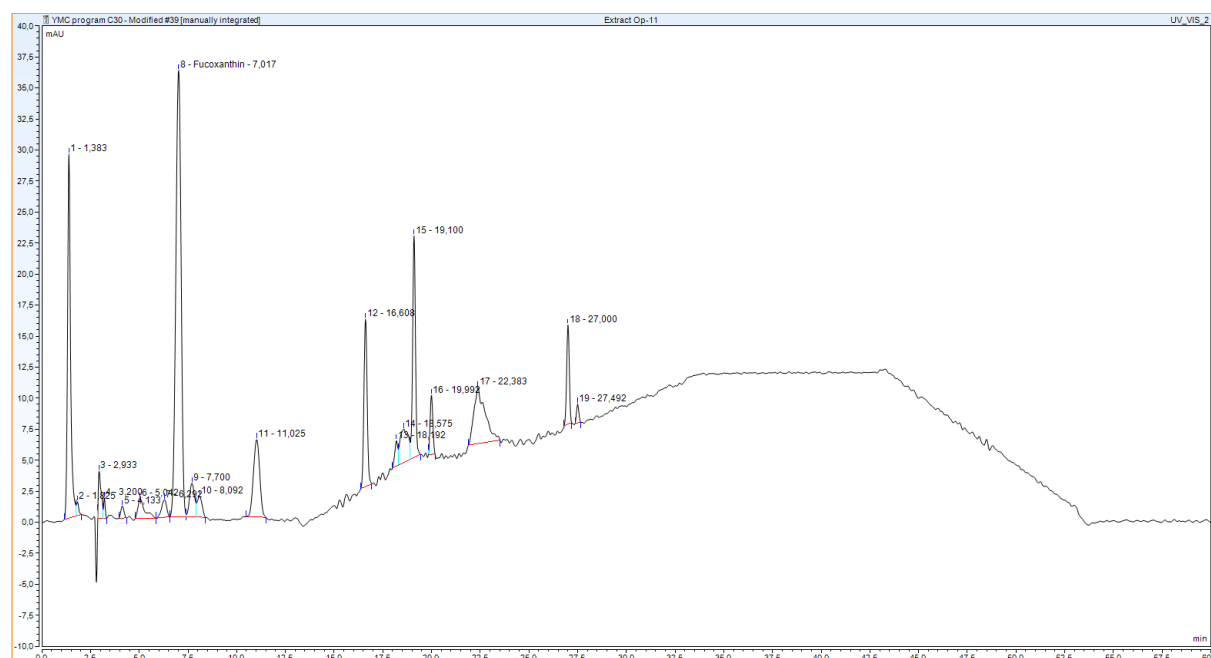
Peak properties neighboring peaks

Property Name	Property Value
No.	4
Peakname	
Ret.Time	6,208 min
Peak Width	0,424 min
Type	BMb*
Height	0,987 mAU
Area	0,2910 mAU*min

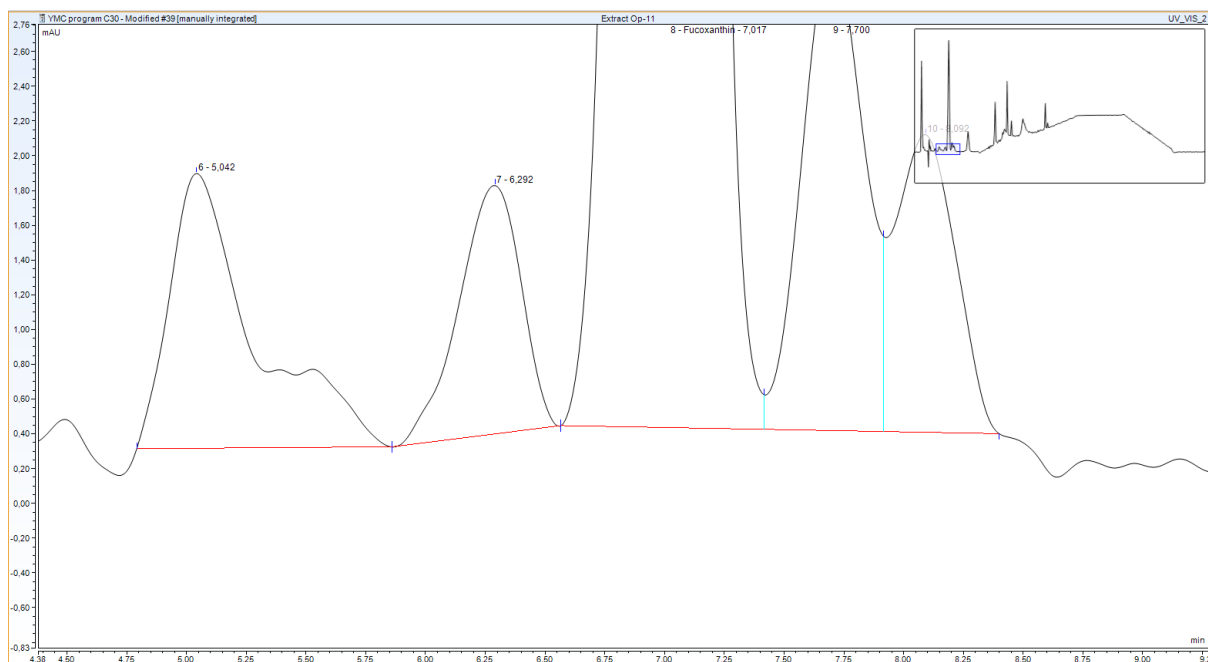
Property Name	Property Value
No.	6
Peakname	
Ret.Time	7,617 min
Peak Width	0,600 min
Type	M *
Height	1,943 mAU
Area	0,6392 mAU*min

Experiment number (Op-11)

448 nm



Zoom



Peak properties Fucoxanthin

Property Name	Property Value
No.	8
Peakname	Fucoxanthin
Ret.Time	7,017 min
Peak Width	0,499 min
Type	bM *
Height	35,994 mAU
Area	11,2376 mAU*min

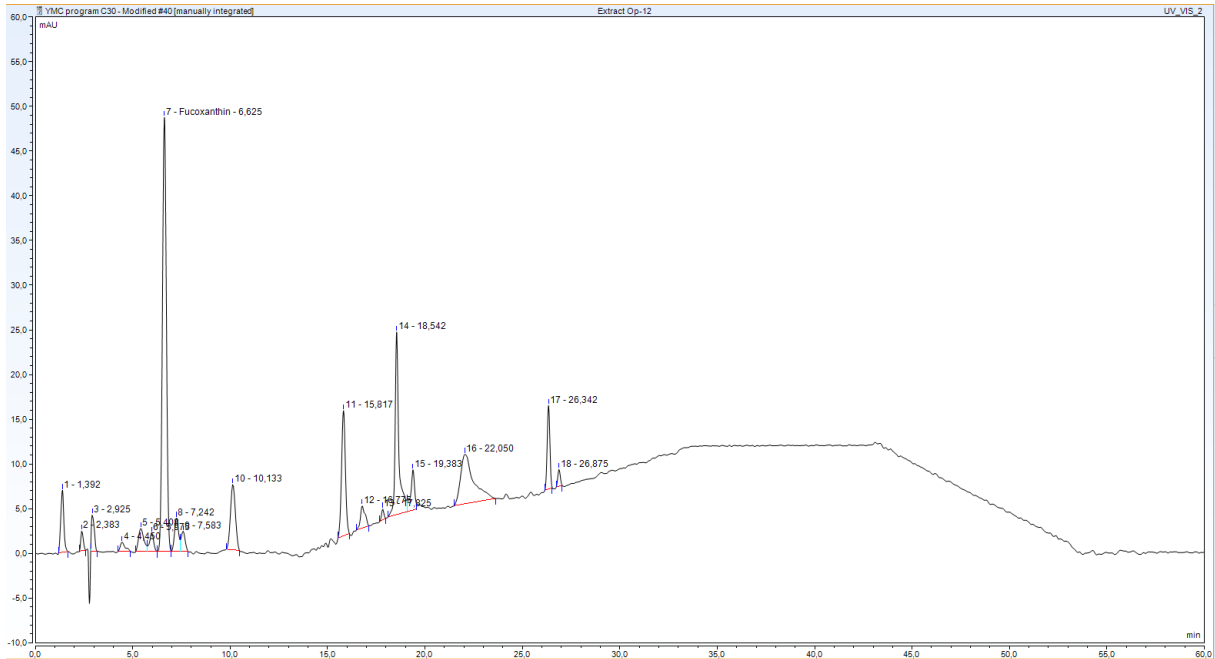
Peak properties neighboring peaks

Property Name	Property Value
No.	7
Peakname	
Ret.Time	6,292 min
Peak Width	0,479 min
Type	bMb*
Height	1,429 mAU
Area	0,4309 mAU*min

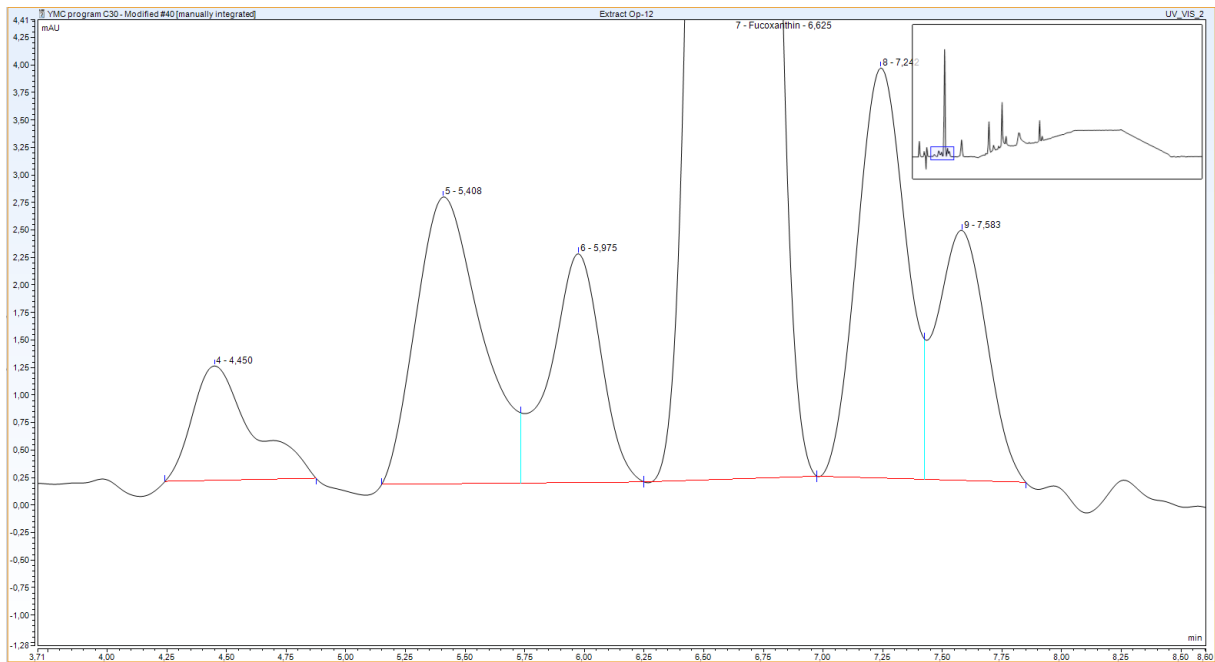
Property Name	Property Value
No.	9
Peakname	
Ret.Time	7,700 min
Peak Width	0,509 min
Type	M *
Height	2,751 mAU
Area	0,8204 mAU*min

Experiment number (Op-12)

448 nm



Zoom



Peak properties Fucoxanthin

Property Name	Property Value
No.	7
Peakname	Fucoxanthin
Ret.Time	6,625 min
Peak Width	0,375 min
Type	bMb*
Height	48,546 mAU
Area	11,3936 mAU*min

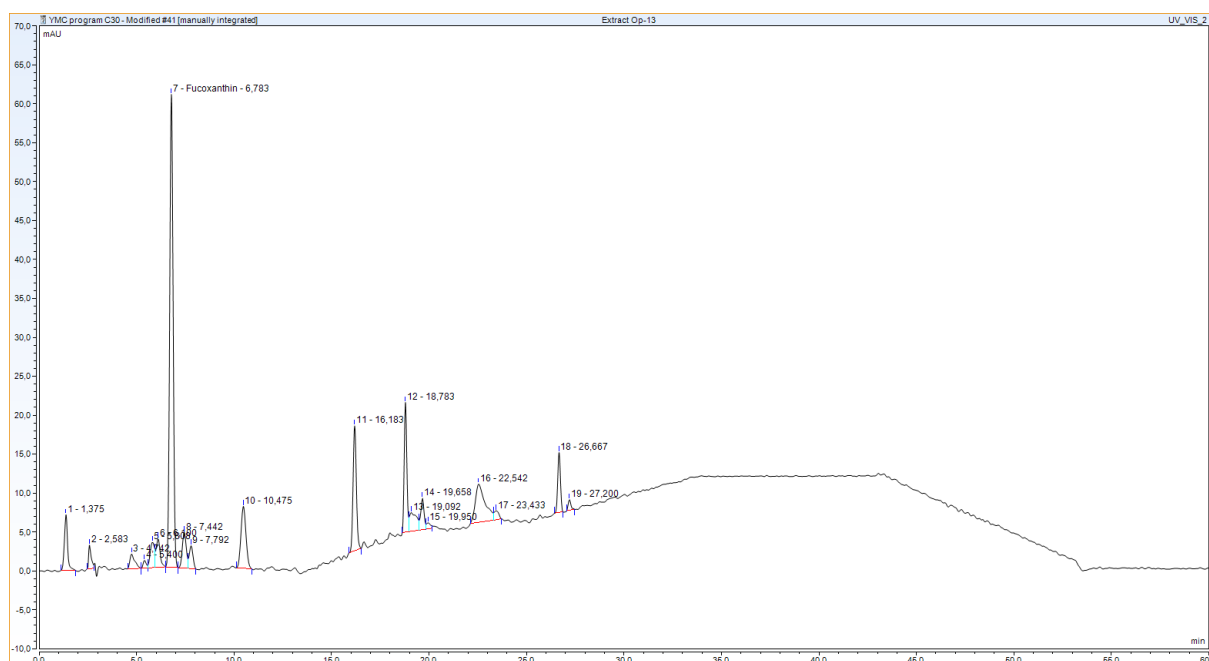
Peak properties neighboring peaks

Property Name	Property Value
No.	6
Peakname	
Ret.Time	6,100 min
Peak Width	0,424 min
Type	Mb*
Height	3,689 mAU
Area	0,8680 mAU*min

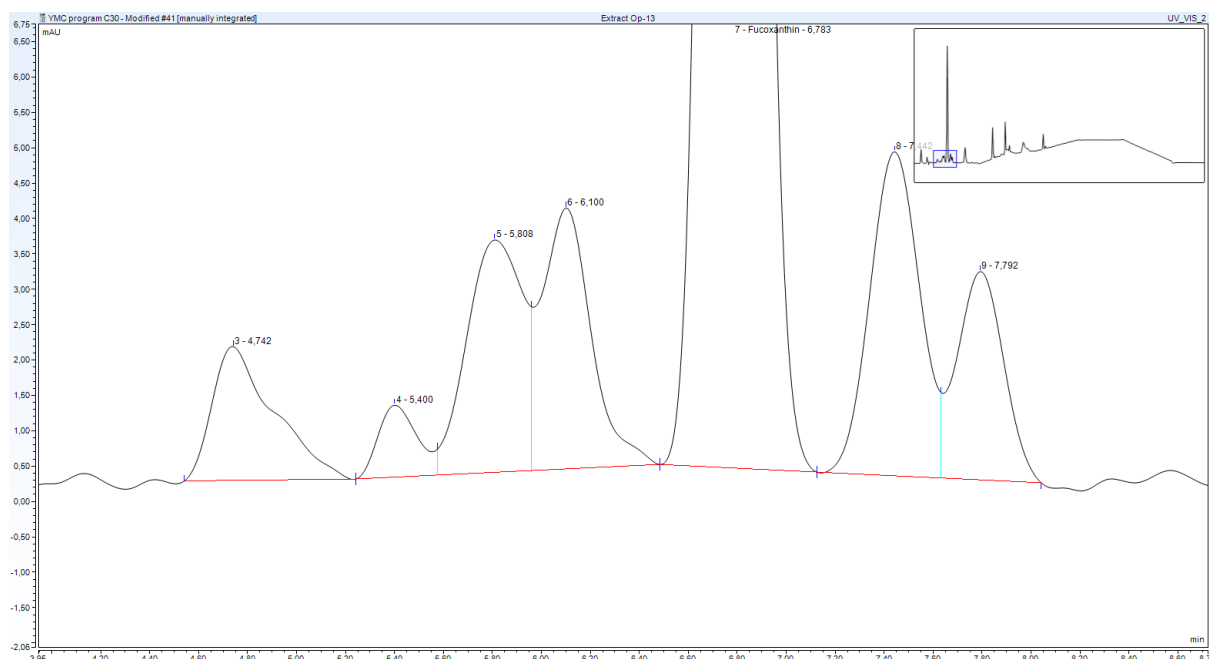
Property Name	Property Value
No.	8
Peakname	
Ret.Time	7,442 min
Peak Width	0,388 min
Type	bM *
Height	4,582 mAU
Area	1,0810 mAU*min

Experiment number (Op-13)

448 nm



Zoom



Peak properties Fucoxanthin

Property Name	Property Value
No.	7
Peakname	Fucoxanthin
Ret.Time	6,783 min
Peak Width	0,325 min
Type	bMb*
Height	60,749 mAU
Area	12,3520 mAU*min

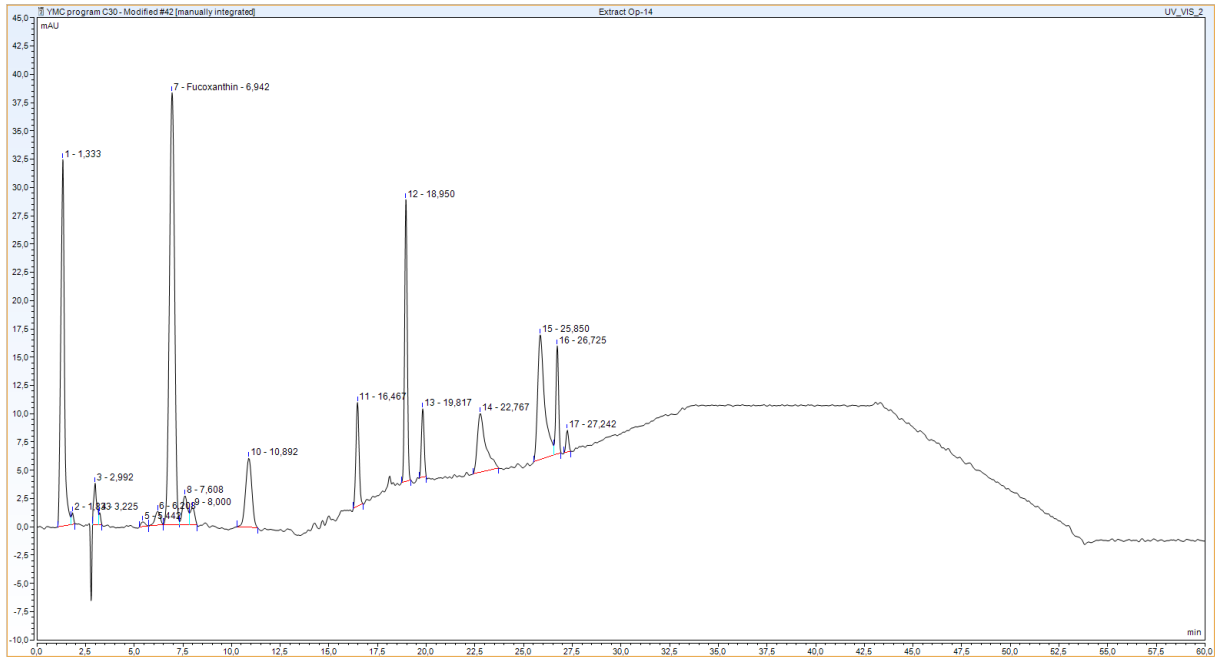
Peak properties neighboring peaks

Property Name	Property Value
No.	6
Peakname	
Ret.Time	6,100 min
Peak Width	0,424 min
Type	Mb*
Height	3,689 mAU
Area	0,8680 mAU*min

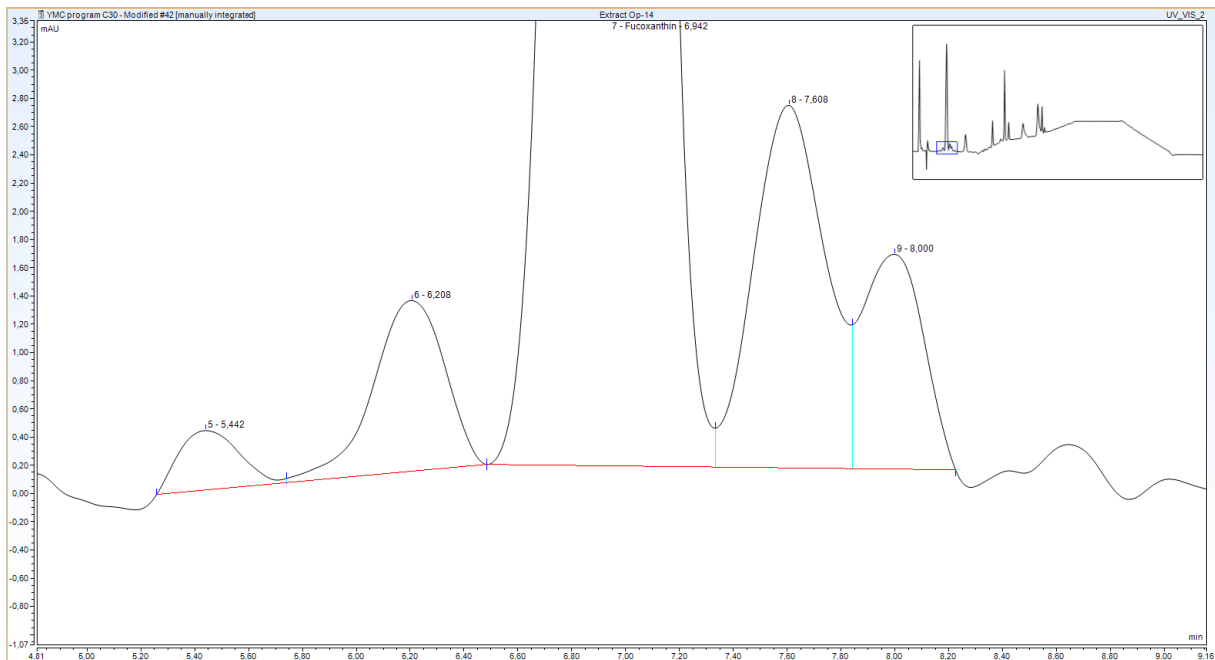
Property Name	Property Value
No.	8
Peakname	
Ret.Time	7,442 min
Peak Width	0,388 min
Type	bM*
Height	4,582 mAU
Area	1,0810 mAU*min

Experiment number (Op-14)

448 nm



Zoom



Peak properties Fucoxanthin

Property Name	Property Value
No.	7
Peakname	Fucoxanthin
Ret.Time	6,942 min
Peak Width	0,490 min
Type	bM *
Height	38,193 mAU
Area	11,6949 mAU*min

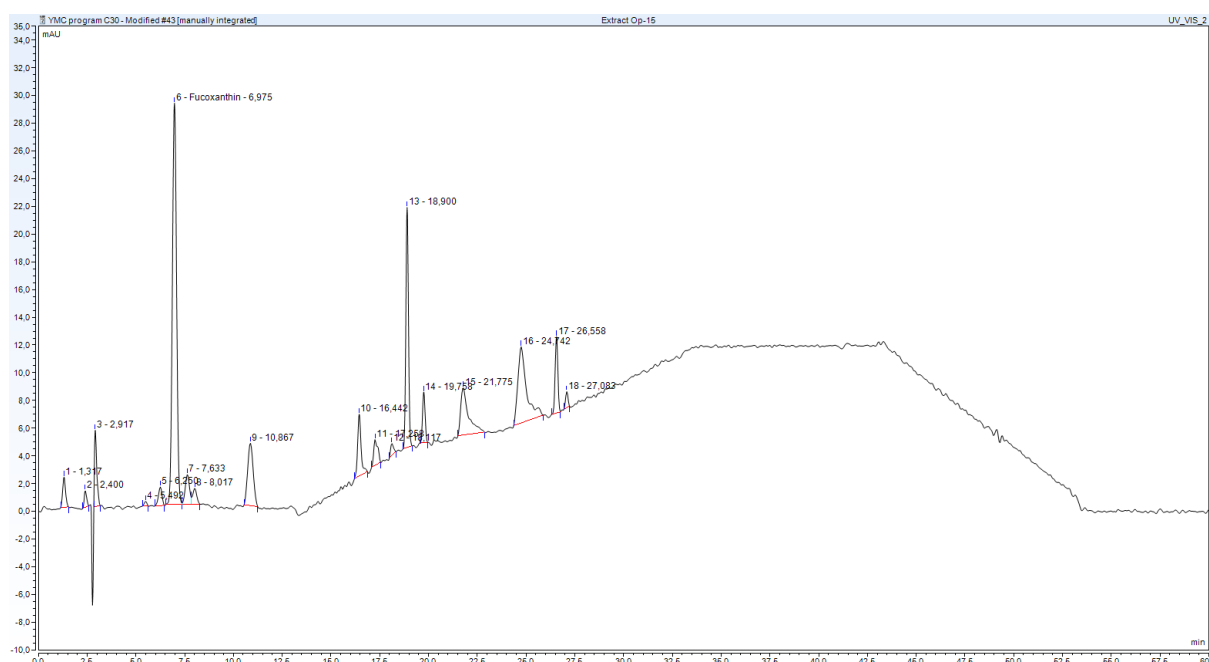
Peak properties neighboring peaks

Property Name	Property Value
No.	6
Peakname	
Ret.Time	6,208 min
Peak Width	0,469 min
Type	Mb*
Height	1,209 mAU
Area	0,3735 mAU*min

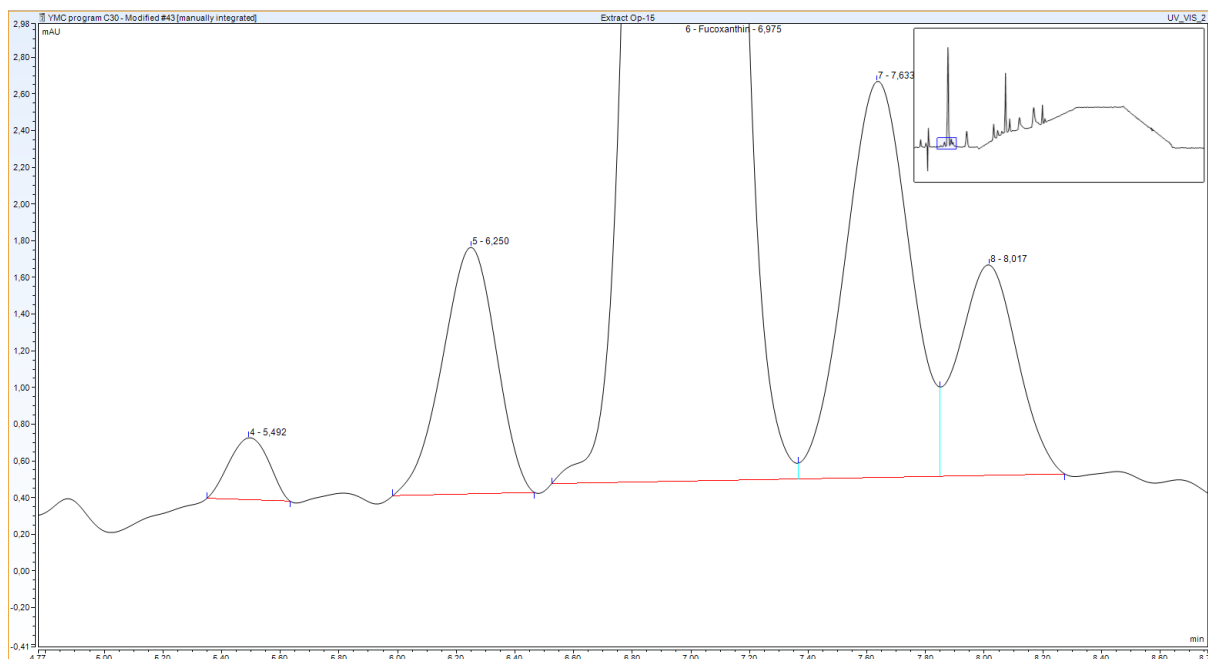
Property Name	Property Value
No.	8
Peakname	
Ret.Time	7,608 min
Peak Width	0,516 min
Type	M *
Height	2,569 mAU
Area	0,7931 mAU*min

Experiment number (Op-15)

448 nm



Zoom



Peak properties Fucoxanthin

Property Name	Property Value
No.	6
Peakname	Fucoxanthin
Ret.Time	6,975 min
Peak Width	0,396 min
Type	BM *
Height	28,972 mAU
Area	7,1941 mAU*min

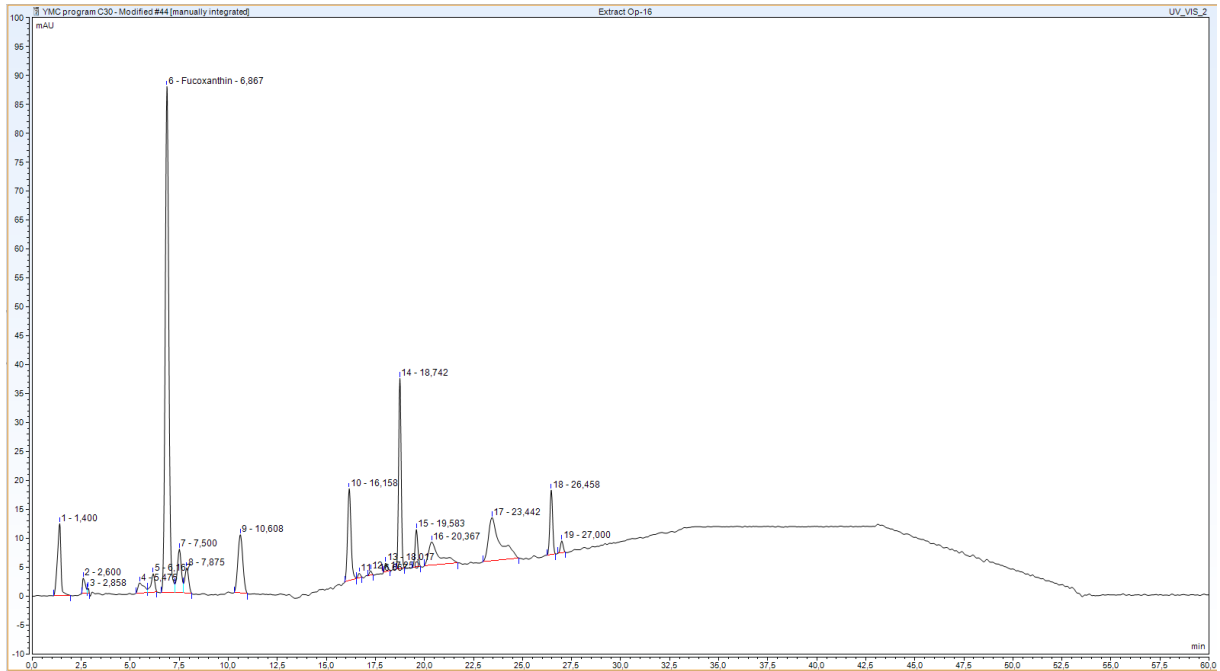
Peak properties neighboring peaks

Property Name	Property Value
No.	5
Peakname	
Ret.Time	6,250 min
Peak Width	0,344 min
Type	BMB*
Height	1,344 mAU
Area	0,2844 mAU*min

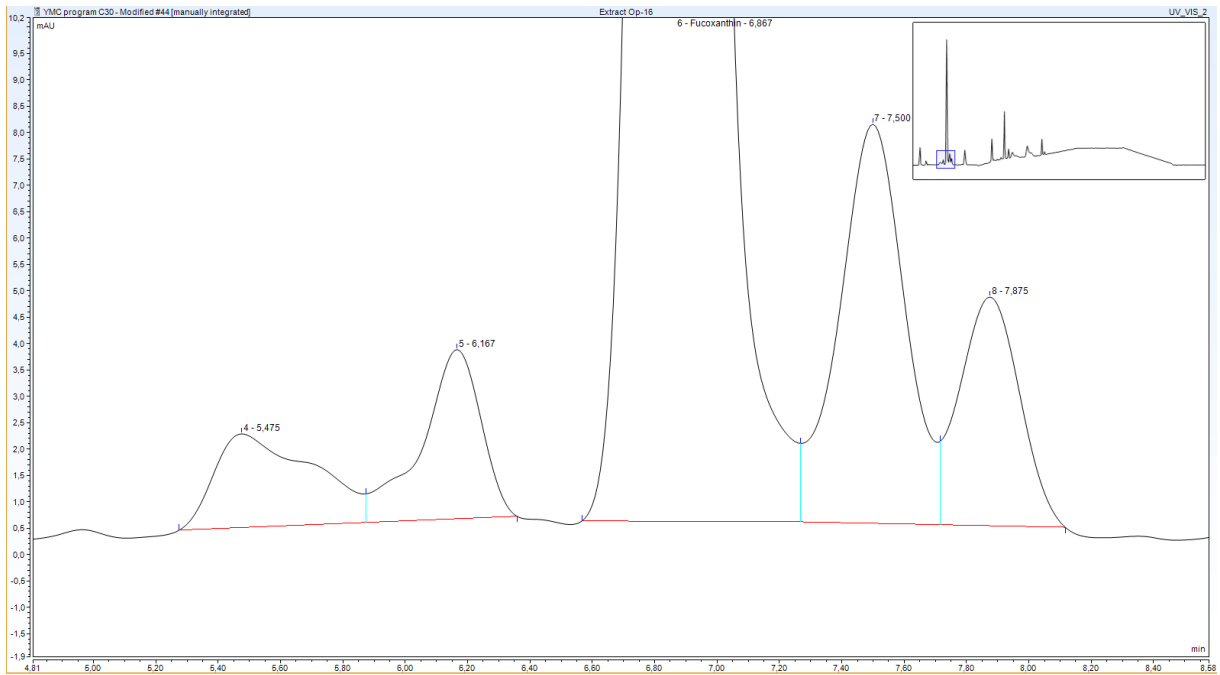
Property Name	Property Value
No.	7
Peakname	
Ret.Time	7,633 min
Peak Width	0,416 min
Type	M *
Height	2,159 mAU
Area	0,5511 mAU*min

Experiment number (Op-16)

448 nm



Zoom



Peak properties Fucoxanthin

Property Name	Property Value
No.	6
Peakname	Fucoxanthin
Ret.Time	6,867 min
Peak Width	0,333 min
Type	BM *
Height	87,477 mAU
Area	18,6804 mAU*min

Peak properties neighboring peaks

Property Name	Property Value
No.	5
Peakname	
Ret.Time	6,167 min
Peak Width	0,313 min
Type	MB*
Height	3,209 mAU
Area	0,7051 mAU*min

Property Name	Property Value
No.	7
Peakname	
Ret.Time	7,500 min
Peak Width	0,384 min
Type	M *
Height	7,567 mAU
Area	1,8603 mAU*min

Rerun Op-16

Peak properties Fucoxanthin

Property Name	Property Value
No.	7
Peakname	Fucoxanthin
Ret.Time	7,967 min
Peak Width	0,386 min
Type	M *
Height	73,945 mAU
Area	18,1608 mAU*min

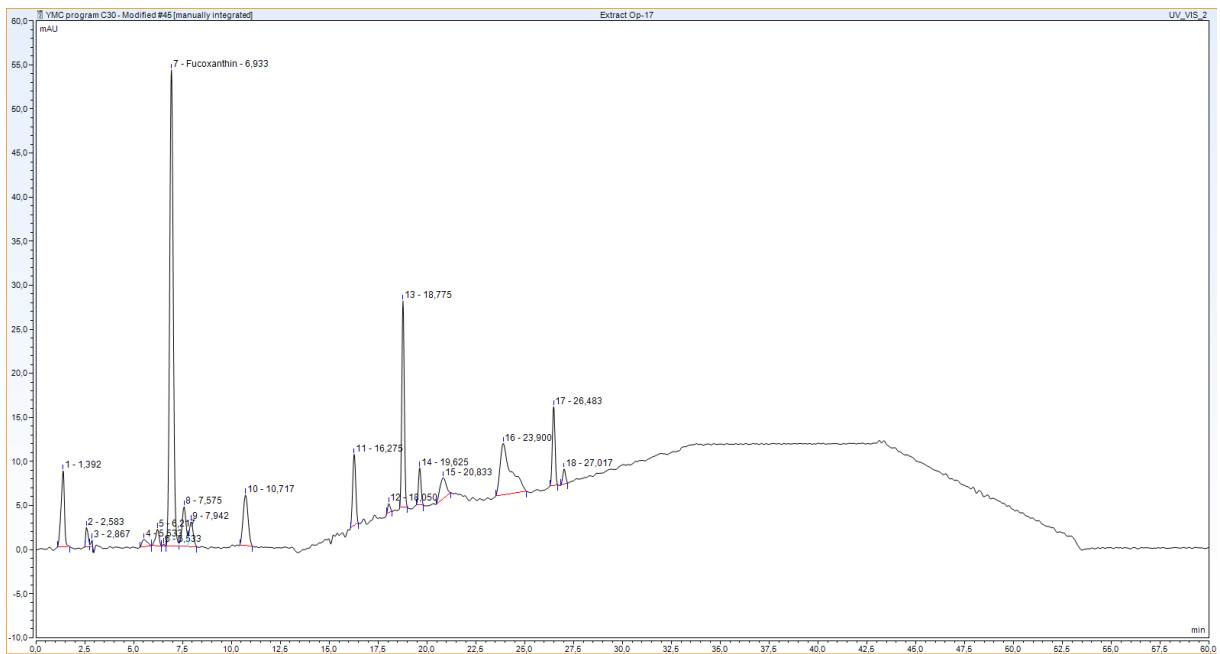
Peak properties neighboring peaks

Property Name	Property Value
No.	6
Peakname	
Ret.Time	7,067 min
Peak Width	0,515 min
Type	M *
Height	4,836 mAU
Area	2,1118 mAU*min

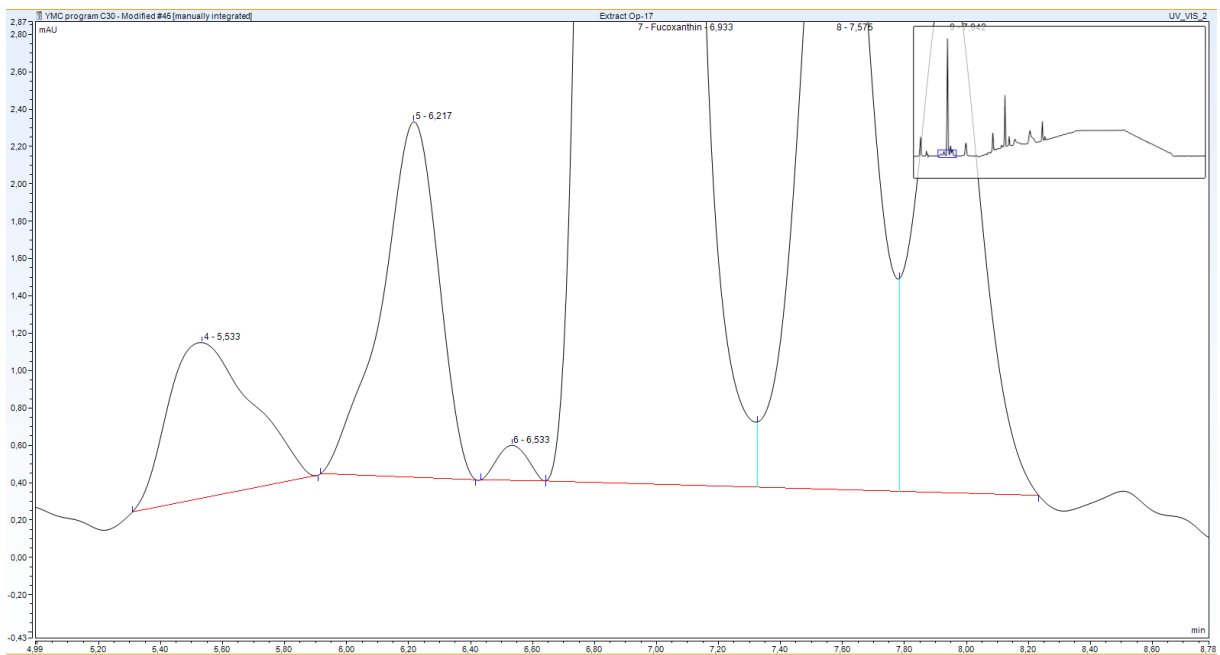
Property Name	Property Value
No.	8
Peakname	
Ret.Time	8,725 min
Peak Width	0,437 min
Type	M *
Height	6,098 mAU
Area	1,6979 mAU*min

Experiment number (Op-17)

448 nm



Zoom



Peak properties Fucoxanthin

Property Name	Property Value
No.	7
Peakname	Fucoxanthin
Ret.Time	6,933 min
Peak Width	0,334 min
Type	bM *
Height	54,046 mAU
Area	11,4333 mAU*min

Peak properties neighboring peaks

Property Name	Property Value
No.	6
Peakname	
Ret.Time	6,533 min
Peak Width	0,185 min
Type	BMb*
Height	0,188 mAU
Area	0,0213 mAU*min

Property Name	Property Value
No.	8
Peakname	
Ret.Time	7,575 min
Peak Width	0,387 min
Type	M *
Height	4,519 mAU
Area	1,0894 mAU*min

Rerun Op-17

Peak properties Fucoxanthin

Property Name	Property Value
No.	7
Peakname	Fucoxanthin
Ret.Time	7,983 min
Peak Width	0,385 min
Type	M *
Height	46,377 mAU
Area	11,2574 mAU*min

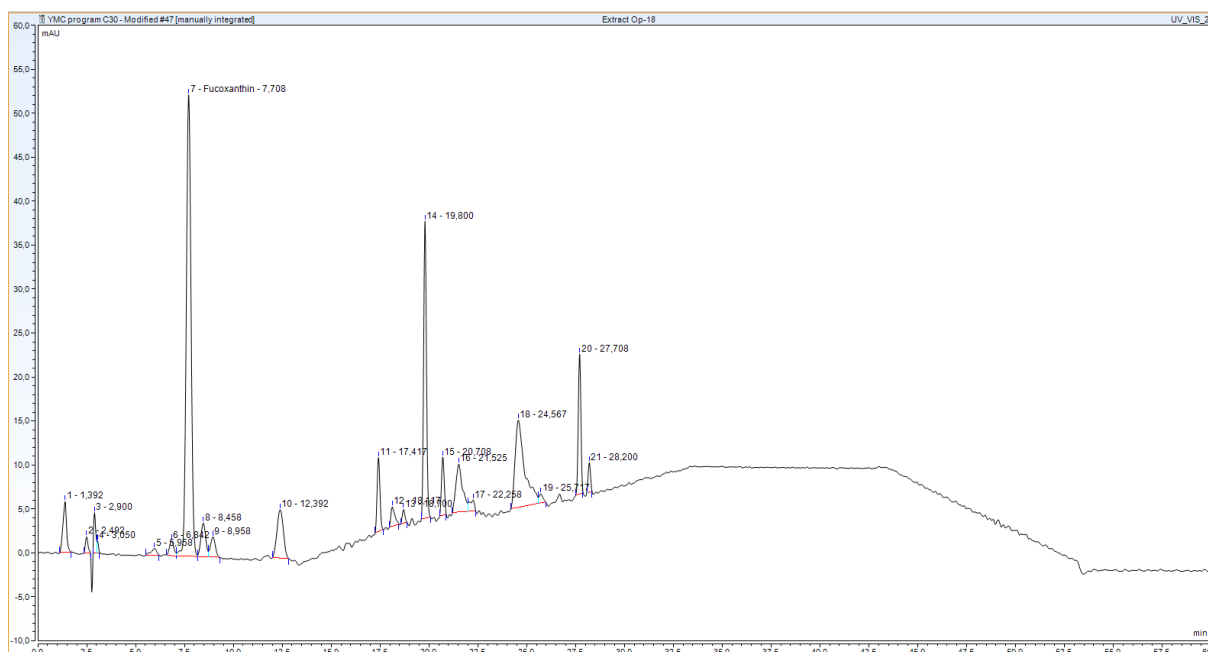
Peak properties neighboring peaks

Property Name	Property Value
No.	6
Peakname	
Ret.Time	7,458 min
Peak Width	0,692 min
Type	M *
Height	0,613 mAU
Area	0,1790 mAU*min

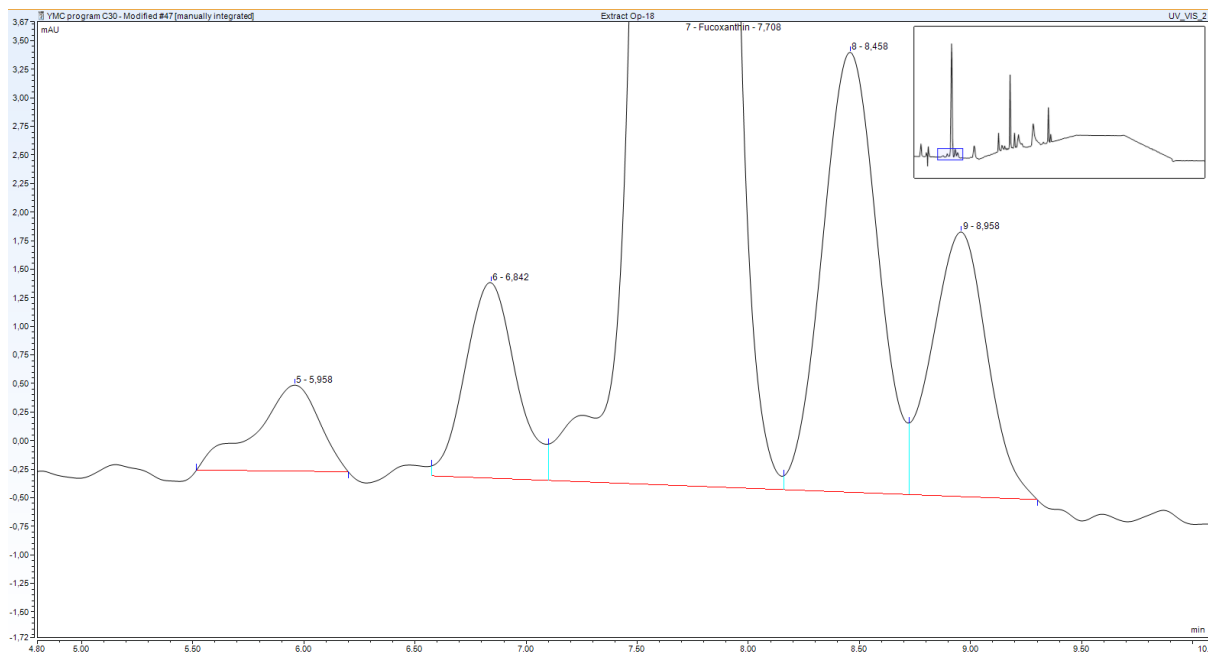
Property Name	Property Value
No.	8
Peakname	
Ret.Time	8,750 min
Peak Width	0,414 min
Type	M *
Height	3,956 mAU
Area	1,0281 mAU*min

Experiment number (Op-18)

448 nm



Zoom



Peak properties Fucoxanthin

Property Name	Property Value
No.	7
Peakname	Fucoxanthin
Ret.Time	7,708 min
Peak Width	0,445 min
Type	M *
Height	52,486 mAU
Area	14,7828 mAU*min

Peak properties neighboring peaks

Property Name	Property Value
No.	6
Peakname	
Ret.Time	6,842 min
Peak Width	0,413 min
Type	M *
Height	1,712 mAU
Area	0,4527 mAU*min

Property Name	Property Value
No.	8
Peakname	
Ret.Time	8,458 min
Peak Width	0,462 min
Type	M *
Height	3,852 mAU
Area	1,1127 mAU*min

Rerun Op-18

Peak properties Fucoxanthin

Property Name	Property Value
No.	7
Peakname	Fucoxanthin
Ret.Time	8,108 min
Peak Width	0,469 min
Type	M *
Height	46,978 mAU
Area	13,7529 mAU*min

Peak properties neighboring peaks

Property Name	Property Value
No.	6
Peakname	
Ret.Time	7,158 min
Peak Width	0,433 min
Type	BMB*
Height	2,082 mAU
Area	0,6090 mAU*min

Property Name	Property Value
No.	8
Peakname	
Ret.Time	8,917 min
Peak Width	0,513 min
Type	M *
Height	3,813 mAU
Area	1,2234 mAU*min

Attachment 7 - Analytes other than Fucoxanthin

Extraction number 12 standard-mixture

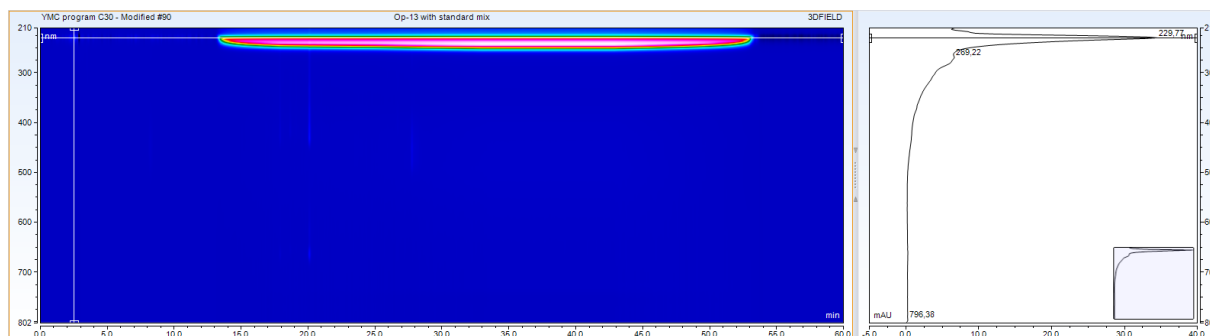
Extraction number 12 (Op-13) in mixture with phloroglucinol, chlorophyll a, β -carotene.

100 μ l of each component, 20 μ l injected.

231 nm – Phloroglucinol:

Property Name	Property Value
No.	2
Peakname	
Ret.Time	2,633 min
Peak Width	0,175 min
Type	bM *
Height	184,039 mAU
Area	20,2412 mAU*min
Amount	Peak is not identified.

Contour plot from 210 nm to 800 nm

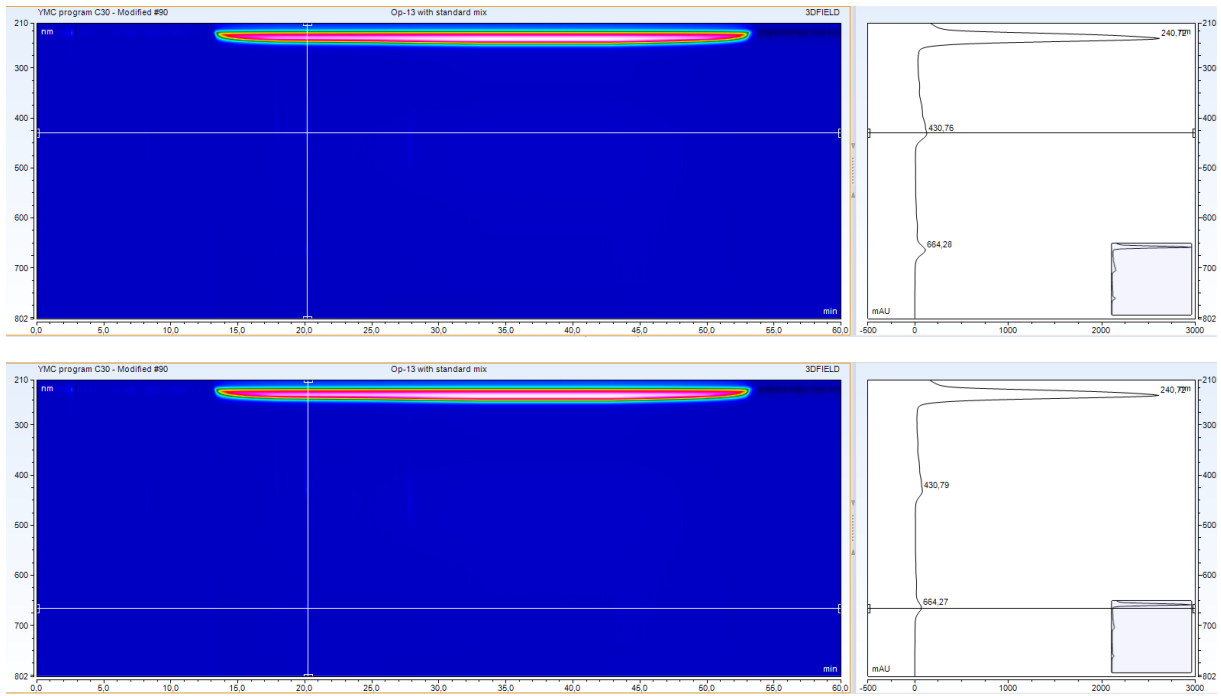


431 nm – Chlorophyll a

Property Name	Property Value
No.	2
Peakname	
Ret.Time	2,633 min
Peak Width	0,175 min
Type	bM *
Height	184,039 mAU
Area	20,2412 mAU*min
Amount	Peak is not identified.

Property Name	Property Value
No.	6
Peakname	
Ret.Time	20,133 min
Peak Width	0,258 min
Type	BMB*
Height	121,649 mAU
Area	19,8570 mAU*min
Amount	Peak is not identified.

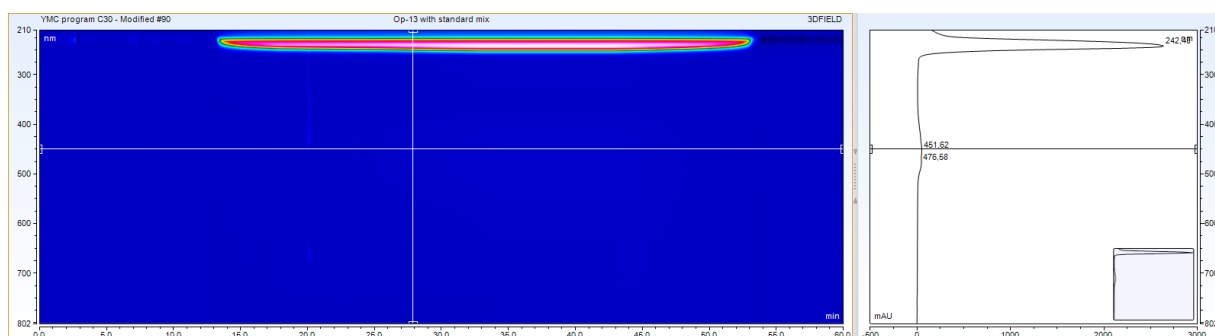
Contour plot from 210 nm to 800 nm



451 nm - β -carotene

Property Name	Property Value
No.	16
Peakname	
Ret.Time	27,792 min
Peak Width	0,292 min
Type	BMB*
Height	49,434 mAU
Area	13,4003 mAU*min
Amount	Peak is not identified.

Contour plot from 210 nm to 800 nm



Extraction number 12

20 μ L injected

231 nm – Phloroglucinol:

Property Name	Property Value
No.	1
Peakname	Phloroglucinol
Ret.Time	2,525 min
Peak Width	0,241 min
Type	BMB*
Height	341,344 mAU
Area	61,9090 mAU*min

431 nm – Chlorophyll a

Property Name	Property Value
No.	7
Peakname	Fucoxanthin
Ret.Time	7,683 min
Peak Width	0,377 min
Type	M *
Height	47,041 mAU
Area	11,3487 mAU*min
Amount	At least 2 calibration level(s) are/is required, but there are/is only 0.

Property Name	Property Value
No.	10
Peakname	
Ret.Time	12,258 min
Peak Width	0,544 min
Type	BMB*
Height	6,364 mAU
Area	2,1202 mAU*min
Amount	Peak is not identified.

Property Name	Property Value
No.	11
Peakname	
Ret.Time	17,342 min
Peak Width	0,281 min
Type	BM *
Height	56,488 mAU
Area	10,1076 mAU*min
Amount	Peak is not identified.

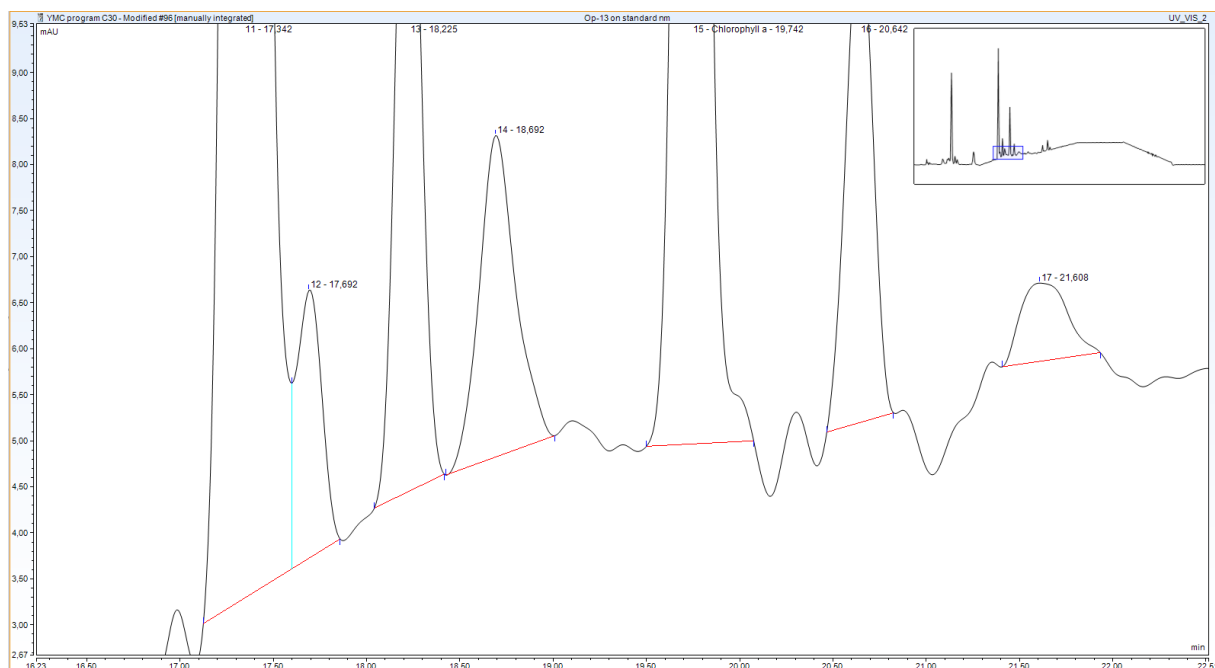
Property Name	Property Value
No.	15
Peakname	Chlorophyll a
Ret.Time	19,742 min
Peak Width	0,262 min
Type	BMB*
Height	24,600 mAU
Area	4,1055 mAU*min

Property Name	Property Value
No.	16
Peakname	
Ret.Time	20,642 min
Peak Width	0,269 min
Type	BMB*
Height	5,539 mAU
Area	0,9126 mAU*min
Amount	Peak is not identified.

Property Name	Property Value
No.	20
Peakname	
Ret.Time	27,525 min
Peak Width	0,247 min
Type	BMB*
Height	5,034 mAU
Area	0,7664 mAU*min
Amount	Peak is not identified.

Property Name	Property Value
No.	21
Peakname	Beta-carotene
Ret.Time	28,025 min
Peak Width	0,250 min
Type	BMB*
Height	1,296 mAU
Area	0,1946 mAU*min

Zoom



448 nm - Fucoxanthin

Property Name	Property Value
No.	7
Peakname	Fucoxanthin
Ret.Time	7,683 min
Peak Width	0,379 min
Type	M *
Height	54,734 mAU
Area	13,3274 mAU*min

Property Name	Property Value
No.	10
Peakname	
Ret.Time	12,258 min
Peak Width	0,547 min
Type	BMB*
Height	6,944 mAU
Area	2,3302 mAU*min
Amount	Peak is not identified.

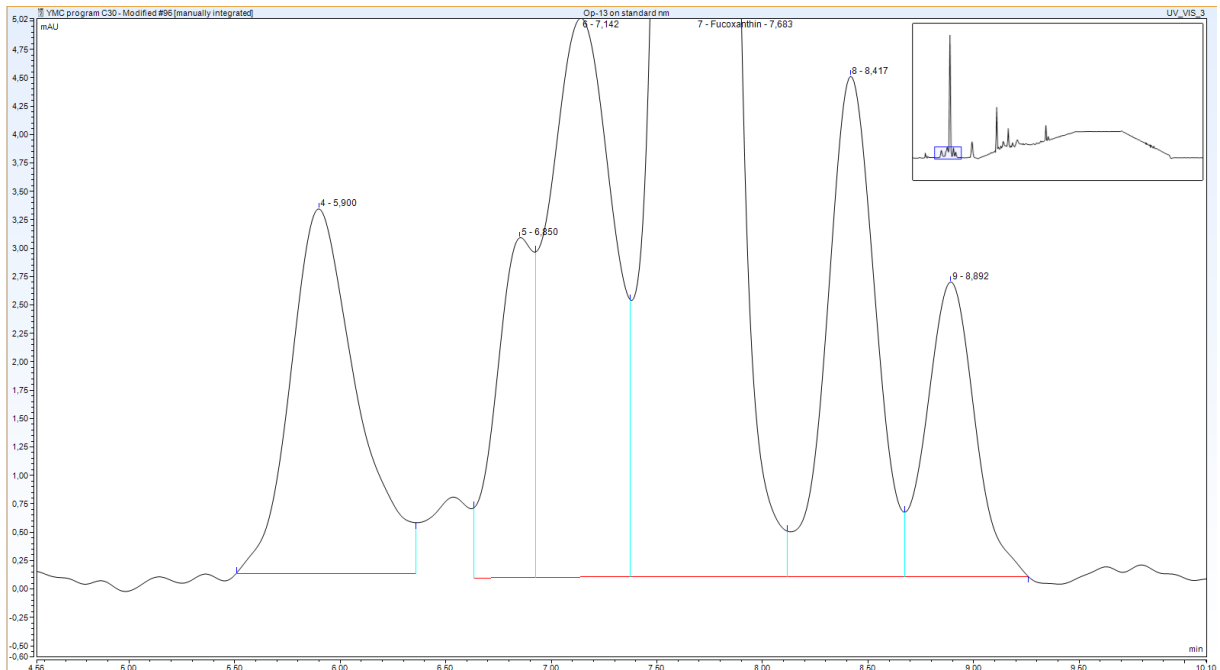
Property Name	Property Value
No.	11
Peakname	
Ret.Time	17,350 min
Peak Width	0,285 min
Type	BM *
Height	19,488 mAU
Area	3,5262 mAU*min
Amount	Peak is not identified.

Property Name	Property Value
No.	17
Peakname	
Ret.Time	21,600 min
Peak Width	0,621 min
Type	BMB*
Height	2,234 mAU
Area	0,9842 mAU*min
Amount	Peak is not identified.

Property Name	Property Value
No.	18
Peakname	
Ret.Time	27,525 min
Peak Width	0,246 min
Type	BMB*
Height	6,630 mAU
Area	1,0064 mAU*min
Amount	Peak is not identified.

Property Name	Property Value
No.	19
Peakname	Beta-carotene
Ret.Time	28,025 min
Peak Width	0,247 min
Type	BMB*
Height	1,531 mAU
Area	0,2268 mAU*min

Zoom



451 nm - β -carotene

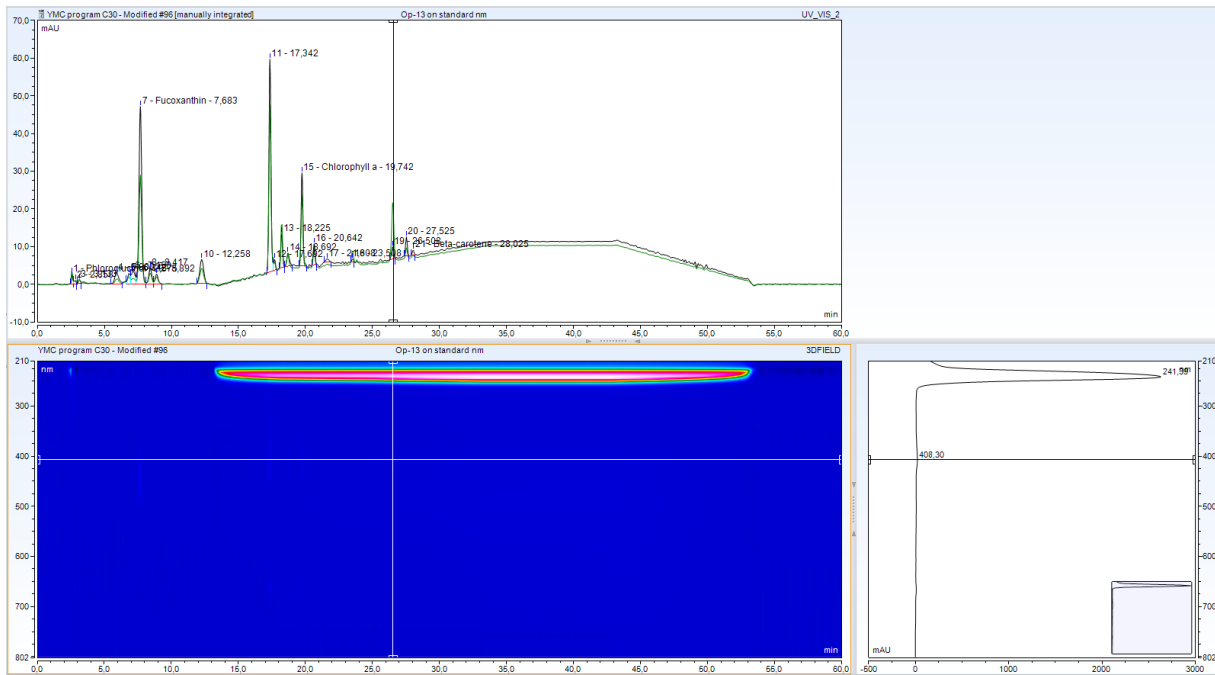
Property Name	Property Value
No.	9
Peakname	
Ret.Time	12,258 min
Peak Width	0,548 min
Type	BMB*
Height	6,914 mAU
Area	2,3286 mAU*min
Amount	Peak is not identified.

Property Name	Property Value
No.	10
Peakname	
Ret.Time	17,350 min
Peak Width	0,288 min
Type	BM *
Height	13,238 mAU
Area	2,4198 mAU*min
Amount	Peak is not identified.

Property Name	Property Value
No.	16
Peakname	
Ret.Time	27,525 min
Peak Width	0,242 min
Type	BMB*
Height	6,604 mAU
Area	0,9779 mAU*min
Amount	Peak is not identified.

Property Name	Property Value
No.	17
Peakname	Beta-carotene
Ret.Time	28,025 min
Peak Width	0,239 min
Type	BMB*
Height	1,435 mAU
Area	0,2053 mAU*min

Unknown:



Contour plot from 210 nm to 800 nm

